Data Aspects in the Reinforcement of Polymer Gears Manufactured by Injection Moulding

by

Xingguang Xu

Thesis Submitted to the University of Warwick

for the Degree of

Doctor of Philosophy

School of Engineering

Apr 2021

To dedicate this thesis

to my most beloved mother and father

谨以此文献给我最亲爱的

妈妈和爸爸

Contents

Acknowledgements

The author wishes to express his sincere gratitude to Dr Ken Mao for the supervision and support in both work and life during the study. Thanks for always supporting whenever and whatever needed help. Without his help, there would be no possibility to reach the destination of this study.

The author also wishes to express his sincere gratitude to Dr Vannessa Goodship for the supervision, support and encouragement. Especially for the guidance in material science research, manufacturing study and writing. Without her great help, I could have easily got lost along the path of my research, and this work would never reach its present stage.

Grateful thanks to Fei Gao, Dr Kylash Makenji, Dr Adrian Lopera Valle, Martin Millson, Zihan Zhang, Dr Saskia Bakker and Dr Chinemelum Nedolisa, for their kindest help and cooperation of the work.

Finally, but by no means least, the author wishes to thank the university technical staffs: Huw Edwards, Philip Gibbons and Mike Green, for the help on experiments undertaken.

Declaration

This thesis is submitted to the University of Warwick in support of my application for the degree of Doctor of Philosophy. No part of this thesis has been submitted for a research degree at any other institution.

The work presented in this thesis has been published in the following peer-reviewed articles:

Xingguang Xu, Fei Gao, Adrian Lopera Valle, Kylash Makenji, Chinemelum Nedolisa, Yuanfang Zhao, Vannessa Goodship, and Ken Mao. “Wear Performance of Commercial Polyoxymethylene Copolymer and Homopolymer Injection Moulded Gears.” Tribology in Industry, in press, accepted in March 2021, DOI: 10.24874/ti.1039.01.21.04.

Mao, K., P. Langlois, Z. Hu, K. Alharbi, X. Xu, M. Milson, W. Li, C. J. Hooke, and D. Chetwynd. "The wear and thermal mechanical contact behaviour of machine cut polymer gears." Wear 332 (2015): 822-826.

Abstract

This study is data driven research, focusing on injection moulded polymer gears. With the help of big data, python scripts were created to summarise academic papers automatically, and bibliometrics research was conducted to discover the main challenges in polymer gears. Challenges were found in the whole life cycle of polymer gear manufacturer including design, manufacturing, and testing. As a practical research topic, the study on polymer gears crossed with many disciplines including mechanical engineering, material science, computer science, electrical engineering and statistics. Following the literature based review, a targeted experimental programme was undertaken using injection moulding. Mould designs were examined and improved to create optimum mouldings and high quality gears were produced. A study on the effect of injection moulding parameters revealed the relationship between the injection moulding parameter settings and the polymer gear performance for material reinforcement in gears with optimisation in the injection moulding process. Further research was undertaken on widely applied POM gears and it was concluded that the homopolymer and copolymer POM gears perform in service differently. It was a novel finding for this commonly applied material. Further, a new effective polymer gear analysis procedure was introduced, putting more emphasis on the material science aspects. This procedure successfully explained differences in performance between POM types was due to the inherent crystallinity. Finally, a new cloud-based Internet of Things (IoT) solution for polymer gears was explored. This offers a potential future ability to collect data from real polymer gear applications and to help secure applications with real-time gear status monitoring.

Abbreviations

IM	Injection moulding
WoS	Web of science
LLR	Log-likelihood ratio
ANOVA	Analysis of variance
ANN	Artificial neural network
OA	Orthogonal array
BP	Backpropagation
DOE	Design of experiment
MT	Melting temperature
CT	Cavity temperature
IS	Injection speed
HP	Holding pressure
POM-C	Copolymer POM
POM-H	Homopolymer POM
CAE	Computer-aided engineering
MQTT	Message queuing telemetry transport
IoT	Internet of things
AWS	Amazon web services
SNS	Simple Notification Service
SMS	Short message service
CAV	Connected autonomous vehicles

List of Figures

List of Tables

List of Symbols

F_{t}	tangential force (N)
P_{d}	diametral pitch (mm)
b	face width of the tooth (mm)
Y	the Lewis form factor of the gear tooth
S_{b}	the maximum root bending stress (MPa)
K_{l}	lubrication condition factor
K_{h}	humidity condition factor
K_{t}	temperature condition factor
K_{v}	speed condition factor
K_{s}	material grade condition factor
K_{m}	mating gear material condition factor
K_{f}	metal gear surface roughness condition factor
C_{s}	service condition factor
Y_{e}	contact ratio factor
K_{a}	application factor
S_{c}	the maximum contact stress (MPa)
Z_{f}	contact ratio factor
K_{a}	application factor
v_i	Poisson ratios of material i
E_i	elastic moduli of material i (MPa)
u	ratio of the number of teeth of the large gear to that of the small gear
θ_{a}	ambient temperature of surround air (°C)
T	transmitted torque (N m)
ρ	specific gravity ($\mathrm{g/cm^3}$)
c	specific heat (kJ/kg/K)
r_{a}	outside radius (mm)
r	reference radius (mm)
Z	tooth number
μ	friction coefficient
k	thermal conductivity (w/m/K)

E	elastic modulus (MPa)
R	relative radius
V_i	sliding velocity for gears i (m/s)
V_f	volume fractions of the fibre
V_m	volume fractions of the matrix
E_f	modulus of the fibre (MPa)
E_m	modulus of the matrix (MPa)
a_{ij}	weight from the i-th input neuron to the j-th hidden neuron
x_i	output value from X_i towards all hidden neurons
b_{jk}	weight from the j-th hidden neuron to the k-th output neuron
X_i	i-th input neuron
Y_j	j-th hidden neuron
Z_k	k-th output neuron
W_{ij}	weight from the i-th input neuron to the j-th hidden neuron
Q_{ij}	the importance of i-th input weight among all inputs connected to Y_j
R_i	relative importance of the i-th input neuron
n	number of samples
Y_i	the performance of each sample
h	step size for gradient descent method
x_i	value after the i-th iteration using gradient descent method
Δw	weight adjustment
δ	local gradient
v^{out}	output signal from the previous layer
δ_k^P	local gradient at the k-th output neuron (out of a total number of P output neurons)
$u_j^{\mathrm{out}}(n)$	output value from the j-th hidden neuron at the n-th iteration
$e_k(n)$	error at the k-th output neuron at the n-th iteration
x_i	output value of the i-th input neuron
k_s	wear rate (mm/cycle)
V_w	wear volume (m^3)
F	normal force (N)
s	sliding distance (m)

Q	wear depth (m)
b	gear pitch circle diameter (mm)
N	number of cycles the gear takes
$\theta_{\max}$	maximum gear contact surface temperature (°C)
θ_{b}	body temperature (°C)
θ_{f}	flash temperature (°C)
c_{r}	constant relating to the contact ratio of the two gears
a	crack length (mm)
K	stress intensity factor
ΔK	the stress intensity factor range
ΔF	load range for a cycle (N)

1 Introduction

This chapter introduces polymer gears. It identifies the current application limitations of polymer gears in industry, which leads to the project aims, plans and thesis structure.

1.1 Background

As a key element in a machine system, gears perform duties including load transmission and changing speed and changing rotation direction. Gears transmit motion providing high accuracy and efficiency even with the heavy loads. Gears have a long history tracing back to about 400 to 200 B.C. of Chinese compass [1]. The earliest gear in Europe was designed by the Greek polymath Archimedes [2] between 150 and 100 B.C. The design of gears has been upgrading and developing since 17th century. Then in the 18th century Leonard Euler, regarded as the originator of modern gears, discovered the involute curve and conjugate motion [3]. By the late 19th century, the machine tools were invented so that involute gears were manufactured and widely applied in industry. Meanwhile, gears characteristics have been studied such as gear lubrication [4] and failure [5].

The environment has become an increasingly important factor in the developing world. For instance, air pollution has become one of the most serious issues, phasing diesel cars out from the market. At the same time, electric vehicles are being rapidly developed to complete with traditional fossil fuel ones. Each demands an increase in the work efficiency. One method to do this is to replace with polymer gears the metal ones that are present in any system containing a transmission mechanism. This method not only increases the transmission efficiency but also decreases the weight of the system.

For polymer gears manufacturing, injection moulding (IM) is one of the most popular techniques and around one third of plastic products are produced with this method in industry [6]. IM offers accurate geometry in short cycle times, and can produce complex shaped products [7]. When compared with 3D printing production, IM can meet higher volumes manufacturing demands with a much higher production speed and a lower component cost.

Polymer gears have unique advantages over metal ones such as lower weight, quieter running, lower cost, self-lubricating and excellent mouldability. However, the potential

application of heavy-duty polymer gears is limited due to the lack of heat resistance and mechanical strength. That is why polymer gears are mainly applied in light load applications such as food machines, toys and textile machines. To solve that problem, research to enhance polymer gears performance is an effective method to expand utilisation. When it comes to the material aspect, this enhancement is usually implemented by adding third party components such as carbon fibres, glass fibres and nanotubes [8].

1.2 Scope of the thesis

Section 1.1 highlighted some reasons why the polymer gears provide pressing industrial research needs especially for high load applications with the gear qualities such as mechanical performance needing to be improved in order to fulfil the requirements. As polymer gears are real industrial products, the gear reinforcement could be considered in each part of the manufacturing process which includes gear shape design, injection moulding mould design, injection moulding process setting, material formulation and the study of tribology mechanics. A two-dimensional study structure is proposed in this project. One dimension addresses the inherent material science in polymer gears because the material influences performance. The other dimension considers the process more widely encompassing design, manufacture and performance carrying out improvements in each of the section with the help of data collection and analysis.

Moreover, further implications are considered in trends for digital transformation which influences not only science development but also people's daily life. Therefore, in this project, a novel creation utilising techniques such as cloud and the Internet of Things (IoT) has been applied to solve the bottleneck of polymer gears usage.

1.3 Research objectives

The overall aim of this project is to study and optimise the manufacturing process of injection moulding polymer gears as well as the working performance.

In order to achieve these aims, the objectives are:

- To study injection moulding and gear testing methods and procedures.
- To undertake injection moulding optimisation for gear manufacturing.

- Explore potential sample analysis methods which can be applied on polymer gears to enhance development.
- Design new polymer gear solutions for practical applications.

1.4 Layout of the thesis

Chapter 2 summarises the research review related to this study. It includes gear design methods as well as the commonly used reinforcement methods in material aspect. Two further methods are used to enhance the literature review. The bibliometrics analysis is applied to find out the main challenges in the study of polymer gears. And a specific python script is designed by the author to automatically summarise the academic publications.

Chapter 3 describes the details of the polymer gear designs. It describes different kinds of gear shapes as well as designs of the injection moulds. They are compared and the optimised design confirmed as the primary design in this project. It describes methodology used to make the polymer gears compatible with the test rig used for the testing.

Chapter 4 presents the injection moulding process for the polymer gears. A study is carried out to find out the impact factor on each of the parameter settings before final optimisation.

Chapter 5 presents a study of a representative polymer gear. As Polyoxymethylene (POM) are one of the most applied material in polymer gears, this chapter shows some new findings related to the POM gears.

Chapter 6 presents a new procedure for the polymer gear sample analysis, using advanced techniques for material analysis rarely applied on polymer gear studies. Frequently studied POM gears have been re-examined to confirm the new procedure is meaningful.

Chapter 7 introduces a creative solution for the application of polymer gears using the IoT and cloud technology. This solution will help gain testing data more efficiently and can monitor the real-time working status of polymer gears. This chapter will explain the concepts as well as the architecture building up procedures.

Chapter 8 presents the conclusions, the novel contribution of this research and draws future recommendations for the future of polymer gear research.

2 Review of polymer gears

2.1 Introduction

This chapter reviews the research on polymer gears. First, a general review is generated focusing on the design, mechanism and reinforcement of polymer gears. On the other hand, as a practical project, the polymer gear has connections to many categories such as manufacturing, material science and mechanical engineering, and there are a lot of related publication resources available online. Those resources are extracted and then statistical methods, namely bibliometrics, are applied to study the topic further. Finally, a specifically created Python script is applied to generate the literature review automatically and some of the most important literatures are selected for the demonstration.

2.2 Design and mechanisms of polymer gears

Even though there is a large quantity of knowledge for metallic gears in practice, they cannot been applied directly on polymer gears because of the unique character of polymers such as sensitive to temperature and easier to deform. However, polymer gears mechanisms have been evaluated with some formulas which were originally developed for metal gears, with correction factors to eliminate the differences between them. The characters of polymer gears were summarized in ref [9] covering the material variety, thermal behaviour, wear performance, failure modes, dynamic mechanism and acoustic emissions.

2.2.1 Design methods of polymer gears

2.2.1.1 Bending strength

The Lewis equation for the bending stress S of metal gears is

$$S = \frac{F_{\mathrm{t}} P_{\mathrm{d}}}{bY} \tag{2.1}$$

where F_{t} is the tangential force, P_{d} is the diametral pitch, b is the face width of the tooth, and Y is the Lewis form factor of the gear tooth.

In order to make the equation fit for polymer gears, a more precise equation for root bending failures was suggested by Yelle [10]. The maximum root bending stress S_{b} allowance is

$$S_{\mathrm{b}} = S\frac{K_{\mathrm{l}}K_{\mathrm{h}}K_{\mathrm{t}}K_{\mathrm{v}}}{K_{\mathrm{c}}K_{\mathrm{s}}K_{\mathrm{m}}K_{\mathrm{f}}C_{\mathrm{s}}} \tag{2.2}$$

where S is given by Equation 2.1, K_{l} is lubrication condition factor, K_{h} is humidity condition factor, K_{t} is temperature condition factor, K_{v} is speed condition factor (pitch line velocity), K_{c} is manufacturing process condition factor, K_{s} is material grade condition factor, K_{m} is mating gear material condition factor, K_{f} is metal gear surface roughness condition factor, and C_{s} is service condition factor.

Later, the British Standard provides an equation for non-metallic gears to calculate the maximum bending stress S_{b} [11]:

$$S_{\mathrm{b}} = SY_{\mathrm{e}}K_{\mathrm{a}} \tag{2.3}$$

where S is given by equation 2.1, Y_{e} is contact ratio factor, and K_{a} is application factor.

2.2.1.2 Surface contact strength

One widely used equation on maximum contact stress is provided by the British Standard [11]:

$$S_{\mathrm{c}} = Z_{\mathrm{h}}Z_{\mathrm{e}}Z_{\mathrm{f}}\sqrt{\frac{F_{\mathrm{t}}}{bd_{\mathrm{p}}}\frac{u+1}{u}K_{\mathrm{a}}} \tag{2.4}$$

where

$$Z_{\mathrm{h}} = \sqrt{\frac{2}{\cos\alpha\sin\alpha}}$$

and

$$Z_{\mathrm{e}} = \sqrt{\frac{1}{\pi\left(\frac{1-{v_1}^2}{E_1}+\frac{1-{v_2}^2}{E_2}\right)}}.$$

Z_{f} is contact ratio factor, and K_{a} is application factor. v_1 and v_2 are Poisson ratios of material 1 and 2 respectively. E_1 and E_2 are elastic moduli of material 1 and 2 respectively. u is the ratio of the number of teeth of the large gear to that of the small gear.

2.2.1.3 Design method introducing wear and surface temperature

Mao [12] provided an equation specifically for polymer gears which took the surface temperature into consideration. The maximum surface temperature is calculated as

$$\theta_{\max} = \theta_{\mathrm{a}} + k_1 T + k_2 T^{3/4} \tag{2.5}$$

where

$$k_1 = \frac{0.625\mu}{bc\rho Z(r_{\mathrm{a}}{}^2 - r^2)}$$

and

$$k_2 = \frac{1.11\mu\left(V_1^{1/2} - V_2^{1/2}\right)}{2r^{3/4}b^{3/4}(k\rho c)^{1/2}}\left(\frac{\pi E}{R}\right)^{1/4}.$$

θ_{a} is the ambient temperature of surround air. T, ρ and c are transmitted torque, specific gravity and specific heat, respectively. r_{a}, r, b, Z and μ are outside radius, reference radius, tooth face width, tooth number and friction coefficient, respectively. k, E, R, V_1 and V_2 are thermal conductivity, elastic modulus, relative radius, sliding velocity for gears 1 and 2, respectively.

2.2.2 Failure modes of polymer gears

Up to now, the service life of polymer gears is difficult to predict because the polymers are not as stable as metal. Each tiny variation in either manufacturing or working condition could lead to huge difference in performance. In order to study the mechanisms of polymer gears more deeply, it is important to understand why polymer gears fail.

2.2.2.1 Wear

Wear is a natural phenomenon which occurs when two surfaces contact with each other with a relative motion. AGMA [13] defines the gear tooth wear as a mechanism in which layers of material are uniformly removed from the meshing surface. Halling [14] summarised wear into four types, which are abrasive, corrosive, adhesive and fatigue wear. Abrasive wear is the displacement of material caused by hard particles. Corrosive wear is a process where electrochemical or chemical reactions occur. Adhesive wear is that the material transferred from one surface to the other during relative motion. Fatigue wear is that the small amount of material gets removed during sliding cycles.

2.2.2.2 Fracture

In most cases fracture occurs because of fatigue or overload on gear teeth. For the fatigue fracture, when the number of working cycles under the load exceeds the endurance limit of the polymer, crack starts to form, and it usually occurs at the root of the tooth where the highest stress concentrates. Then the crack develops towards fracture. The overload fracture happens when the applied load exceeds the tensile strength of the polymer. What is more, the fracture often occurs at the pitch circle which occurrence might be related to the temperature.

2.2.2.3 Pitting

AGMA [13] defines the pitting as repeated stresses of surface and subsurface exceeding the allowance of material. It usually leads to pits on the surface because small cracks on or near the surface get material pieces removed from the surface. Pitting is influenced by the working cycles and contact stress; this progress is enhanced as pitting occurs, leaving non-pitted area unable to hold the load.

2.2.2.4 Scuffing

Scuffing is caused by welding and tearing of small areas which leads to material being rapidly removed from the tooth surface [15]. The use of high loads is usually implicated causing friction overheating between surfaces of two meshing teeth, while the low heat conductivity of polymers makes the temperature rises rapidly.

2.2.2.5 Plastic flow

As a permanent failure, plastic flow results from the yielding of the surface and subsurface material and is caused by high contact stress during sliding [15]. Material flow is caused by thermal softening and the whole deformation processed is influenced by high surface temperature. Also, the deformation rate increases while the yield strength deceases.

2.3 Review on enhancement of polymer gears

The ever-increasing demands for more efficient applications in engineering have resulted in a rapid increase in the use of polymer composites due the unique advantages over metal gears such as low weight, quiet running, low cost and excellent mouldability. However, the application of heavy-duty polymer gears is limited due to lack of heat

resistance and mechanical strength. In these cases, polymer gears cannot be utilised in current automotive systems. To solve this problem, the enhancement of the polymer material and therefore the properties of the resultant gears, can be used effectively [8]. Adding fillers is one of the most common methods to strengthen them. In summary, the enhancement of polymer gear is usually implemented by adding third party components such as carbon fibres, glass fibres and nanotubes.

2.3.1 Polymer enhancement

As polymers continue to develop, they are more and more widely applied in industry. But some applications require high load capacities, high temperature resistance or low wear friction such as gears, bearings, pumps and cans [16]. So, it is necessary to enhance the particular properties of polymers to enable for example the wear of composites to be enhanced as much as 1/50 of that of unreinforced materials [17]. The use of short fibres usually yields an improvement in wear resistance when being incorporated in a polymeric matrix. In the matrix, any change of materials, or even a change in the proportion of each material, can lead to huge differences in matrix properties [18]. Also, the polymeric matrix behaviour is further affected by factors such as the type, amount, size, shape and orientation of the fibres [19, 20].

2.3.2 Material types

There are common polymers which are frequently used as matrices in gears. Examples include polyoxymethylene (POM) [21], polyetheretherketone (PEEK) [22], polyethylene (PE) [23] and polycarbonate (PC) [24]. Fillers can be either inorganic or organic and they usually improve the wear resistance due to either the enhanced chemical properties (bonding between transfer films and metallic counterparts) or improving mechanical properties (modulus and hardness) [25]. Inorganic fillers usually enhance the mechanical and tribological properties of polymers [26] as they usually do not bond with matrices except that some inorganic particles are of help to enhancing the bonding between the transfer film and the metallic counterpart [25]. For example, if copper acts as a filler in PEEK [22], CuS filled PEEK [27] and SiC filled PEEK [28], those fillers act as enhancers to the transfer film and help on the reducing of the wear rate. Commonly used organic fillers are fibres such as carbon fibres (CF)and aramid fibres (AF) [16], [29-31]. Glass fibre is the most commonly applied reinforcement in

about 95% of fibre reinforced plastics [32]. Organic fillers can affect not only the chemical but also the mechanical properties.

2.3.3 Effect of filler size

The size of fillers will influence the performance of the final composite. Fillers can be divided into microparticles and nanoparticles. When compared with microparticles, nanoparticles, namely particles smaller than 100 nm, perform very differently [33]. Durand et al. [17] undertook experiments with inorganic particles in polymers from 5 to 100 μm with the conclusion that large particles (of about 100 μm) protect the polymer matrix better than small particles (of about 20 μm). Furthermore, if the sizes of particles are lower than 20 μm, it will not reinforce the polymer matrix because it will be removed along with polymer debris. Similar results had been found by Friedrich [34]. In contrast, Xin et al. [35] studied the spherical silica particles in epoxy with a filler size of 120 to 510 nm and concluded that the smaller sized particles seemed to be more effective to improve the wear resistance. [33]. Not only are the mechanical properties improved such as strength, modulus and elongation, but also some of the chemical properties are enhanced significantly [36]. Additionally, Xue [28] compared the nano with micro SiC particles incorporated into PEEK and concluded that nanoparticles performed better. In short, the results from researchers are not unified, and are sometimes contradictory when considering the influence of size. In the aspect of wear resistance alone, nanoparticles generally perform better than microparticles.

2.3.4 Effect of filler proportion

Generally, the performance of wear resistance gets better when the filler proportion increases but after a certain amount of filler, it will reach a plateau and not improve even with more particles added. As show in Fig. 2.1, the volume of particles will affect the wear coefficient, but when the particle volume fraction is higher than 20%, it does not significantly increase the wear resistance of the composites [17]. Wang [37] reached similar conclusions about the wear coefficient influenced by volume of fillers but they found the relationship between the wear rate and the volume of fillers. It is reported that when the filler (ZrO_2) is 7.7 wt. %, the wear rate is the lowest (Fig. 2.2). As well as Zhao and Bahadur [38], they concluded that most of the beneficial wear-reducing effect was achieved with 20–30 vol. % filler proportion.

For randomly orientated short fibre reinforced polymers, the modulus E can be calculated with the equation [39]:

$$E = \frac{3}{8}E_{\mathrm{L}} + \frac{5}{8}E_{\mathrm{T}} \tag{2.6}$$

where

$$E_{\mathrm{L}} = E_{\mathrm{f}}V_{\mathrm{f}} + E_{\mathrm{m}}V_{\mathrm{m}}$$

and

$$E_{\mathrm{T}} = \frac{E_{\mathrm{f}}E_{\mathrm{m}}}{E_{\mathrm{m}}V_{\mathrm{f}} + E_{\mathrm{f}}V_{\mathrm{m}}}.$$

V_{f} is the volume fractions of the fibre, V_{m} is the volume fractions of the matrix, E_{f} is the modulus of the fibre, and E_{m} is the modulus of the matrix.

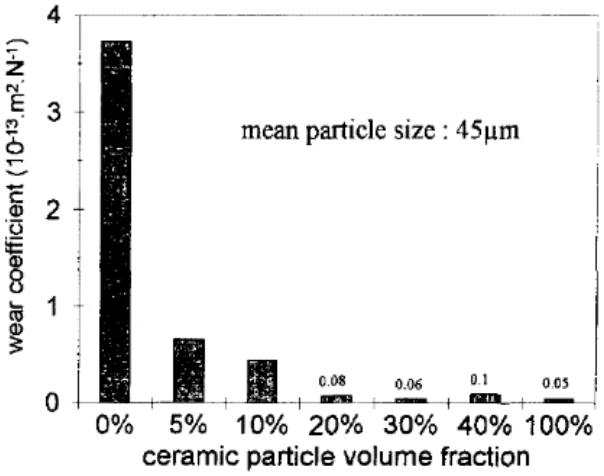

Fig. 2.1 Effect of ceramic particle volume fraction on the wear of Composites [17]

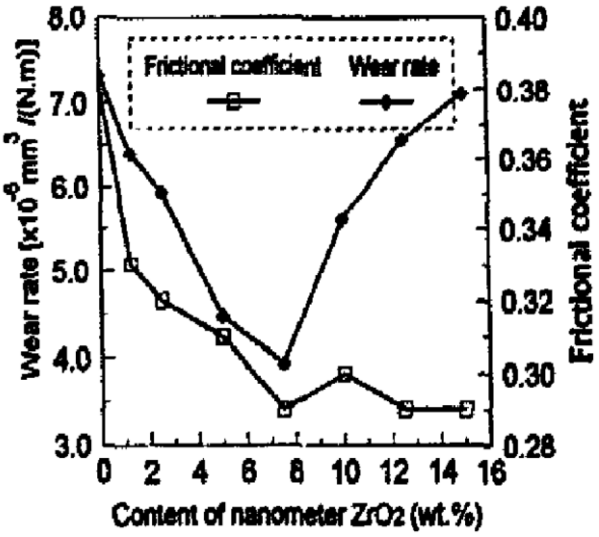

Fig. 2.2 Effect of the content of nanometre ZrO_2 (size of 10 μm) on the frictional coefficient and wear rate of the filled PEEK (load: 196 N; sliding velocity: 0.445 m/s)[37]

2.3.5 Reinforcement of polymer gears

When it comes to the specific reinforcement of polymer gears, the available publications are not as many as those for reinforcement of polymer itself. As expected, reinforced gears perform better in general than the unreinforced ones. For example, Ikegami et al. [40] announced that the reinforced gears were superior to the gears without reinforcement as to wearing durability. Gurunathan et al. [41] stated that the wear rate would reduce with the increase of hardness and crystallinity when adding fillers to polymer gears. Meanwhile, the thermal property was enhanced so that the gears can keep the strength for longer times, namely higher gear life. Also, Senthilvelan and Gnanamoorthy [42] concluded that unreinforced gears (Nylon 6/6) showed more hysteresis loss than fibre reinforced ones did. Furthermore, carbon fibre reinforced gears gained less hysteresis loss than glass fibre ones did. In thermal properties, not only can the reinforcement with fibres reduce the internal heat generation capacity in the matrix when under periodic working conditions, but also gears reinforced with high modulus fibres demonstrated lower heat generation when compared with unreinforced ones [42]. Another reinforcement method showed that gears reinforced with glass cloths was twice as strong as the epoxy resin gear without the reinforcement in both static and dynamic bending tests [40].

In contrast, the reinforced gears also bring weakness such as that the lead form deviation and profile form deviation of reinforced gears are more than those of unreinforced ones

because the hard glass fibres on the teeth surface increase the surface roughness. What is more, the fibres as fillers influence the material homogeneity so that more deviation of reinforced gears will be created than that of unreinforced gears [43]. And it is obvious that gears reinforced with high modulus fibres generate higher noise compared with unreinforced gears [42], which weaken the advantage of the quiet operation of polymer gears. An experiment demonstrated that reinforcement with carbon cloths did not improve the tooth strength due to the low interlaminar strength in the reinforcing layers [40].

Importantly, the influences of the above factors to polymer gears are not that clear, and they are much more complicated to research than those of polymer materials. For example, not only does the form of carbon fibre worn debris largely influence the wear properties, but also the formation of the transfer film that will affect the depths of gear teeth. Furthermore, the more abrasive the carbon fibre becomes, the more wear occurs. In addition, the difference in the compression modulus and the surface hardness between the paired gears also has an influence on intervention of the carbon fibre worn debris at the engagement region [44]. Kurokawa [45] found that the gears did not perform better in line with increasing of the high strength in mechanical properties. But the more amorphous fractions in the base polymer, the stronger the lubrication effect of grease on the engagement region. Most importantly, the teeth fracture usually occurs in the fibre direction, in other words, it will change the failure mode in some occasions [40].

2.3.6 Conclusions

Even though there are a lot of articles focusing on polymer enhancement, they could not be applied directly because the gear pair meshing is a complicated process in which the teeth thickness, pressure angle, surface roughness, pressure value and temperature will affect gear performance and even these factors will affect each other under working condition. For example, the chemical and mechanical properties of polymers are related to the temperature, which could not be controlled during meshing. In this case, the future work may consider more about the relationship between general material studies and the specific polymer gear studies. For example, it has been shown that there are many factors which may influence the mechanical behaviour of a material, but it deserves further study to find out what are the main factors which affect the wear

behaviour when the material is applied on polymer gears. Meanwhile, undertaking more laboratory experiments to obtain sufficient data for gear study is always valuable. Finally, if more design methods or standards can be created for polymer gears, it will be helpful to apply polymer gears more widely in industry.

2.4 Review with bibliometrics

Bibliometrics is the application of statistical methods to analyse publications. In the field of scientific publications, it is called scientometrics. In order to review the development process of the polymer gear industry further, the software CiteSpace was applied to study this topic from the aspect of bibliometrics, which included the countries which are studying this topic, the cooperation between different groups, the citing conditions and the most related topics. This method helped understand the most relevant areas to polymer gear and made a prediction on the future development of this topic.

2.4.1 Review with Web of Science

1441 articles including reviews from the database of Web of Science (WoS) were found. The keyword search process was as follows: The first keyword group was a set of keywords—"polymer", "plastic", "PC", "PE", "acetal", "POM", "nylon" and "PEEK", all connected with the `or` function. The second group was "gear". Then these two groups were combined with the `and` function in the advanced search section of WoS. All the data were filtered with "All languages" in the language setting and document types were set as "articles" or "reviews" or "books" to exclude unwanted resources such as presentations and meeting abstracts. After a quick check, it was found that many resources related to marine and pollution were selected because they used "fishing gear" as another name of the fishing tackle. Thus, 'fishing gear' as a compound using the `and not` function to exclude the relevant publications. Finally, 1179 publications as extracted as the final output.

Firstly, from the WoS, the analysis results of "Total Publications" (Fig. 2.3) and "Sum of Times Cited Per Year" (Fig. 2.4) were exported. Fig. 2.3 showed that the number of publications increased from 1991 and from 2014 it increased faster. Fig. 2.4 showed the total number of citations to the 1179 found results per year. It showed the number of citations started to rise from 1995. From the two figures, the increase of these two numbers proved that the studies related to polymer gears got more and more popular,

and researchers became more interested in this area. From 1970 to 1990, the average publications per year are less than 10, and the condition of citation is similar. During that period, the study of polymer gears had just started, and researchers were more focused on the material choice as well as the production methods for polymer gears [46-48]. Then the number of citations kept increasing every year. When it comes to the number of publications, from 2014, the number of publications was more than 50 every year and the number of citations per year were more than 950. The researching outbreak continued till 2020. As the data for 2021 is not complete, it is not included in this study.

When undertaking the "Analyze Results" function in WoS, it showed that this topic was related to 126 science categories, while the main studying areas were Engineering Mechanical (33.3%), Materials Science Multidisciplinary (24.0%), Polymer Science (9.8%), Engineering Manufacturing (8.2%), Engineering Multidisciplinary (6.7%), Metallurgy Metallurgical Engineering (5.3%), Mechanics (5.2%), Physics Applied (5.1%) and Nanoscience Nanotechnology (5.0%). There were 519 publication sources, and the five main sources were from "Wear" (3.8%), "Tribology International" (2.5%), "International Journal of Advanced Manufacturing Technology" (2.0%), "Proceedings of the Institution of Mechanical Engineers Part C Journal of Engineering Tribology" (2.0%) and "Bulletin of the JSME Japan society of mechanical engineers" (1.9%), which covered the area of mechanics, manufacturing, wear and tribology. In summary, the topic of polymer gear is a practical research direction with highly interdisciplinary connections.

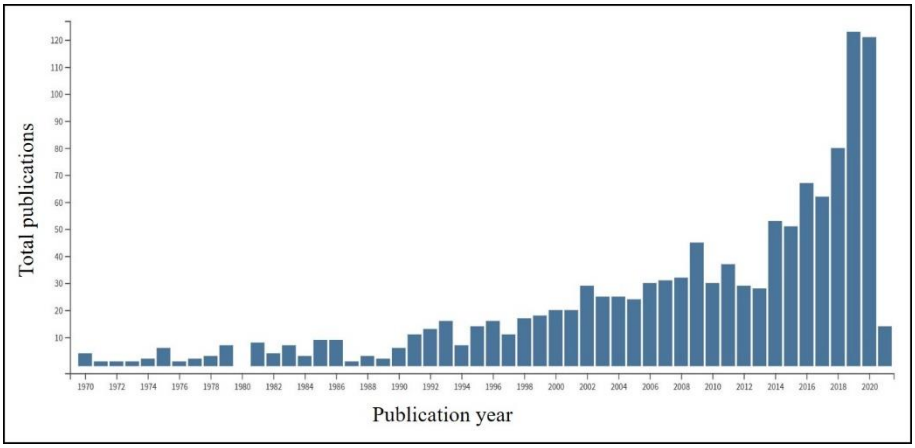

Fig. 2.3 Total publication numbers from 1972 to 2021 according to the Web of Science. Note: Data updated to January 2021.

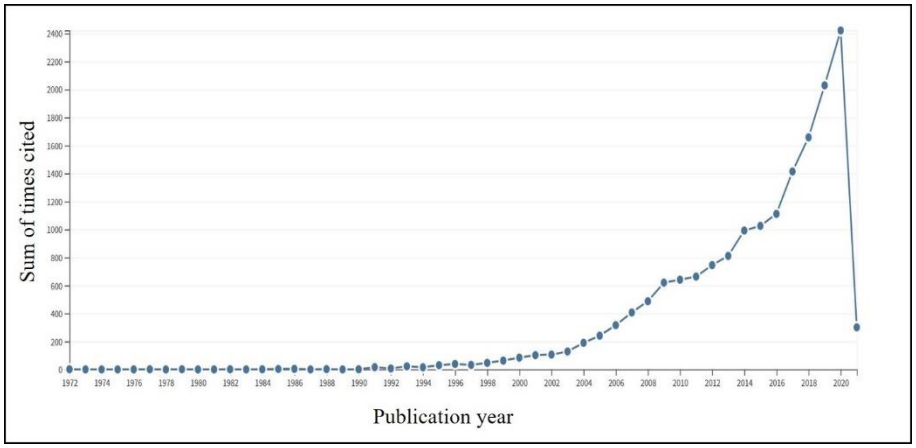

Fig. 2.4 Sum of cited publication numbers from 1972 to 2021 according to the Web of Science. Note: Data updated to January 2021.

2.4.2 Review with CiteSpace

The data gained from WoS were imported to the CiteSpace 5.7 R4 software for further bibliometric analysis. These data were originally exported from WoS in plain text format with the record content setting "full record and cited references" to get the most details. In CiteSpace, they have been filtered to remove duplication. Then the setting for CiteSpace was undertaken. As the earliest article found was in 1970, the time slicing range was set from 1970 to 2021 (as the time range for the bibliometrics purpose), and the slice is set as 1 year per slice by default. The term sources—"Title", "Abstract", "Author Keywords" and "Keywords Plus", were all selected for analysis. These four terms covered the most important information from the raw data, which could then be processed by the software.

Firstly, the co-authorship analysis was taken which included country type and institute type. For the country type analysis (Fig. 2.5) regarding the citation numbers, the top 10 countries are the USA, China, Japan, India, Germany, England, South Korea, Canada, Poland and France, meaning that these countries have been cited more for their publications in the field of polymer gears. Then these 10 countries were ranked again by centrality. In CiteSpace, the nodes (each node here represents a country) with centrality higher than 0.1 means that they have relatively high influence in this field and are coloured as purple (Fig. 2.6). In this condition, the high influencing countries are Germany (0.4), the USA (0.32), England (0.25), China (0.23), France (0.22), Greece (0.16), India (0.14), Belgium (0.12) and Australia (0.11). What is more, the thickness of the connected lines between different counties determines how well the countries

cooperate with each other in general. The USA and China had cooperation with most of the main countries while Japan, Germany and England have relatively low cooperation with each other.

Fig. 2.5 Contribution of the main countries. Ranked by number of citations.

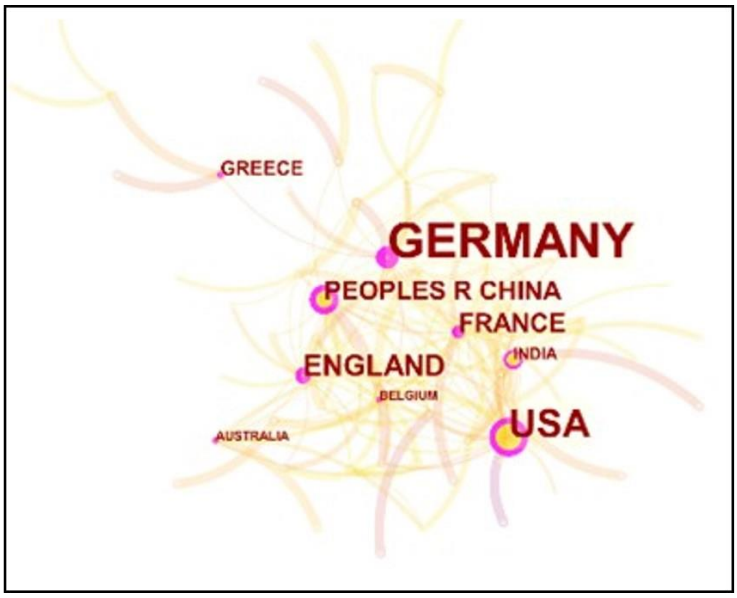

Fig. 2.6 Contribution of the main countries. Ranked by centrality.

When it comes to the institute analysis (Fig. 2.7), it showed that most of the main countries had at least one institute ranked top in this list, e.g. the Indian Institute of Technology, the Chongqing University in China, the Chinese Academy of Sciences, the University of Birmingham in the UK and the University of Warwick in the UK.

India is developing fast in this field. It began studying this area only from 1993 but with a relatively high citation number of 88 during this period and ranked fourth in the list. They gathered 23 universities as one institute, namely the Indian Institute of Technology, making it rank first among all the institutes in regard to citation numbers, which also gained influence due to the result. It showed that the Chongqing University, Chinese Academy of Sciences and the Wuhan Technology University played an important role in China. The University of Warwick and the University of Birmingham are the two major institutes in England. For Germany and Japan, Technology University Munich and Nagasaki University are the most representative institutes, respectively. It is interesting to see that there are no key institutes in the USA ranking top even though the USA is one of the main countries researching on this topic. It is because there are many institutes in the USA doing this topic such as Georgia Institute of Technology, the Pennsylvania State University and Massachusetts Institute of Technology but the average number of publications per institute is low. What is more, the USA is regarded as one of the earliest countries studying this topic. This fact also contributes to the influence.

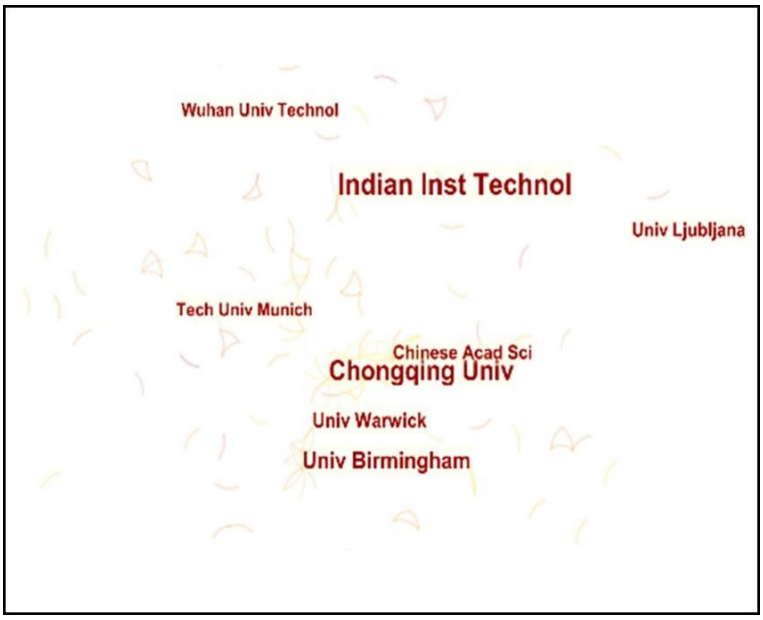

Fig. 2.7 Contribution of the main institutions.

The main contributed authors were also researched. When ranking by the citation numbers (Fig. 2.8), the top five authors were N. Tsukamoto, K. Mao, R. Gnanamoorthy, S. Senthilvelan, Huaiju Liu and Caichao Zhu (tied for fifth). When ranked by the centrality (Fig. 2.9), the five authors were K. Mao, D. Walton, Huaiju Liu, Caichao Zhu

and Jinyuan Tang. As marked with the most influence, K. Mao worked on a variety of topics on polymer gears which included wear analysis, peformance simulation and test facility designing[12, 49, 50]. D. Walton was mainly focusing on gear geometry design and peformance of both metallic and non-metallic gears[3, 51, 52]. Huaiju Liu and Caichao Zhu were in a same group, they had various research areas such as gear lubrication, gear application and gear coating; and their group is mainly focusing on transmission of both metallic and polymer gear systems[53-55]. Jinyuan Tang's interest was on dynamic responses of gears[56, 57]. N. Tsukamoto contributed much to the area of transmission efficiency of polymer gears[58, 59]. R. Gnanamoorthy and S. Senthilvelan were frequently working together on polymer gear performance related to material, manufacturing methods and profile design[41-43].

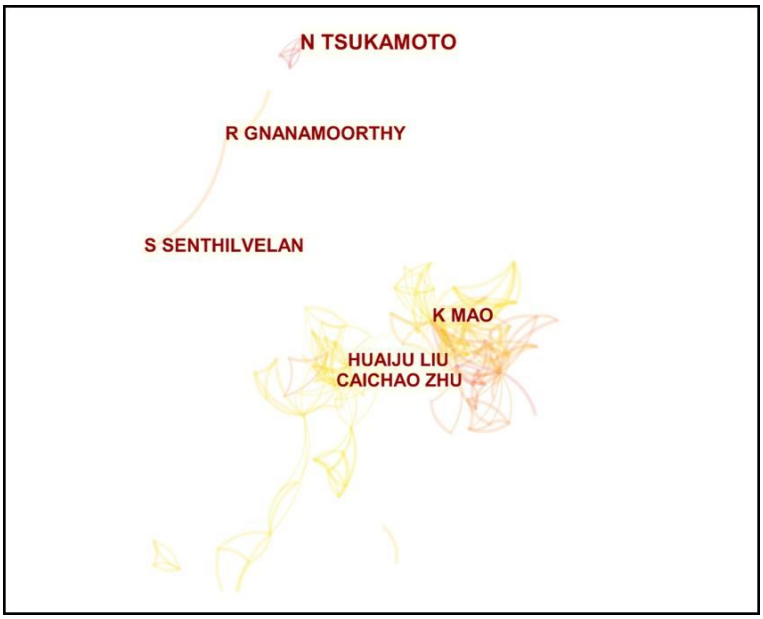

Fig. 2.8 Contribution of the main authors. Ranked by number of citations.

Fig. 2.9 Contribution of the main authors. Ranked by centrality.

The keywords analysis could help find out the main topics in polymer gear research. In CiteSpace there are two methods for keywords analysis. The first one uses the keywords in publications directly; and the second one summarises all the keywords in titles, keywords and abstracts to generate the keywords. In this study, we used the first method and Table 2.1 shows the top 10 keywords sorted by frequency and centrality. The two sorting methods are both effective to reveal the importance. The "by frequency" method shows the most used keywords and the "by centrality" method lists the keywords which occur in wider categories of publications. The keywords such as "gear", "polymer", "plastic gear", "plastics and "spur gear" define the research area. The keywords such as "behaviour", "performance" point out the research purpose. And the "friction", "wear", "deformation", "temperature" and "damage" are the main research objectives most related to the research outcome. Finally, the keywords like "simulation", "model design" and "composite" are possible solutions for the research issues.

Table 2.1 Most important keywords.

Rank	Keywords	Frequency		Rank	Keywords	Centrality
1	behavior	111		1	polymer	0.07
2	gear	109		2	model	0.07
3	wear	103		3	growth	0.07
4	friction	91		4	damage	0.06
5	polymer	85		5	Surface roughness	0.05
6	performance	69		6	plastics	0.05
7	plastic gear	63		7	water	0.05
8	simulation	55		8	design	0.04
9	temperature	54		9	composite	0.04
10	spur gear	50		10	deformation	0.04

The document co-citation analysis is a method pioneered by Henry Small [60] to synthesise research networks. The synthesised network is divided into co-citation clusters of references to show an overview of the research process. In this study, the co-citation analysis was undertaken based on publications from 1970 to 2021. The top 80 most cited publications were collected to build a cited reference network for each individual year. Then all the results were combined into one network. As recommended by the software designer, the log-likelihood ratio (LLR) method was applied and the keywords of publications were chosen for analysis. The whole network contained 9555 references, namely the nodes in the pictures. It had 2388 clusters in total and there were 523 clusters which had more than one reference. The network had a modularity (Q) value of 0.50 and a mean silhouette score of 0.80 (S). Generally, if Q has a value larger than 0.3, it means that each field represented by a co-citation cluster inside the whole network is clearly defined. If the S value is greater than 0.5, it means that the clustering effects are reasonable, and the level of homogeneity is relatively high, suggesting that clusters are well matched with each other[61]. Thus, the cluster results are considered reasonable. The top 10 clusters were shown as Fig. 2.10. The colours of the clusters were related to the citation time which would be analysed later. It also showed that the fields were ranked as: #0 “polymer gears”, #1 “material valorisation”, #2 “block copolymers”, #3 “polymer matrix composites”, #4 “quality improvement”, #5 “three dimensional printing”, #6 “electrochemical properties”, #7 “cycloidal gear”, #8 “gear

mesh and contact path", #9 "soft robotics". The overlapping area implied that the clusters had close relationship with each other such as #4 with #5, and #7 with #8. In summary, it covered different aspects including materials (#1, #2 and #3), applications (#7 and #9) and mechanics (#8) of gear.

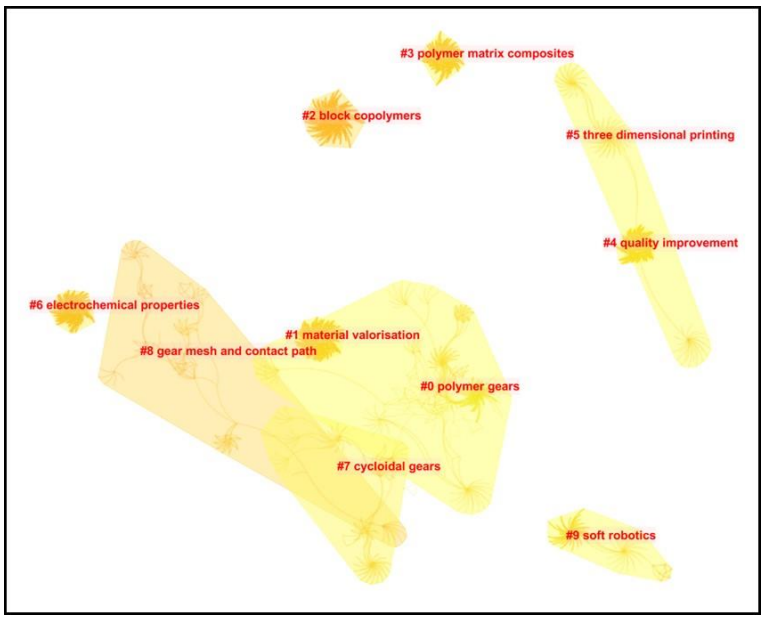

Fig. 2.10 A landscape view of the co-citation network.

Then the timeline visualisation was presented which depicted the top 10 clusters along horizontal timelines (Fig. 2.11), according to the time of publication on the top of the picture, from left to right. Clusters were vertically listed in the descending order of size. The coloured arcs represented the co-citation links. The larger the nodes (solid dots on the horizontal lines) were, or the denser tree rings the nodes had, the more importance these fields had because it meant that they were highly cited or had citation bursts or both. Those references were listed below each timeline. From the timeline view, the clusters showed different levels of sustainability represented by arc lengths. Some kept active for 15 to 20 years while some were alive for a relatively short time. Important nodes deserved deep studies as they were key references. Thus, more research will be carried out in Section 2.5.

It was interesting to see that there were no co-citation links (represented by coloured arcs) found before 2000. One possible reason would be that there were not as many citations in that duration. Another possibility was that prior to 2000, the information from the database was not as detailed. To get a better understanding of the whole

development process of polymer gears regarding the circumstance above, the co-occurrence term analysis was then taken.

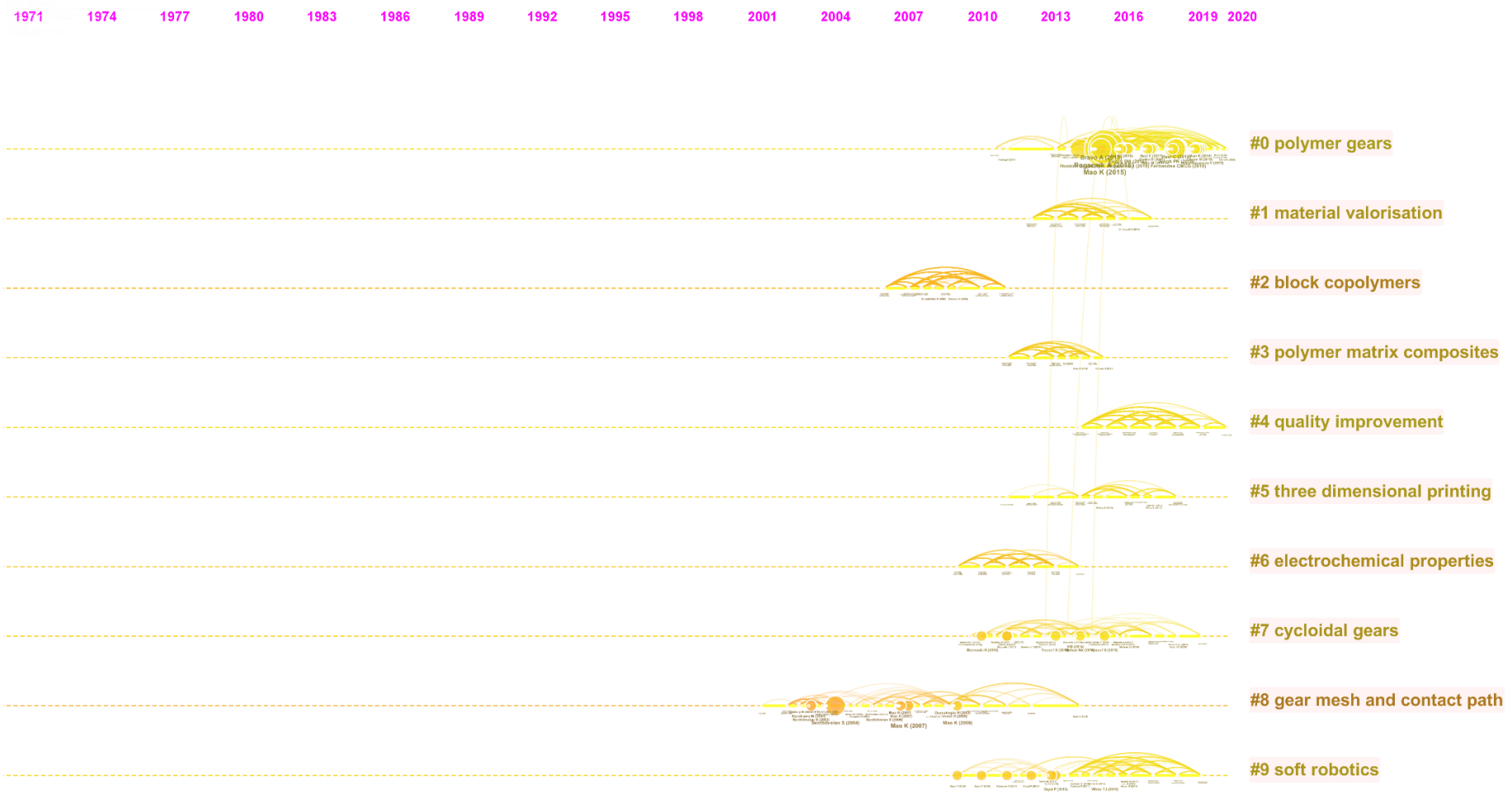

Fig. 2.11 A timeline visualization of the largest clusters

In CiteSpace, the co-occurrence term analysis can extract noun phrases from the content of the bibiographic records. Then it finds out important phrases from titles, authors and keywords of publications. The phrases with count numbers greater than 3 were summarised in Table 2.2, with the years indicating the first time they occurred. It showed that from 1970 to 1979, the studies on polymer gears started; and the research was relatively more basic and focusing on the concepts such as wear rate, deformation, rolling methods and wear resistance. Then from 1980 to 1989, the topics extended to material, gear tooth design, transmission system, etc.. When it came to 1990–2000, one of the key characteristics for polymer gears, namely temperature has been paid attention; advanced techniques such as finite element analysis were applied in simulation, and composites were introduced in material.

Table 2.2 Most important topics from 1970 to 2000.

Noun Phrases	Year
Plastic gears; nylon gears; wear resistance; wear rate; plastic deformation; rolling method(s);	1970–1979
Power transmission; gear teeth; tooth profile change; plastic material; tooth surface; mating metal gear(s); lubracating;	1980–1989
Degrees; temperature; gear pump; flow rate; finite element analysis; tooth profile; surface layer; high strength; composite gear(s); fatigue; friction coefficient; carbon fiber(s);	1990–2000

Furthermore, the reference burst analysis adds up more details about the references which have relatively high importance due to the burst in cited numbers. The results were shown in Table 2.3. The Begin and End years displays the burst duration for the reference. Year means the year of publication. And the Entity column lists basic information of publications. Those publications will be reviewed later with a new method in Section 2.5 using computer science.

Table 2.3 Top cited publications by bursts.

Begin	End	Strength	Year	Entity
2010	2014	2.5971	2010	Mao K, 2009, WEAR, V267, P639, DOI 10.1016/j.wear.2008.10.005
2018	2019	3.4797	2017	Walvekar AA, 2017, INT J FATIGUE, V95, P264, DOI 10.1016/j.ijfatigue.2016.11.003
2018	2019	2.9819	2017	Li S, 2017, INT J FATIGUE, V98, P81, DOI 10.1016/j.ijfatigue.2017.01.020
2018	2021	2.9684	2016	Evans SM, 2016, TRIBOL INT, V97, P379, DOI 10.1016/j.triboint.2016.01.052
2019	2021	8.516	2015	Mao K, 2015, WEAR, V332, P822, DOI 10.1016/j.wear.2015.01.084
2019	2021	6.494	2015	Pogacnik A, 2015, MATER DESIGN, V65, P961, DOI 10.1016/j.matdes.2014.10.016
2019	2021	5.6379	2018	Fernandes CMCG, 2018, TRIBOL INT, V120, P255, DOI 10.1016/j.triboint.2017.12.027
2019	2021	5.4936	2018	Tavcar J, 2018, J ADV MECH DES SYST, V12, P0, DOI 10.1299/jamdsm.2018jamdsm0006
2019	2021	5.0102	2018	Singh PK, 2018, TRIBOL INT, V118, P264, DOI 10.1016/j.triboint.2017.10.007
2019	2021	5.0102	2018	Hasl C, 2018, J ADV MECH DES SYST, V12, P0, DOI 10.1299/jamdsm.2018jamdsm0016
2019	2021	4.6747	2015	Bravo A, 2015, ENG FAIL ANAL, V58, P113, DOI 10.1016/j.engfailanal.2015.08.040
2019	2021	4.3828	2018	Singh AK, 2018, P I MECH ENG J-J ENG, V232, P210, DOI 10.1177/1350650117711595
2019	2021	3.6597	2017	Zorko D, 2017, J ADV MECH DES SYST, V11, P0, DOI 10.1299/jamdsm.2017jamdsm0083
2019	2021	3.4095	2016	Duhovnik J, 2016, TEH VJESN, V23, P199, DOI 10.17559/TV-20151028072528
2019	2021	3.129	2017	Hu ZD, 2017, TRIBOL INT, V116, P394, DOI 10.1016/j.triboint.2017.07.029
2019	2021	3.0616	2018	He HF, 2018, INT J MECH SCI, V141, P512, DOI 10.1016/j.ijmecsci.2018.03.044

As another overview on polymer gears, Fig. 2.12 is a dual-map overlay of the polymer gear publications in the context of the global science map based on more than 10,000

journal records in the Web of Science. It showed the relationship between the disciplines (map part on the left) and the science categories (map part on the right). More information about this method is on the publication of Chen and Leydesdorff [62]. In this dual-map overlay, the node area on the left are the disciplines of the citing publications, i.e. the more than 10,000 publications in our original datasets. The node area on the right were the disciplines of the cited publications, which were the references cited by the publications in the original datasets. Generally, the disciplines on the left showed what categories the searched topics were related to; and those topics are either related to or based on the disciplines on the right. In this figure, the curves stood for reference clues; and the ellipses contained information of the number of authors (monitored by the minor axis length) and the number of publications (monitored by the major axis length). It showed that the polymer gear publications occurred in many disciplines. This topic mainly belonged to two major disciplines, which were "physics, materials, chemistry" and "mathematics, systems, mathematical". When it came to the cited publications, the disciplines became much wider, such as "systems, computing, computer" and "sports, rehabilitation, sport". It might be because the polymer gears were widely used in many areas and as practical research, it was related to many scientific areas as well.

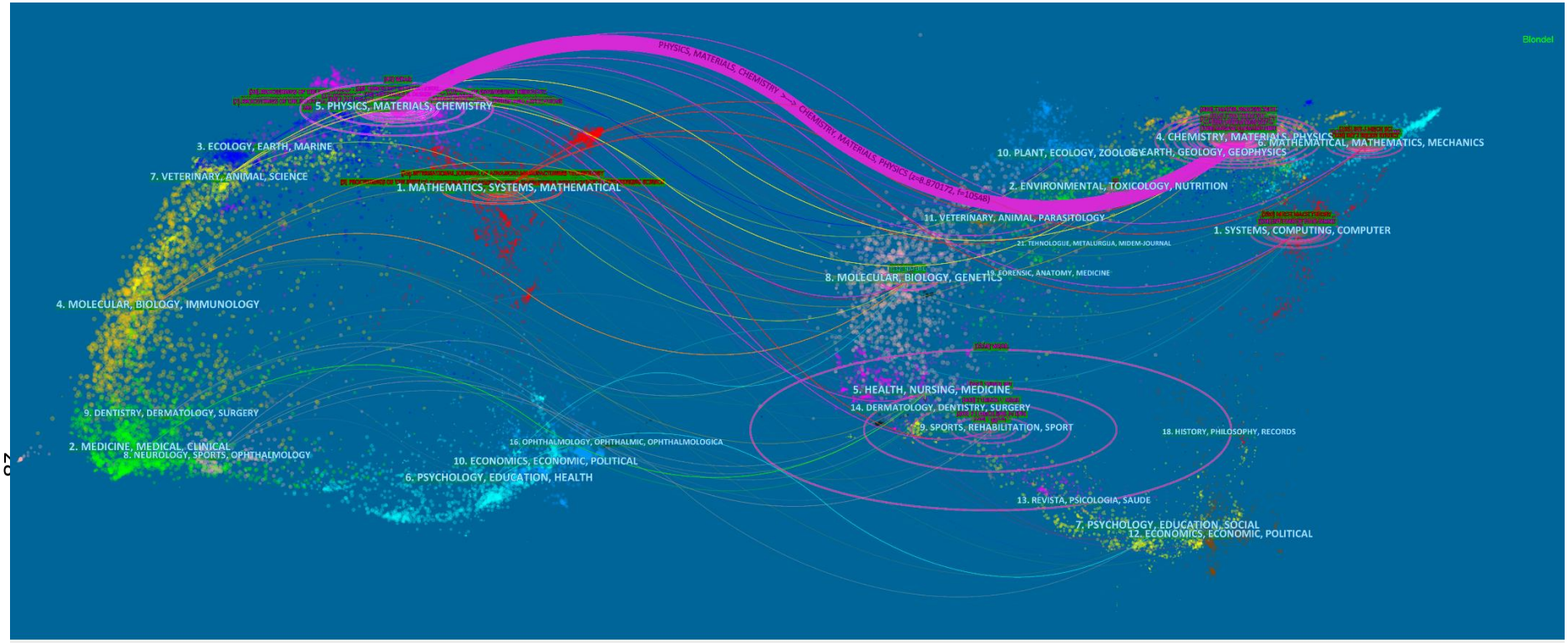

Fig. 2.12 Dual-map overlay visualisation for polymer gear research.

Finally, this bibliometric method was used to target the main challenges for the research of polymer gear. Fig. 2.13 is the category analysis which presents the most related fields to polymer gears. Each node stands for one category. Nodes are linked by curved lines showing that they are related. Generally, the bigger the node size is, the more important its category stays; The thicker the line is, the stronger the bonding between two nodes is [63]. In this project, it shows that "engineering", "engineering mechanical", "material science", "material science multidisciplinary" and "polymer science" are the most important categories for polymer gears. But "engineering" and "engineering mechanical" have relatively weaker connections to nodes related to materials.

Similar conclusions were drawn when checking the publications in detail. There are a large amount of polymer testing references [64, 65]. However, only few of them are currently applied to polymer gear analysis. In polymer gear applications, reported research methods stayed at a macroscopic level such as the wear performance [66-69], temperature influences [70-73] and oil influences [74, 75] on different kinds of polymers [76-80]. Due to the complex interactions in gear applications, the vast majority of findings could not be directly applied on polymer gears, meaning that there is a gap between the study of polymer science and polymer gear performance.

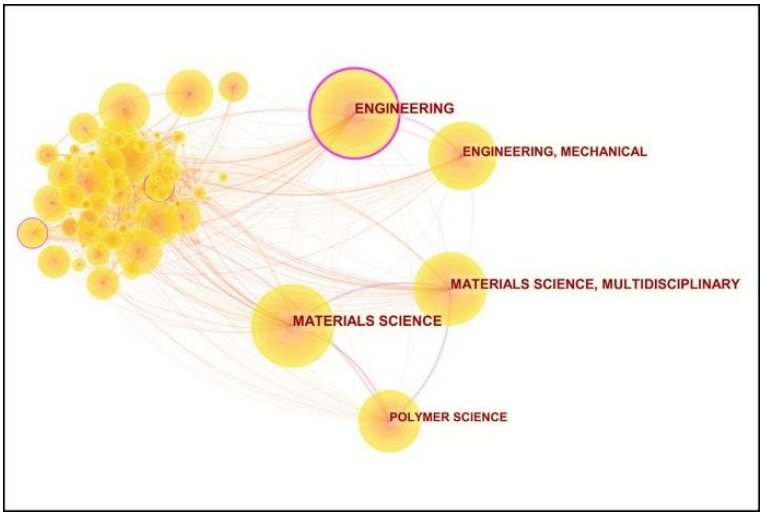

Fig. 2.13 Category cluster

In summary, this method helped on the review of polymer gear research and studied more on the relationships among different disciplines. However, it should be noted that the results presented are also limited by the keywords chosen. For example, the variability of key words such as "PE" and "Polyethylene" will influence the

bibliometric results. Further exploring on the influences of keywords variability would be worthwhile in future research.

2.5 Automatic literature review

As shown previously, the study of polymer gear covers many categories which bring in a large number of publication resources. For higher study efficiency, the author wrote a script using Python (Python 3.7.3) to automatically undertake the literature reviewing process.

2.5.1 Design of the auto-review script

The commonly downloaded publication files with the format of .pdf can be used for reviewing. Due to legal requirements, using a web crawler method to download a large quantity of academic papers automatically is not allowed. So, all the publications are searched and downloaded manually. Then all the pdf files are transferred from pdf to text in script. Many third-party libraries had been tried such as pdfminer, pdfminer.six, PyPDF2 and pdfPlumer. The pdfminer.six has the best performance and it is applied in this project. Then the text files are extracted into the script. All the pdf files in the target folder will be read through one by one. An excel file is created to store all the results, each row stands for a paper. There are four parts of the output results. The first part list the titles. The second part extracts the information of authors and publication years. The third part snips the abstract because it provides the essential information for quick understanding of the publication. The final part provides a summary which is based on the conclusions or results part of the publication. In the excel file, each column stands for one part of the results. As for the methodology of the process, most of the publications are highly formatted, the script tries to track the general format then extracted the required information from the publications which are mostly relying on the regular expression. For example, the abstract part usually begins with the title of “abstract” or it usually follows the author & year part. And the next part is usually called “introduction”. The keywords indicating the start and end of the abstract are searched then the section between them is outputted. When it comes to the summary part, the script tries to search all the sentences with some landmark root words, for example the “conclu-”, “result-”, “show-” and some conjunction such as “however” and “furthermore”.

The script gathers important information from different publications in one table automatically, which increases the efficiency in roughly reading large quantities of publications. And it tries to find out some of the most evident conclusions in the publication, which may help gain further understanding than only having information from the abstract.

2.5.2 Results of the auto-review script

Due to the limitation of the thesis length, only some literatures are auto reviewed. The literature burst analysis using CiteSpace in Chapter 2.4 list some important references (Table 2.3). Those references are selected and the results of the auto-review process on them are detailed in Appendix A. Fig. 2.14 demonstrates two examples of successful and failed processing, respectively. This tool brought in some advantages. First, it listed some information of different publications such as the titles, authors and abstracts in one table, which would help the researchers on review and comparison of the publications. Second, it summarised some key conclusions from the content automatically, researchers could extract more information without reading deeply on each publication or at least receive more information about each publication in few minutes. This would be helpful to support the literature review process especially when the subjects are within a lot of different publications: this tool can be used as a filter to help researchers highlight more interested publications.

Title	Year;Authors	Abstract	SUMMARY
An investigation on the thermal and wear behavior of polymer based spur gears	2018 Prashant Kumar Singh *, Siddhartha, Akant Kumar Singh	A R T I C L E I N F O This study investigates the potential of three different thermoplastic materials viz. Acrylonitrile Butadiene Styrene Keywords: (ABS), High Density Polyethylene (HDPE) and Polyoxymethylene (POM) to be used in plastic gearing applica- Polymer gears Failure tions. The gears are manufactured by injection molding process. Thermal and wear behavior of these gears are Wear rate examined at different torque levels of 0.8, 1.2, 1.6 and 2.0 Nm along with different rotational speeds of 600, 800, Surface temperature 1000 and 1200 rpm. Also, steady state analysis of the gears is carried out at a torque of 1.4 Nm and a rotational speed of 900 rpm to measure the reduction in the gear tooth, durability and failure modes occurring in these gears. ABS gear fails due to excessive wear of the teeth whereas HDPE gear failure is caused by the cracking at the root of gear teeth. ABS and HDPE gears complete 0.5 and 1.1 million cycles, respectively before failure whereas POM gear completes 2 million cycles without any sign of failure. 1.	The results obtained in this study are concluded as follow: 1. It results in a reduced wear rate of gear tooth at higher rotational speed. It is found that ABS gear shows the best agreement (maximum 8% deviation) with Mao model followed by HDPE and POM gears with the maximum deviation of 10% and 11% respectively. It is found that rise in surface temperature is maximum for POM and minimum for HDPE at all torque levels.4 Nm and a rotational speed of 900 rpm and it is found that ABS gear fails due to excessive wear of gear teeth while HDPE gear fails due to root cracking of gear teeth.) to investigate their performance. machine cut gears) can be used to fabricate polymer gears and their performance can be compared with the gears made by current technique (i. Other form of gears such as helical or bevel gears can be fabricated to investigate the performance.
Efficiency and running temperature of a polymer–steel spur gear pair from slip/roll ratio fundamentals	2016 S.M. Evans a,b,n, P.S. Keogh a	a r t i c l e i n f o A new methodology to predict the transient operational temperature of a polymer–steel gear pair under Article history: Received 24 November 2015 loaded running is presented. For the involute gear form, rolling and sliding leads to a loss of gear effi- Received in revised form ciency and generation of heat in the contact zone. The power dissipated is used to set the conditions for a 29 January 2016 series of rod on disc experiments. The rod-on-disc data are processed in a time averaging procedure, Accepted 31 January 2016 which allows prediction of the complete gear temperature. This is assessed with analytical and finite Available online 6 February 2016 element models to validate the predicted temperature rise against the experimental data. The sig- Keywords: nificance is that the experimental procedures may be used to assess gear thermal performance without Gear efficiency testing full gear pairs. Polymer gear temperature & 2016 Elsevier Ltd. All rights reserved. Slip/roll ratio Temperature prediction 1.	error

Fig. 2.14 An example of auto automatically literature review results.

2.5.3 Limitations of the design

First, this model doesn't work on non-searchable pdf files because they are created with image format, but the current tools can not convert them into text. Second, the model

will only work on English publications. The ones with other languages will generate an error output. Third, on some occasions there are issues when attempting transfer pdf to text such as the failed example shown in Fig. 2.14. It is because the text extracting process starts from left to right, from up to down in each page and many of the publications have a two-column lay out. If the words on the right column are higher than the ones on left column such as Fig. 2.15, it may lead to disorder of text extraction then a failure in the summarising process. In short, the current tool does not work well when transferring a pdf file with multi-column format to text. This issue was optimised by adjusting the setting values as well as adding more conditions by the author, but it may still need more optimisation to completely overcome this issue.

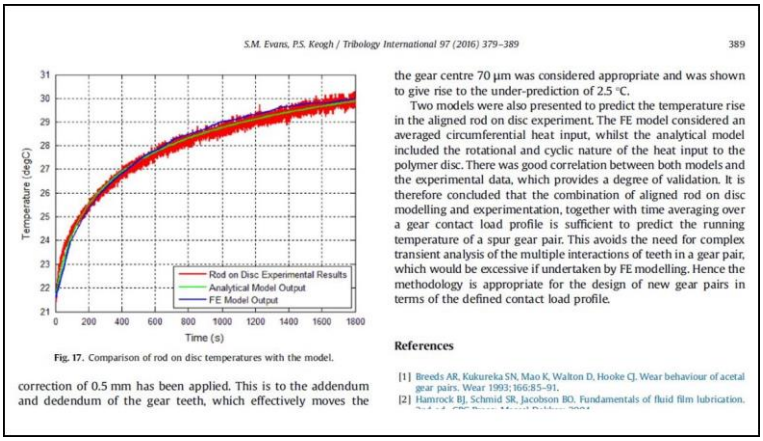

Fig. 2.15 Example of pdf file with failed auto-review process [81]

In the future, with the help of Natural Language Processing (NLP) in Artificial Intelligence (AI) [82], it is believed the automatic literature review process will be much more efficient.

3 Design and manufacturing of polymer gears

3.1 Introduction

As the first step, the design of the gear needed to be confirmed. This chapter describes the gear shape chosen and the details of two iterations of the IM mould design. A comparison between two moulds is made and the upgraded mould edition is chosen for further research. In order to enable the molten polymer to flow symmetrically, the required keyway as well as pin holes are not added into the mould directly. Thus, the manufactured gears need to be modified by a secondary machining process which is detailed here. Once this is all completed, the gears are ready to be tested.

3.2 Injection moulding process

Injection moulding can offer accurate geometry even for complex shaped products within a short cycle time [83]. The process can be summarised as below:

a) Melting and pre-heating the polymer materials in the injection moulding barrel.

b) Injecting a dosed quantity of this melted plastic into a closed and heated mould cavity through a sprue under a pre-set injection pressure.

c) Hold a relatively low pressure until the moulded part becomes solid to minimise shrinkage and add extra material to compensate for this.

d) Open the mould and eject the solid part from the mould.

e) Dose a new fixed weight of material in the injection cylinder

f) Start a new IM cycle.

An overview of the parts of an IM machine is shown in Figure 3.1:

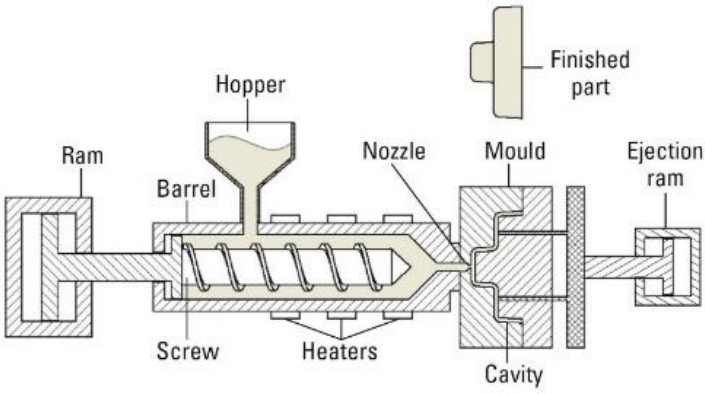

Fig. 3.1 Common IM machine Schematic [83]

The polymer is stored in the hopper as preparation and is fed onto the screw by gravity. The injection cylinder, which contains the screw, is heated by electric heaters, and heats the material to a pre-set temperature. A measured dose of material is injected into the tool cavity through the combination of heat and high pressure. A hydraulic ram is used to generate melt pressure. The screw not only helps melt the resin but also conveys material through to the screw tip. Hydraulic pressure moves the melt plastic through a nozzle then into the part cavity of the mould. Then the ram holds a lower pressure to fill more material in the cavity until the plastic in the runner becomes solid. After that, the pressure is released when part is hard enough and the mould opens, then the part is ejected.

3.2.1 Injection moulding parameters

During the whole IM process, there are numbers of parameters which can be set on the IM machine such as melting temperature, cavity temperature, holding time, holding pressure, cooling time, back pressure, screw speed and injection speed. Most of them are set through manufacture recommendations, trials and experience. Some of the main factors for consideration are listed as below:

- Melting temperature

This is the material specific temperature of the heater set to allow material to be conveyed and moulded. The heater will transfer the heat to the material in the injection barrel. The real temperature of material will be influenced by the heater, screw pressure and screw rotating speed [84]. If the melting temperature is set too high, the material will be burned. If it is too cold, the materials may not inject, or the moulded part may

have defects such as being brittle. Cold material will also place higher demands on injection and holding pressure.

- Mould temperature

The mould temperature is the temperature of the mould cavity inner surfaces which can be controlled by the mould internal cooling system. This is usually either a water or oil system [85] depending on the tool temperature required. It is a key parameter for IM because firstly, it will affect the surface quality, material viscosity, shrinkage, deformation and moulding cycle aspects. Secondly, maintaining the cavity temperature to a specific value will help keep the product as the same quality in each IM cycle. Otherwise, if there is no cavity temperature set, it will be highly affected by the injected material and the injection condition will be varied at each time. Increasing the cavity temperature will help improve the material viscosity and surface quality but the cooling time will be extended and the shrinkage will be higher. Decreasing the cavity temperature will save time for IM cycle and create less material shrinkage, but when the molten material meets the mould surface, it will cool down rapidly, which will cause potential problems such as flow lines, blisters and flanking of the surface.

Some studies show that the mould temperature influences the surface quality [86] as well as the inside residual stress [87] of the IM parts.

- Injection pressure

Injection pressure is the pressure that pushes the liquid plastic into the mould cavity. The value of the pressure should be high enough to force the material to fully fill the cavity. The setting is related to a flow-ability character named melt flow rate (viscosity). If the injection pressure is too low, a related parameter injection time will increase which may lead to higher frozen layer fraction and lower flow rate. While if it is much higher than needed, it may cause high residual stress. The higher the injection pressure needed, the higher clamping force the IM machine should have. Thus, materials with good flow characters are more widely used [88].

- Injection speed

The injection speed is the speed of the volume of molten polymers injected into the mould cavity. It will influence the surface appearance, if the injection speed is too high,

jetting may occur and the shear pressures on the material will be higher causing trapped air, diesel effects and burning, especially when passing through the thin gate. While if it moves too slowly, it may bring defects such cold slugs and short shots. It should be noted that the actual injection pressure cannot been set directly in the IM machine, it is indirectly changed by adjusting the injection speed.

- Holding pressure

When the injection process is finished (approximately 90% to 98% full of volume), the holding process will take over. Holding pressure is the pressure against the cooling plastic in the cavity image while that plastic solidifies. A high holding pressure will cause overfilling of moulds, flash and potential mould damage. While if the holding time is too low, it will produce sink marks, rough surface and high shrinkage [89]. As a thumb of rule, the holding pressure is usually set as 50% of the injection pressure, however it may go up to 80% sometimes [88].

- Holding time under holding pressure

Following the injection process, the holding process will help fill in the gap of the mould cavity as well as decrease diesel effects [90]. Once the gate closes or the part freezes the holding process can stop. If the holding time is too short, the part will have high shrinkage and the part will be poorly shaped. If it is too long, it will increase the cycle process time and may have flash as well [91].

- Back pressure

Back pressure is the pressure required to suck material into the screw occurring when the screw feeds backwards and sucks material from the hopper to the barrel. It can help homogenise the polymer as well as push out unwanted air. It is usually suggested to keep the back pressure as low as possible otherwise excess back pressure will cause too much shearing force in the polymer and it may also lead to thermal degradation [88]. While if it is too low, the screw may not move backwards successfully to the pre-set material dosage point.

- Cooling time

The cooling time is a duration in which the component is left in the closed cavity before mould opening and ejection. If the time is too short, the ejection pins will damage the

surface of part or warpage will occur because of the ejection force. And it is related to the defects such as high shrinkage. While if the cooling time is too long, it will not only increase the injection cycle but also make the part more likely to stick on the mould which will require extra ejection force. Figuring out a balance between efficiency and quality is the main purpose in this process [92]. As the most important parameter which influences the cycle time, much attention has been paid due to the demand of higher efficiency in industry.

There is a new method named rapid cooling which can largely decrease cooling time by changing the cavity temperature fast. Nevertheless the uniform cooling is recommended because it offers better quality with lower level of shrinkage, inner stress, warpage and easier ejection.

3.2.2 Injection moulding gate design

During the injection moulding process, the molten plastic flows from the nozzle to the cavity through a runner. A runner is a channel cut into the mould that allows plastic material to flow from the nozzle to the cavity. And the gate is the part which connects the IM part and runner. The gate performs an important connection function which allows molten polymer from the injection cylinder to enter and fill the mould cavity and should be designed to avoid shrinkage as much as possible. Thus, the design of gate largely influences the final moulded part. The design of gate mainly contains the location, number and the type of the gate. There are many kinds of gates, the most applied ones are as follows:

- Sprue Gate

The sprue gate (Fig. 3.2(a)) is widely used especially for parts with a base. It has the advantages of direct flow without losing pressure or increasing shearing when compared to restricted or side gates. It has disadvantages as well, for example, the gate area may gather high stress concentration and the gate needs to be removed manually after each IM cycle.

- Restricted Gate

As shown in Fig. 3.2(b), the restricted gate is narrow at the neck, it is widely used in multi-cavity tools because the gates usually break off when ejecting without moving

out manually if it is not too large. While if the gate is too small, high pressure as well as the frictional heating occurring at the gate may cause burning and splash marking on the parts. As a rule of thumb, the diameter of the gate should be between 0.6mm to 2mm. In order to protect the IM part, the back taper is designed with some distance (usually 1.5mm) away from the surface of the moulding to avoid any unexpected cracks.

- Side Gate

The side gate (Fig. 3.2(c)) is usually used in multi-impression moulds when the components are flat and relatively small. It offers parallel molecular orientation in the cross section thus has uniform shrinkage in flow direction. The size of the gate is recommended as 75% of the component thickness and the width is the same as the runner.

- Fan Gate

Fan gate (Fig. 3.2(d)) becomes wider from the runner side to the part connection. This design has the advantages of reducing stress concentration at the gate. It fits for relative thick parts with minimal warpage and good accuracy because the gate chills off slowly and can transfer pressure even in cooling process.

- Diaphragm Gate

For the best uniform radial mould filling, the diaphragm gate (Fig. 3.2(e)) is usually considered. This design not only offers symmetrical flow but also reduces weld lines. For fibre reinforced parts, it helps orientate the fibres symmetrically and make the shrinkage even across the part. This gate has to be removed manually after each IM cycle.

- Spider Gate

In order to save material from diaphragm gate, the spider gate (Fig. 3.2(f)) is designed especially for large diameter apertures. It should be noted that as a disadvantage, this design creates several weld lines at the meeting of different flows. This influence on both appearance and mechanical property should be considered.

- Hot Tip Gate

The hot tip gate is one of the most commonly used gating methods. It keeps the plastic inside the runner as well as the gate cavity molten, which means the runner as well as the gate will not be part of the injected moulded parts. Thus, it reduces the waste in each IM cycle. It should be noted the hot tip gate leaves a small mark on the moulded part surface which influences the part appearance.

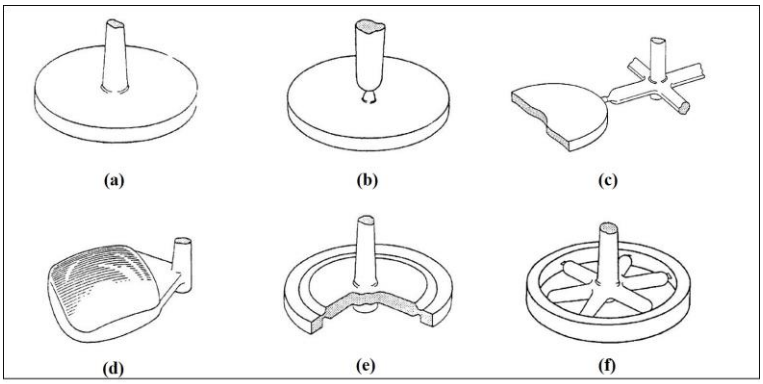

Fig. 3.2 IM gate designs [93]. (a) Sprue gate. (b) Restricted gate. (c) Side gate. (d) Fan gate. (e) Diaphragm gate. (f) Spider gate.

3.3 Preliminary gear and the mould design

A gear design for IM includes two parts which are gear design itself and the IM mould design. For the gear shape, a commonly used design has been applied. With the help of Moldflow software, the details of mould design were simulated then confirmed such as the sprue location, runner size and gate style (Fig. 3.3).

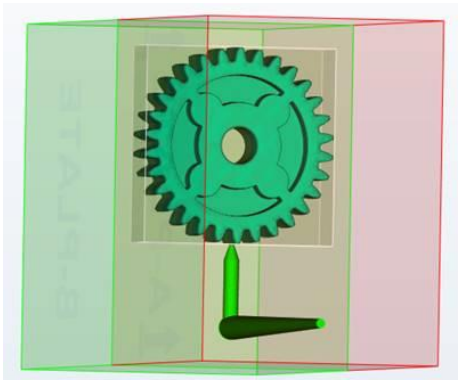

Fig. 3.3 Mould design using Moldflow

3.3.1 Mould design

The IM machine offers a steel tool bolster set with a changeable mould insert cavity (Fig. 3.4(a)). Thus, a focus on the design of inserts which are compatible with the cavity size was necessary. Aluminium inserts were designed as shown in Fig. 3.4(a) and the full details are in Appendix B. The side gate was used in this design. The molten polymer flows from the sprue inlet hole, runner and gate then spreads from the bottom to fill the whole gear cavity while trapped air inside exits from both vent and parting line area. Once the gate becomes solid, the holding pressure is released and leaves the part cooling until ready to eject. As a two-plate mould design, the right-hand side (RHS) plate on the injection side is fixed during the IM and the left-hand side (LHS) insert is attached on the movable side of the mould cavity.

After the cooling time step, the mould opens automatically, then the gear is ejected manually with tools (Fig. 3.4(b)).

There are some limitations on this manufactured gear part which should be highlighted. First, the design of the contour on the gear face (Appendix B) makes the gear quite difficult to eject manually, it needs to be removed (Fig. 3.4(c)). Following further cooling and shrinkage of the gear, the part line is like Fig. 3.4(d). As the gear teeth are the contact area for gear meshing, it is believed to influence the accuracy as well as the performance of the gear. Unfortunately, these disadvantages cannot be eliminated by simply modifying the current mould insert.

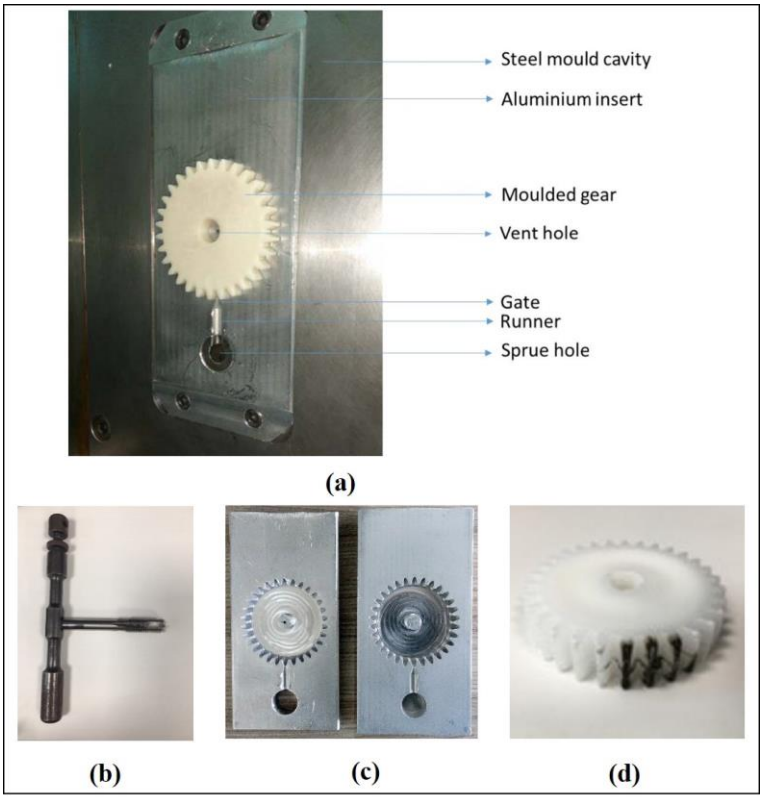

Fig. 3.4 (a) Preliminary mould design (b) Screwdriver tool for gear ejection (c) Preliminary mould cavity design (d) A manufactured gear sample with preliminary mould design

3.3.2 Gear shape design

The gear specification is shown in Fig. 3.5. A number of studies have been carried out with this specification and it has therefore been proven reliable [49, 67, 69, 73, 94]. Thus, it will be easy to make comparison of the results from this study with others. Fig. 3.5 shows the gear geometry design. Four pin holes are cut to insert pins to allow the gears to be fixed in the gear testing equipment. This is for relatively soft polymer such as pure acetal as the keyway hole will be easy to break when holding the whole load during testing. If the gears are relatively rigid such as fibre reinforced polymers, the keyway is strong enough to bear the whole load itself, the pin holes are not needed practically.

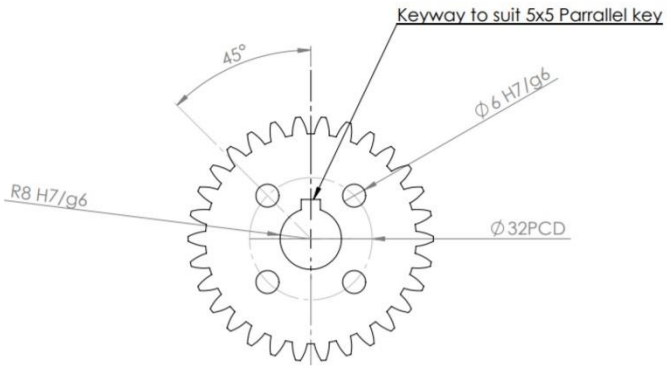

Parameters	Gear Category	Module (mm)	Tooth Number	Pressure Angle (°)	Face Width (mm)	Tooth Thickness (mm)	Contact Ratio	Profile Standard
Value	Spur Gear	2	30	20	15	3.14	1.67	DIN 3960

Fig. 3.5 Gear geometry and specifications.

3.4 Final edition of gear and mould design

As the first gear iteration had some disadvantages which influence the gear performance, an upgraded design was applied to make better quality gears.

3.4.1 Gear shape design

The gear specification as well as the geometry are the same as Fig. 3.5 respectively. As a design update without heavy influence on the gear testing results, a rim has been designed on the gear body (Fig. 3.6) to decrease the body shrinkage as well as the cooling time in IM process. And the fillets are created for better appearance and to make the gear easier to eject. If the IM part adheres tightly to the mould, high force will be necessary when ejecting, potentially damaging the gear. This should be avoided. Thus, in order to make the part easy to eject, with the help of the toolmaker, draft angles were added on the gear. It should be noted that the shaft hole was designed as 15mm while the target is 16mm because a design margin was needed to take account of shrinkage. Details of gear and mould design are shown in Appendix C.

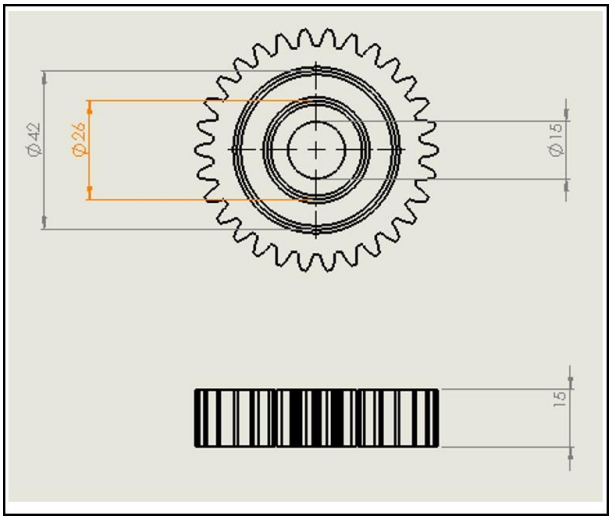

Fig. 3.6 Upgraded gear design with a rim.

3.4.2 Mould design

A centre diaphragm gate is utilised to make the melted plastic flow uniformly in each direction, the section diagram is presented as Fig. 3.7(a). It helps eliminate the influence of differences of molten plastic flow in each orientation on the gear wear performance, especially for a polymer with additives such as fibres. Moreover, the keyway as well as the four-pin holes used for gear installation are not created on the mould directly so as not to create any melted plastic turbulence and weld lines during the injection moulding process. In summary, this design keeps the flow direction as well as the shrinkage uniform in each direction to make the gear accurate in geometry and easy to study without unwanted noise from the IM process. As shown in Fig. 3.7, RHS (Fig. 3.7(b)) is the fixed side and the melted polymer flows from the runner in the centre then spreads into the whole cavity through the diaphragm gate. As the gate was designed as a diaphragm gate instead of a sprue, it needs more time than a sprue gate for the gate to solidify. The LHS (Fig. 3.7(c)) insert contains the whole cavity of the gear part, and is the side the component can be found when the mould opens at the end of each IM cycle. It is ejected automatically by 6 ejection pins. What is more, this design eliminates any embossment produced by the gap of parting line as the previous design and the vent is designed on each side of the gear body face. The full details of mould design are attached in appendix C.

This design overcame all the defects from the previous mould design with better design quality. What is more, the ejection pins allowed automatic gear manufacture once the

IM parameters were confirmed, increasing working efficiency. Therefore, this edition was chosen as the primary IM tool and it was used in the following research.

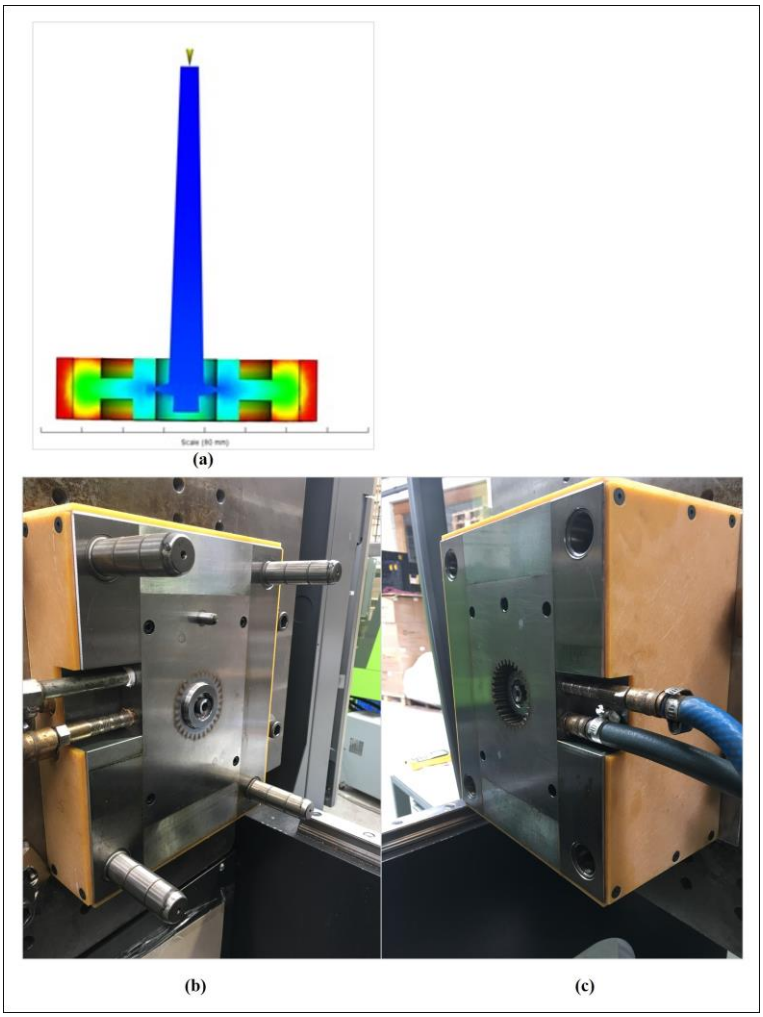

Fig. 3.7 (a) Gear cross section from Moldflow. (b) and (c) Gear moulding tool.

3.5 Gear modification

The gears were manufactured using the mould design showed in section 3.4 and the gear specifications were shown in Fig. 3.5. As the gear injection moulding process were different regarding the materials applied as well as the specific aim of study, it will be explained in more details in each study independently later.

When gears were manufactured from the IM machine, they looked like Fig. 3.8(a). The sprue part as well as gate were connected with the gear and there were no pin holes or keyway. In order to make them available to be tested on the test rig some machining and cutting steps were undertaken.

3.5.1 Removing of sprue and gate parts

The sprue and gate need to be removed first. As the gate is thin, when it was pushed by a press (Fig. 3.8(b)) along with a pin whose diameter was smaller than that of gear shaft hole, it was removed from the gear part easily.

3.5.2 Shaft hole expansion

It was mentioned in the previous section that the diameter of the final shaft hole should be 16mm while it was designed as 15mm. Because different polymers or different IM processes may create very different values of shrinkage, enough allowance should be left in order to avoid making the shaft hole larger than required as it might lead to installation issues. Therefore, the shaft hole was smaller than 16mm hole and expansion was required. A cutting machine tool (Fig. 3.8(c)) was used to expand the shaft hole. It should be noted that the machine needs to be calibrated including centroid and height before cutting. Each gear was cut twice to achieve the target and accuracy.

3.5.3 Cutting the keyway and pin hole

Firstly, a keyway was cut to fit the test rig. The press as well as a keyway broach set are applied to cut a 5mm x 5 mm keyway. For some gears, such as glass fibre reinforced acetal, they are hard enough to bear the load with only one keyway, thus they are ready to be tested on the test rig. For soft materials like pure acetal gears, deformation may occur holding the whole load with only one keyway and deformation around the contact area of keyway occurs. In this situation, pin holes are required to share the load.

With an automatic cutting machine, it was difficult to position the pin holes and to keep the relative distance with the keyway accurately, therefore a special clamp (Fig. 3.8(d)) was designed and manufactured to help cut pin holes. The clamp can hold two gears at a time. Firstly, the drill was calibrated to fit with the directive holes when the drilling power was off. Then the electric drill is used to cut the holes by going along the directive holes on the clamp.

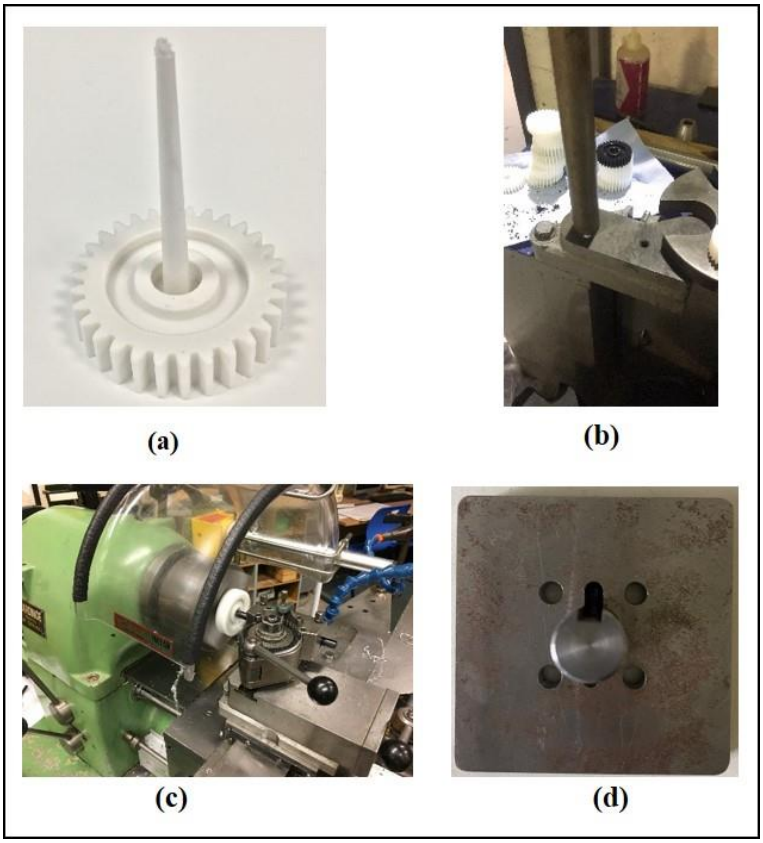

Fig. 3.8 (a) manufactured gear sample. (b) press for gear modification. (c) cutting machine tool for gear modification. (d) clamp for gear modification.

After modifying the gears, they were ready to be installed on the test rig for testing.

4 Injection Moulding Process Impact Analysis

4.1 Introduction

Injection moulding (IM) is one of the most commonly used methods and about one third of plastic products are produced using this technique in industry [95]. It has the ability of offering accurate geometry in short cycle times even when producing complex shaped products [96]. The quality of the IM product is very important because once the moulding tool has been designed it usually remains unchanged over thousands of part manufacture. Unfortunately, unlike metal manufacturing, plastic IM consists of setting many separate processing parameters for each component. The optimisation of parameter settings is usually carried out in production by experienced engineers using the trial-and-error method [97]. Taguchi is a method which can be readily applied to this process. A large quantity of research has been carried out on the influence of mould geometry in the IM process [98-102], while fewer researchers have focused on the influence on other characteristics such as strength [103, 104] and weight [105] validation. Polymer gears are core mechanical components under complex working conditions [66, 71, 106]. Hence the research on working gears is largely different from basic character studies on plastic bars [107, 108] and discs [109-111]. On the other hand, a number of researchers on polymer gears are studying the performance of the gear itself [12, 112-115], overlooking the effect of manufacturing techniques on the product leading to unreliable results due to the outcome of this study. The service life of polymer gear is difficult to predict because it is influenced by many factors such as temperature, wear and pressure. Moreover, they, along with the characteristics of polymer types, all influence each other during the process. As well as research in mechanism of material and wear, it also requires an attempt to focus on real applications in respect to data analysis.

4.2 Methodology

The process flow of this study is shown in Fig. 4.1. First, the IM parameter settings were designed from the starting point of the manufacturers recommended settings and the Taguchi method was applied to produce a factorial design for IM polymer gears. Selected gears were then tested to reveal the service life. Finally, the results were

analysed using Taguchi, analysis of variance (ANOVA) and artificial neural network (ANN).

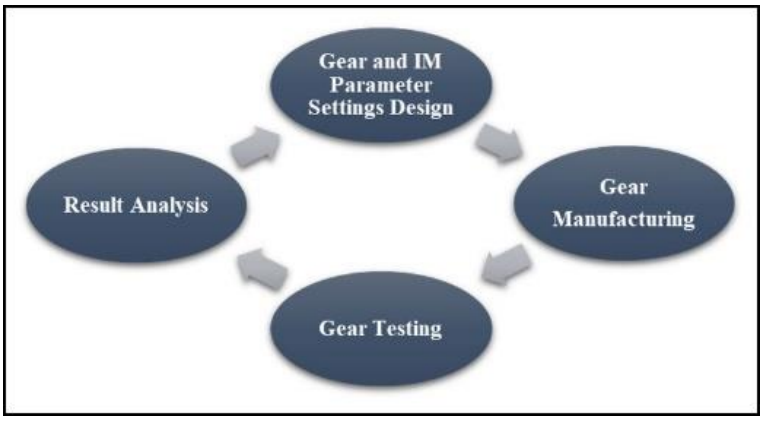

Fig. 4.1 Flow chart of work process

4.2.1 Taguchi Method

Taguchi method [116-118] is a commonly used statistical method to improve the quality of manufactured products and reduce the trial-and-error attempts. It is being widely applied in marketing[119], biotechnology [120, 121] and engineering [122, 123], in which parameter design is one of the most trusted applications of the method [124]. To simplify the setting combinations, the four variable factors with three-level L_9 orthogonal array (OA) were selected for this study as shown in Table 4.1. This design is relevant to the choosing of the IM parameters which are explained in chapter 4.3.1.

Table 4.1 Layout of the L_9 orthogonal array (OA)

Deney No.	A	B	C	D
1	1	1	1	1
2	1	2	2	2
3	1	3	3	3
4	2	1	2	3
5	2	2	3	1
6	2	3	1	2
7	3	1	3	2
8	3	2	1	3
9	3	3	2	1

4.2.2 Injection Moulding (IM) Process

The plastic IM process for acetal (POM) can be very simply summarised: a polymer material is plasticised and heated (melting temperature) until it is molten and can flow under pressure. The molten material is rapidly injected (injection speed) into a heated

mould cavity (cavity temperature). A holding pressure is applied to counteract the effects of material shrinkage. Finally, the pressure will be released; and the moulding is allowed to cool and solidify before it is injected.

4.2.3 Artificial Neural Network (ANN)

ANN is a method usually applied in machine learning in which a model learns to perform classification jobs from the data directly. The more layers it has, the deeper the network is. This method has been applied in the IM industry by some researchers [105, 125-127]. It is widely used in industry but most of the research is focusing on big data projects [102, 128, 129].

4.2.3.1 Backpropagation (BP) Neural Network

The BP neural network is one of the most used training methods for the feedforward ANN [130]. The neural network contains multiple layers in three types: input, hidden and output layers. As shown in Fig. 4.2, each neuron is connected to all neurons of adjacent layers; but within the same layer, neurons are mutually not connected to each other. Each solid arrow from a neuron A to B has a weight value, which represents a level of importance of neuron A to B [131]. For a BP neural network with M input neurons, one hidden layer consisting of N hidden neurons, and P output neurons, in the direction of arrows, i.e. how signal is transferred, the following information is obtained. The input at the j-th hidden neuron is given as the weighted sum of signal from all connected input neurons:

$$u_j^{\text{in}} = \sum_{i=1}^{M} a_{ij} x_i \,, \qquad j = 1, 2, \dots, N \tag{4.1}$$

where a_{ij} is the weight from the i-th input neuron X_i to the j-th hidden neuron Y_j, and x_i is the output value from X_i towards all hidden neurons.

Then inside hidden neurons, an optimisation function is applied to shrink all input values to an output of range $(0, 1)$. Therefore, the output value from the j-th hidden neuron Y_j is

$$u_j^{\text{out}} = f\left(u_j^{\text{in}} + \text{bias}\right), \qquad j = 1, 2, \dots, N \tag{4.2}$$

where the optimisation function f is a sigmoid function of S-shaped curve, as

$$f(x) = \frac{1}{1 + e^{-x}} \,. \tag{4.3}$$

There are many kinds of optimisation functions. The sigmoid function was proved to be a precise method [111], and hence is chosen as the optimisation function in this study. However, due to the range of the inputs u_j^{in} causing deviation from the centre of the original sigmoid function domain, a bias adjusted according to the inputs could be introduced to make sure the sigmoid function provides more evenly spread outputs.

For output layer, an input signal is received at the k-th output neuron Z_k, as

$$v_k^{\text{in}} = \sum_{j=1}^{N} b_{jk} u_j^{\text{out}} \tag{4.4}$$

where b_{jk} is the weight from the j-th hidden neuron Y_j to the k-th output neuron Z_k.

Finally, with the help of another activation function g, typically a linear function, the output at Z_k would then be

$$v_k^{\text{out}} = g\left(v_k^{\text{in}}\right). \tag{4.5}$$

BP neural network has the powerful ability to generate nonlinear functions ([132],[133]) with different learning methods ([134-137]). After data are transferred from the input through hidden layers to the output, the algorithm of backpropagation starts the training of weight by returning from the output to the input and adjusting weights layer by layer, along the path of reducing the error. After the weights from the input layer to the first hidden layer are adjusted, one iteration of backpropagation is completed. The new set of weights will be used for another iteration of signal going forward and then backpropagation. Simulation of a large enough number of loops optimises all weights between neurons and stabilises the model.

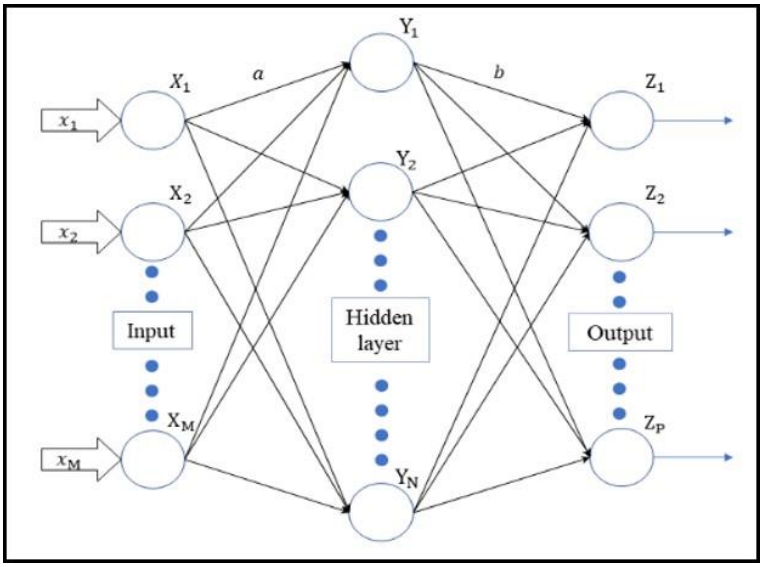

Fig. 4.2 Backpropagation (BP) neural network structure

4.2.3.2 Garson's Method for Relative Importance

Relative importance is a key concept to express the relationship between two quantities such that how much one could affect another. In neural network it is useful to see how much the change of one input parameter could affect the output. Garson introduced a method of partition connection weights to determine the relative importance of various inputs[138].

First, a neural network of M input neurons $X_1, \ldots, X_M$ and N hidden neurons $Y_1, \ldots, Y_N$ is set up. For each hidden neuron Y_j, we have a sum of connection weights from all input neurons to this hidden neuron, as $\sum_{i=1}^{M} |W_{ij}|$, where W_{ij} is the weight from the i-th input neuron to the j-th hidden neuron.

Then a data set of $M \times N$ elements can be constructed, containing the ratio between the weight of an individual input-hidden connection, and the sum of all weights connected to that hidden neuron Y_j, i.e. the importance of an input weight among all inputs connected to Y_j. One such element is represented as

$$Q_{ij} = |W_{ij}| \Big/ \left| \sum_{i=1}^{M} W_{ij} \right| , \qquad j = 1, 2, \ldots, N. \tag{4.6}$$

By applying summation across all hidden neurons, Q_{ij} will be used to find the relative importance of each input towards all outputs. Note that in the equation there is no

output-related term involved since connection towards all hidden neurons are covered. The relative importance of the i-th input neuron is shown as

$$R_i = \sum_{j=1}^{N} Q_{ij} \Big/ \left(\sum_{j=1}^{N} \sum_{i=1}^{M} Q_{ij} \right) \times 100 \,. \qquad (4.7)$$

4.3 Experiments

4.3.1 Influence Factor and Level Setting for the IM Process

The experiment of IM process was based on various parameter settings. Past researchers studied the influence of process parameter settings on the characteristics of products [99, 100, 111]. General parameters were melting and cavity temperature, injection speed, holding pressure and cooling time [139]. Thus, in this study, the design of experiment (DOE) included melting temperature (MT), cavity temperature (CT), injection speed (IS) and holding pressure (HP). The cooling time was set to a sufficient value to eliminate the influence of itself. The levels of the MT and CT were referred to the material data sheet [140] in order to make sure that the manufacturing process fulfilled the quality requirement. The IS values were optimised with the support of Moldflow software as well as material data sheet. As the HP is related to the injection pressure which is also influenced by the IS, the value of HP was defined as 25%, 50% and 75% of the highest injection pressure, noted as low, medium and high relatively. As studied in chapter 2.3, the fibre reinforced polymer gears have relatively better performance than unreinforced ones, thus the polymer used in this study was a commercial Acetal (POM), grade Hostaform C 9021 GV 1/20, with example materials properties illustrated in Table 4.2. Following manufacturers recommended settings as the basis of the DOE, the chosen IM parameter settings were summarised in Table 4.3.

Table 4.2 Injection moulding (IM) material data

Density (kg/m^3)	1550
Tensile strength (MPa)	120
Flexural modules (MPa)	6900
Melting point (°C)	166
Fibre content (wt %)	20

Table 4.3 IM parameter setting

MT (°C)	CT (°C)	IS (mm/s)	HP
190	80	20	Low
200	100	45	Medium
210	120	70	High

4.3.2 Polymer Gear Geometry Design and Manufacturing

The ENGEL Victory 80 IM machine was used for manufacturing. The details of gear and injection mould design are shown in chapter 3.4. In order to make the IM environment refreshed for new settings, three times of fully purging was taken each time after renewal of the setting. Then 10 gears were made at each set of moulding process.

4.3.3 Gear Wear Test

A gear transition test rig (Fig. 4.3), designed and manufactured in the University of Warwick, UK, can continuously measure the wear of gears under specific added loads. A contact sensor was designed to monitor and record the displacement change of gear wear in the PC with a data-logging software. The layout of the design is shown in Fig. 4.4. The motor provides the power for the gear box then the gear box transmits the load to test polymer gears through the shafts. The test gears are held on the pivot block on which the load can be applied by imposing a 'constant weight' torque. This pivot component and loading method offer a large amount of tooth wear without significantly affecting the applied load. What is more, the pivot block concept provides the ability of monitoring the progressive wear while maintaining thermal conditions similar to those in normal operation. The reason is that the gear wear can be measured indirectly using the degree of the pivot block rotation. The contact between the gear teeth defines the equilibrium position of the block. When the teeth are worn, the pivot block slightly rotated from the one set initially by new teeth. Thus, this rotation indirectly provides a continuous indication of wear during the whole test. In practice, it is measured by the linear movement of a defined point which is on a rigidly tangent arm attached on the block with that displacement sensor. More details about the test rig using as well as the accurate wear measurement methods were published elsewhere [50, 69, 94, 112]. In this study, all the tests were run at the speed of 1000 rpm and with the torque of 7.5 N m. As the machine allows testing under deliberate misalignment, in this study, the misalignment parameter was set to nominally zero. And that tested gears operated at a centre distance of 60 mm.

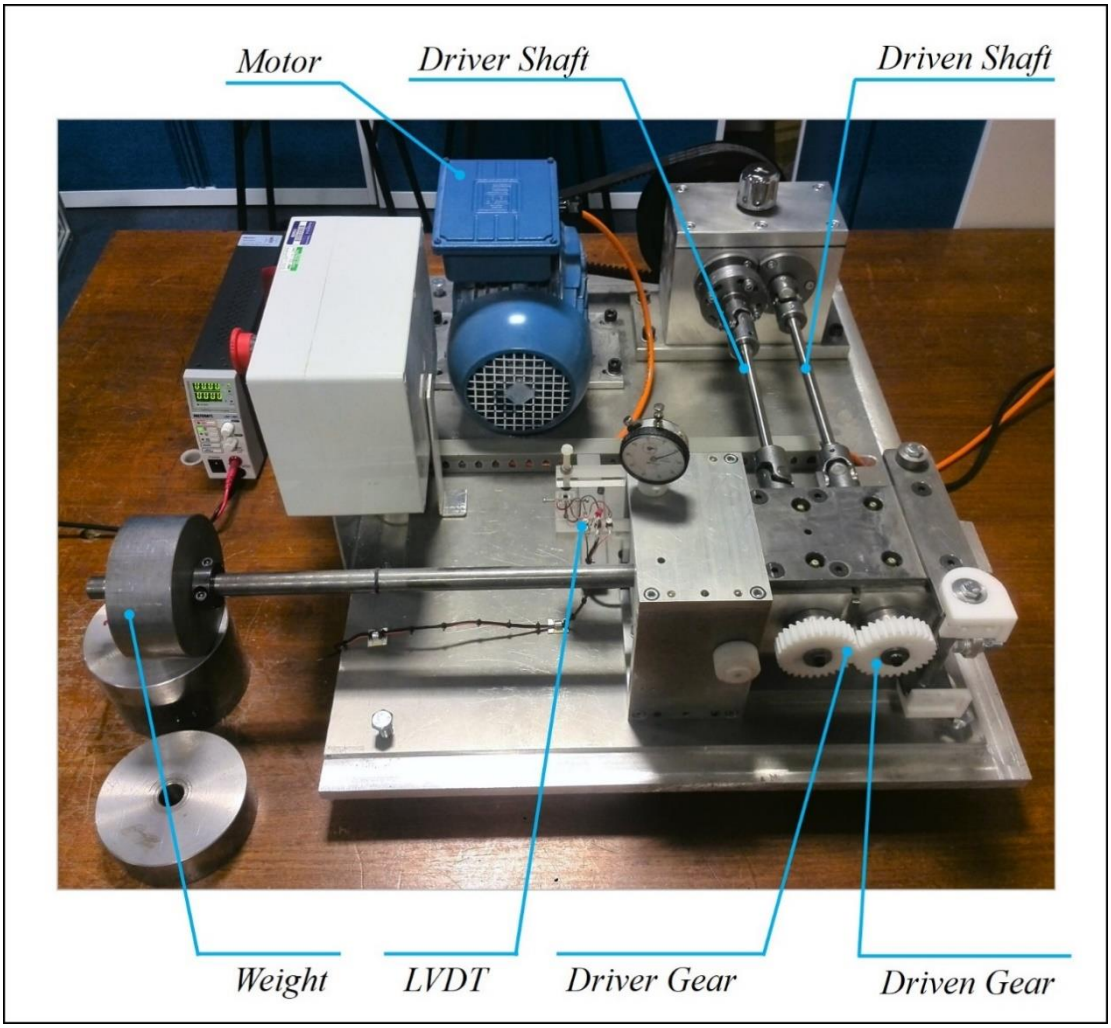

Fig. 4.3 Polymer gear test rig

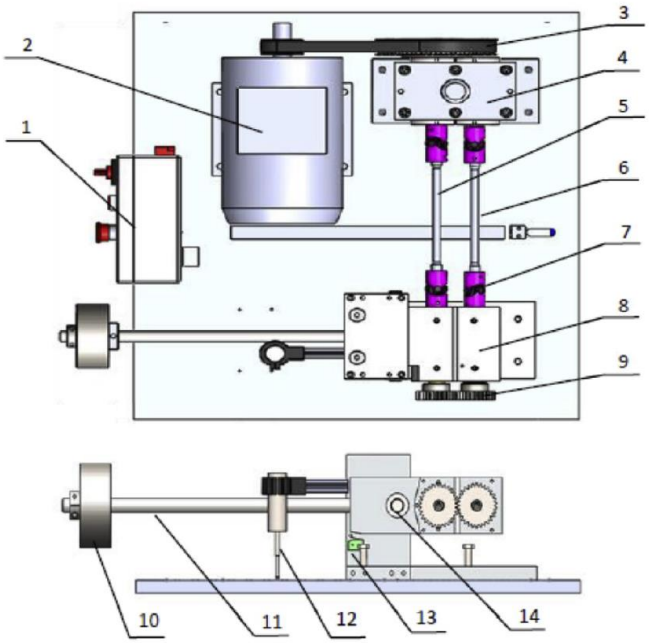

1. Power control
2. Motor
3. Pulley
4. Gearbox
5. Driving shaft
6. Driven shaft
7. Four universal couplings
8. Pivot block assembly
9. Test gears
10. Weight
11. Loading bar
12. Transducer
13. Micro switch
14. Pivot

Fig. 4.4 Mechanical schematics and layout for the test rig design[50]

4.3.4 Data Analysis Procedure

Following completion of the experimental array (Table 4.4), the result revealed the influence of parameter settings on gear wear performance. The commercial software Minitab 18 was used for data analysis. After applying Taguchi method to design the experiment, the response variation was studied by displaying the signal-to-noise (S/N) ratio in the response table, using larger-is-better (Z_L) option, involving the equation

$$Z_L = -10 \log \frac{1}{n} \sum_{i=1}^{n} \frac{1}{Y_i^2} \tag{4.8}$$

where n is the number of samples, and Y_i is the performance of each sample.

Then the widely used ANOVA [141] was applied to predict the service life of gears and calculate the factor contribution. It was noted that multivariate analysis of variance was unavailable due to the shortage of samples of this study. Within ANN there was no need to define a regression method or which pattern data samples should fit in. Since ANN was usually regarded as a black-box simulation, it was considered worth consideration of whether a project with a small sample size works. If it does, IM engineers would have one more tool in hand on the experiment design. In this project, the original data of nine training samples were tried with the BP method, the code was finished by the author with MATLAB. The BP neural network consisted of 9 input neurons, each of which contained a 4-dimensional vector, whose data came from 4-factor IM samples describe above, i.e. a 4×9 matrix. The output layer contained 9 neurons, each of which had a single value of breaking point, i.e. a 1×9 matrix. For hidden layer, there was just one containing 5 neurons. This number of neurons were chosen after several simulation trials since it provided the best simulation result with minimal residual error. The whole procedure using BP neural network comes with a pre-setup black-box simulation package of MATLAB. With its theories explained in Section 4.2.3.1, the user simply configures the input and output sets and the neural network will start its own training.

The gradient descent method was chosen in this study since it was a frequently used method to approach the local minimum of a function [142-144]. For a real function $f(x)$, if it is defined and differentiable at point x_0, the gradient descent method involves

iteration along the direction of $-f'(x_0)$ at which the function decreases fastest. Therefore, the equation of iteration is

$$x_{i+1} = x_i - hf'(x_i) \tag{4.9}$$

where h is the step size and x_i is the value after the i-th iteration using the method.

The general rule of weight adjustment is defined as

$$\Delta w = h \cdot \delta \cdot v^{\text{out}} \tag{4.10}$$

with Δw as the weight adjustment, h as the step size (also known as the learning rate in neural network analysis), δ as the local gradient and v^{out} as the output signal from the previous layer.

For simplicity with small amount of data only one hidden layer was considered. The adjustment of weight between hidden and output layers at the n-th iteration is given as

$$\Delta b_{jk}(n) = h\delta_k^P u_j^{\text{out}}(n) \tag{4.11}$$

where h is the learning rate; δ_k^P is the local gradient at the k-th output neuron (out of a total number of P output neurons); $u_j^{\text{out}}(n)$ is the output value from the j-th hidden neuron at the n-th iteration.

The total error of the network at the n-th iteration is

$$e(n) = \frac{1}{2}\sum_{k=1}^{P} e_k^2(n) \tag{4.12}$$

where $e_k(n)$ is the error at the k-th output neuron at the n-th iteration.

Due to the gradient descent method

$$\delta_k^P = -\frac{\partial e(n)}{\partial v_k^{\text{in}}(n)} = e_k(n)g'\left(u_j^{\text{out}}(n)\right) \tag{4.13}$$

where $g' = 1$, since the transfer function g at the output layer is usually a linear function. Usually in the output layer, the output of a neuron without threshold is expected, therefore a linear function, such as the identity function, would be a typical choice.

The adjustment of weight can be simplified to

$$\Delta b_{jk}(n) = he_k(n)u_j^{\text{out}}(n)\,. \tag{4.14}$$

As the adjustment is going back towards the input layer, in a similar manner the input-hidden layer weight adjustment at the n-th iteration can be represented as

$$\Delta a_{ij}(n) = h\delta_j^N x_i(n) \tag{4.15}$$

where x_i is the output value of the i-th input neuron.

Here

$$\delta_j^N = -\frac{\partial e(n)}{\partial u_j^{\text{in}}(n)} = -\frac{\partial e(n)}{\partial u_j^{\text{out}}(n)} f'\left(u_j^{\text{in}}(n)\right) = f'\left(u_j^{\text{in}}(n)\right)\sum_{k=1}^{P}\delta_k^P b_{jk} \tag{4.16}$$

is the local gradient at the j-th hidden neuron (out of a total number of N hidden neurons). It originally contains the partial derivative $\frac{\partial e(n)}{\partial u_j^{\text{in}}(n)}$ which cannot be calculated directly due to the invisible hidden layer. Alternatively, it can be written in the form of the weighted sum of the local gradients of the forward layer. Therefore, the weight optimisation process in a BP neural network always starts from later to earlier layers.

Table 4.4 Parameter setting applied of the L_9 OA

Deney No.	MT (°C)	CT (°C)	IS (mm/s)	HP
1	190	80	20	Low
2	190	100	45	Medium
3	190	120	70	High
4	200	80	45	High
5	200	100	70	Low
6	200	120	20	Medium
7	210	80	70	Medium
8	210	100	20	High
9	210	120	45	Low

4.4 Result and Analysis

4.4.1 Gear Wear Testing Results

All the gears with different IM parameter settings were tested on the wear rig. For the purpose of uniform comparison, the gear breaking point was defined as the instant at

which any gear tooth ran into a total fracture (Fig. 4.5(a)). It shows like Fig. 4.5(b) which revealed the sensor reading on wear of gear teeth. The data were collected into our own data-logging system then figured using Origin 2018b. The breaking point data were collected in Table 4.5, which included samples of L_9 tables and three extra samples for result validation.

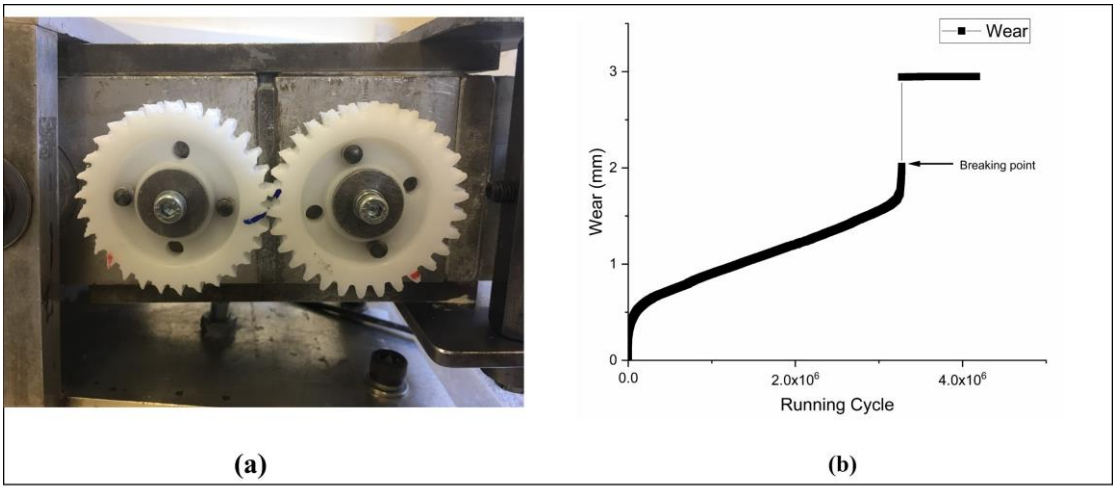

Fig. 4.5 Wear testing of gears on Test Rig: (a) Broken gear pair; (b) Wear testing result

Table 4.5 Service life results for gear meshing

MT (°C)	CT (°C)	IS (mm/s)	HP	Breaking point (10^6 running cycles)
190	80	20	Low	3.51
190	100	45	Medium	3.37
190	120	70	High	3.17
200	80	45	High	3.91
200	100	70	Low	3.97
200	120	20	Medium	3.73
210	80	70	Medium	2.75
210	100	20	High	3.27
210	120	45	Low	3.44
190	120	45	Medium	3.06
200	100	45	Medium	3.97
210	120	45	Medium	3.35

4.4.2 Data Analysis

The Taguchi method analysed the effect of parameter settings on the service life. The main effect for signal-to-noise (SN) ratios is shown in Fig. 4.6, in which "the larger the better" quality characteristic was chosen and the best combination set could be optimised by selecting the highest value for each of the factor, namely 200 ℃ of MT, 100 ℃ of CT, 45 mm/s of IS and low of HP.

ANOVA tested the significance of factors by calculating the mean square against an estimated error in designed confidence levels. The result of ANOVA analysis is shown in Table 4.6, where DF is the degree of freedom, Adj SS is the adjusted sum of squares, Adj MS is the adjusted mean squares. DF is calculated as:

Total DF = number of samples – 1,

Main effect DF = number of factor levels – 1,

Residual error DF = Total DF – sum of DF for all terms included in the model.

It was noted that there are zero degrees of freedom for residual error, since this Taguchi design was a saturated model.

In order to make the error calculable to get a full picture of the model, the number of samples needed to be increased. In this situation, the method of replicating the design was applied, namely adding one more sample by predicting a sample result using general linear model. The regression function ANOVA simulated was

$$\begin{aligned} 3.458 - 0.1078\mathrm{MT}_{190} + 0.4122\mathrm{MT}_{200} - 0.3044\mathrm{MT}_{210} - 0.06778\mathrm{CT}_{80} \\ + 0.07889\mathrm{CT}_{100} - 0.0111\mathrm{CT}_{120} + 0.04556\mathrm{IS}_{20} + 0.1156\mathrm{IS}_{45} \\ -0.1611\mathrm{IS}_{70} + 0.1822\mathrm{HP}_{0.25} - 0.1744\mathrm{HP}_{0.5} - 0.00777\mathrm{HP}_{0.75}\,. \end{aligned} \qquad (4.17)$$

For each factor, the chosen level would be active as value 1 and otherwise inactive as value 0. The set of 4 randomly chosen levels and the predicted sample result are in Table 4.7. After adding this result in, the model was regenerated, with results shown in Table 4.8. Individual factor contribution could be calculated using the equation for contribution shown below, the Factor SS is the adj SS values of each source and the Total SS is the sum of all the adj SS values in Table 4.8. Those results are added in Table 4.8 as well. The factors influence ranking on the gear service life from high to

low was MT, HP, IS and CT. The MT influenced the service life mostly at about 3/4 contribution, while the CT affected very little at about 3%.

$$\text{contribution} = \frac{\text{Factor SS}}{\text{Total SS}} . \qquad (4.18)$$

Finally, three more random experiment results were applied to verify the linear model (Table 4.9).

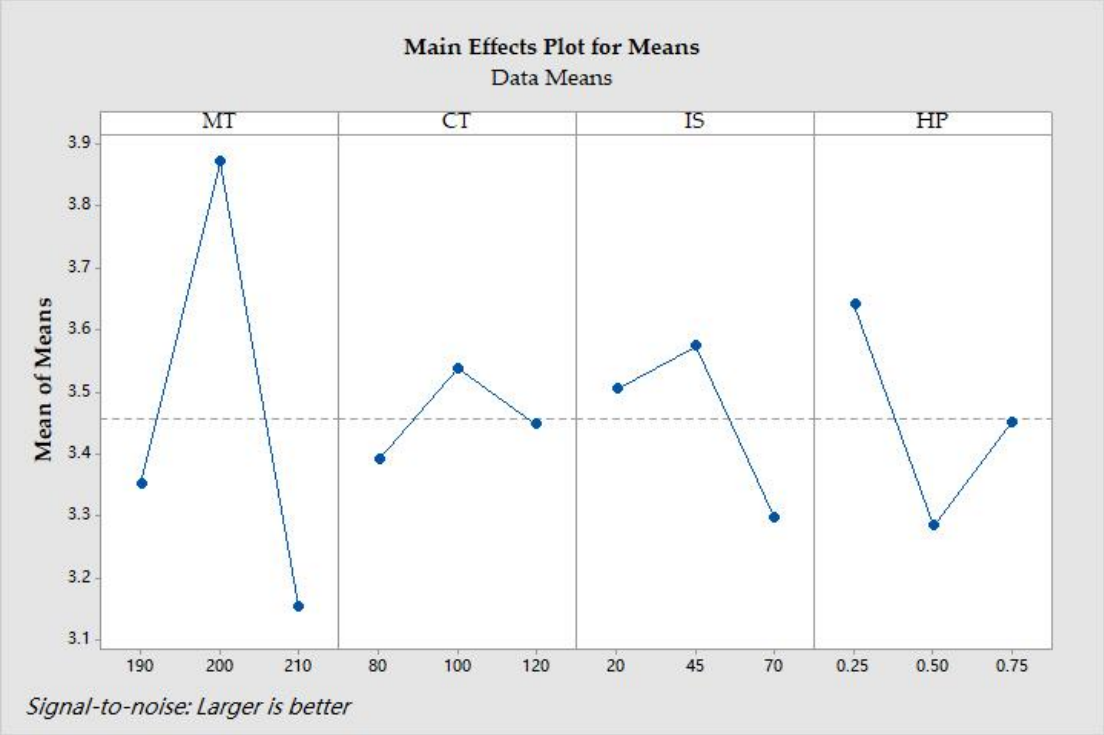

Fig. 4.6 Effect of process parameters on service life

Table 4.6 Analysis of variance for running cycles

Source	DF	Adj SS	Adj MS	P-value	F-value
MT	2	0.82269	0.41134	*	*
CT	2	0.03282	0.01641	*	*
IS	2	0.12416	0.06208	*	*
HP	2	0.19109	0.09554	*	*
Error	0	*	*		
Total	8	1.17076			

Table 4.7 Add-in data of simulation result

MT (°C)	CT (°C)	IS (mm/s)	HP (bar)	Estimated broken Point (x10^6 cycles)
200	80	70	low	3.82

Table 4.8 Recalculation of Analysis of variance for running cycles

Source	DF	Adj SS	Adj MS	F-value	P-value	Factor Contribution
MT	2	0.91673	0.458364	82505.50	0.002	71.13%
CT	2	0.03566	0.017831	3209.50	0.012	2.77%
IS	2	0.13936	0.069681	12542.50	0.006	10.81%
HP	2	0.20908	0.104542	18817.56	0.005	16.22%
Error	1	0.00001	0.000006			
Total	9	1.28884				

Table 4.9 Extra experimental results validation of linear model

MT (°C)	CT (°C)	IS (mm/s)	HP (bar)	Estimated Broken Point (x10^6 cycles)	Real Broken Point (x10^6 cycles)	Relative Error (%)
190	120	45	medium	3.28	3.06	7.19%
200	100	45	medium	3.89	3.97	2.02%
210	120	45	medium	3.08	3.35	8.06%

These three sets of chosen levels and breaking points were extra experimental results not selected in the Taguchi design. The estimated breaking point value was determined by the prediction using general linear model. Errors of 7.19%, 2.02% and 8.06% implied the model to be reasonable.

Fig. 4.7 demonstrates a sample of prediction on testing experimental data with a trained BP model showing an error which was too large to be acceptable (averagely larger than 10%).

The life cycle prediction graph varied for each simulation with a weight initialisation randomly generated using different seeds. It was found that the result was not the same each time when the same simulation was run. It obtained different results which even largely influenced the ranking of factor contribution (Table 4.10). That was because each time the system generated a random initialisation in weight to start the simulation

and it usually led to differentials in results. In this situation, the initialisation condition was set by fixing the initial seeds and optimised using for-loop trials of a large number of seeds; and the result is in Table 4.11.

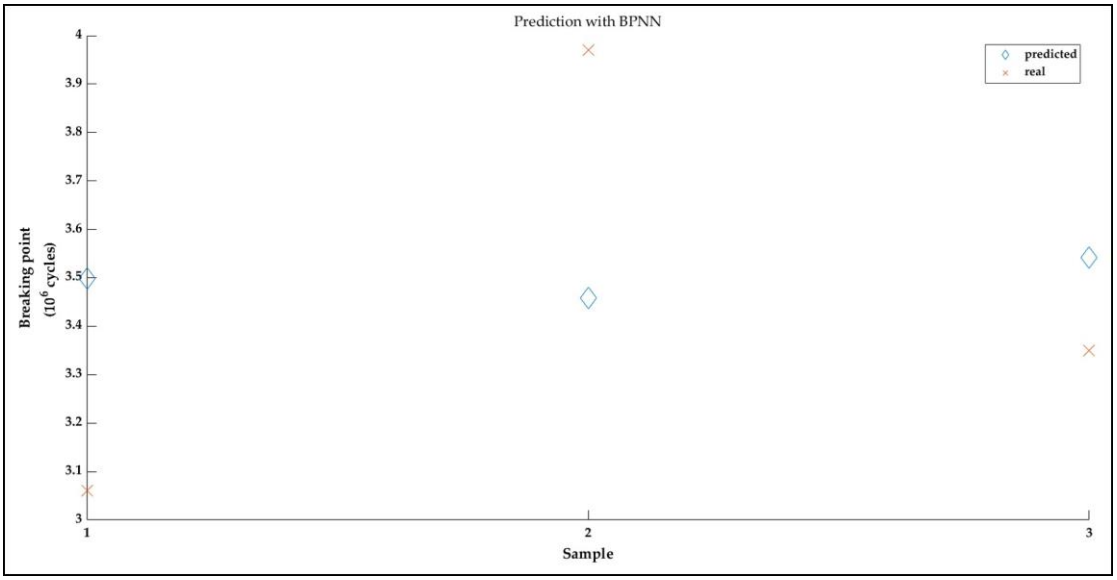

Fig. 4.7 BP neural network prediction

Table 4.10 Factor contribution with Garson's method

Factor Contribution Percentage	MT	CT	IS	HP
1	33.3723	20.2875	23.5628	22.7774
2	18.2137	28.7271	36.2583	16.8009
3	29.7704	35.2615	7.7870	27.1811
4	21.4138	34.2266	25.9687	18.3910
5	25.9069	25.8493	20.9183	27.3255

Table 4.11 Optimised factor contribution with Garson's method

Factor Contribution Percentage	MT	CT	IS	HP
1	28.2635	20.0373	31.2485	20.4508

This work reveals for the first time, the relationship between IM process and gear working performance, namely service life of polymer gears. It also shows how important the IM process is on the gear function quality. This work could not be replaced by only running well-known software simulations such as Moldflow, Ansys

and Abaqus, and there are no regulations of gear manufacturing for the purpose of better performance. It is believed that this work is helpful for improving the gear function quality without extra cost and giving IM engineers guidelines for future gear manufacturing.

4.5 Discussion

It is clear that IM parameter settings have an influence on the performance of polymer gears due to property-processing relationships that exist between the IM process and the tooling set. Heuristic parameter setting from Moldflow recommendations for example, can produce mouldings with acceptable appearance but not necessarily optimum mechanical performance. From this work it appears that choosing the mid-value manufacturers recommended settings but with a lower holding pressure actually produced the optimum results, however this could only be considered applicable to this mould tool design until further experiments are undertaken to confirm whether this had any wider applicability. Therefore, this chapter provides a suggestion, which could be easily applied without extra cost, for IM engineers working on polymer gears. For high volume manufacturing application such as automotive industry, this optimisation advice may save a lot in cost meanwhile offering better quality of products.

ANOVA, and neural network with gradient descent BP neural network, were used in order to analyse factors influencing the wear performance of polymer gears, during IM manufacturing process. Results show that applying general linear model using ANOVA techniques provides a better prediction in wear performance than the BP neural network does.

One possible reason is that the sample size is relatively small; and BP neural network might not be sufficient to handle the case. Modifying the number of hidden neurons could also cause a big change in simulation results. Another reason could be that the simulation results of BP neural network also relies on the initial values of weights, randomly generated by MATLAB. A larger number of simulations using various initial data, which depends on the seeds of MATLAB's built-in random number generator, could possibly improve the performance (as reducing the mean square error), and therefore make the whole trained network more reliable and better for prediction. Even though the BP has been proved working successfully in relatively small sample size such as from about 160 to 230 [105] [145] and even as 27 [146], in this study, at the

total sample size of 12, BP doesn't work efficiently. In short, even though BP method was proved to be helpful in some cases with a relatively small amount of data, in this study, it didn't work with a small sample size of 12.

On the other side, there are more options offered in the method of using neural network to analyse experimental data. There are other training algorithms to fit the neural network, such as Levenberg-Marquardt, quasi-Newton and gradient descent with momentum. Relative contribution of input factors can also be worked out by using methods like partial derivatives method, "Perturb", and Olden's method (which took care of issues of Garson's method, by concerning signs of connection weights of input-output interactions into consideration). These other techniques to solve similar problems are worth further work in the future to check whether those possible methods work on the small sample size case. What is more, as ANN a powerful tool for data analysis, if more experimental data can be collected in the future for this study, it still deserves an attempt and may probably provide a better result.

5 Wear Performance of Commercial Polyoxymethylene Copolymer and Homopolymer Gears

5.1 Introduction

Polymer gear development has shown high potential to replace metal gears, with advantages such as lower weight, lower cost, higher efficiency, and work without lubrication. Previous research revealed that polymer gears could provide about 70% in mass reduction, 80% improvements in inertia, and up to a 9% reduction in fuel consumption over the use of metal in automotive engineering [147]. However, due to a lack of research on material performance, polymer gear applications are currently limited. Further research and implications for the development and application of acetal gears are therefore timely.

As an engineering thermoplastic resin, and potential substitute for metals, acetal, also known as polyacetal or polyoxymethylene (POM), has many advantages such as high chemical resistance, friction wear resistance, fatigue resistance (especially when normalised with respect to the modulus of elasticity) and creep resistance [148]. It is applied widely across applications in automotive, medical, electronics, and household product sectors [149-152]. POM was first introduced by the 1953 Nobel Laureate Hermann Staudinger [153]. As a formaldehyde-based thermoplastic, POM is thermally sensitive and decomposes into formaldehyde gas at low temperatures. In 1960, Dupont Company developed a commercial homopolymer acetal (POM-H) through a condensation reaction of polyformaldehyde and acetic acid to increase its thermal stability and named it Delrin™. In 1962, a copolymer acetal (POM-C) was developed using the reaction of trioxane, a cyclic trimer of formaldehyde, and a cyclic ether, by Celanese Company [154]. The differences in structure can be seen in Fig. 5.1(a) and Fig. 5.1(b) and are reflected in different properties whereby POM-H has aligned uniform chains which allow for the formation of large crystalline domains. On the other hand, the random comonomer of the copolymer helps block the whole structure even under thermal influences.

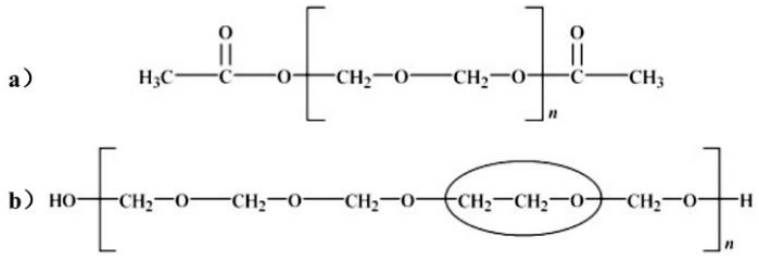

Fig. 5.1 Chemical structure of polyoxymethylene (a) homopolymer and (b) copolymer [154].

Previous studies of POM polymer offered a comparison between POM-H and POM-C. Tajima and Itoh [148] studied the creep rupture strength of the two polymers with different molecular weights. Their work reported that POM-H showed higher creep-rupture resistance than POM-C due to its higher molecular weight and tensile strength. However, POM-C performed better in fatigue resistance and yield strength than POM-H. Archodoulaki et al. [155] researched the degradation behaviour of POM which indicated that POM-C was more resistant against thermal oxidation than POM-H. Besides the different chain structures, POM-C had a better thermal aging property than that of POM-H. Hertzberg et al. [156] studied the fatigue crack propagation of various polymers and concluded that acetal had the highest fatigue resistance found in semi-crystalline polymers to date and that the POM-H version performed better than copolymer. Stohler and Berger [157] found that different chemical reinforcement methods of preventing degradation could be applied, these included capping of end groups by esterification to POM-H while adding epoxides as a comonomer to POM-C.

As POM is one of a number of materials of interest in polymer gears, previous work has been summarised in recent literature reviews of the field e.g. [158-160]. More specific and pertinent previous studies include aspects such as gear meshing mechanisms [94, 161, 162], materials [67, 163, 164], and thermal analysis [165, 166]. Interestingly many previous studies that have evaluated the performance of POM in gear applications, did not report the type of POM [167, 168], i.e. homo- or co-[8, 94, 162, 169]. In addition, most previous studies have assumed commercial POM-H and POM-C as one and the same, indistinguishably, for performance of these polymers in wear and fatigue applications like gears. Limited information has been presented around the comparison between these two types of commercial polymers. Unfortunately, this makes direct comparisons of performance very difficult as it ignores the effects of additives to the polymer formulation which can drastically effect properties such as

friction, crystallinity, and tensile strength. The aim of this chapter is to evaluate the viability of commercial POM-H and POM-C gears and to compare their performance under wear and fatigue in a gear application relative to previous findings. These performance tests were conducted in a novel test rig, designed and manufactured at the University of Warwick, to study the effects of misalignment on polymer gear contact and to continuously measure the wear of the gear surfaces under constant load conditions.

5.2 Sample preparation and experiments

5.2.1 Materials and gear injection moulding

Commercially available injection moulding grades of POM-H (Delrin® 500T BK602, Wilmington, Delaware, USA) and POM-C (Hostaform C9021, Irving, Texas, USA) were purchased from DuPont and Celanese.

The gear specimens were manufactured through IM. An ENGEL 60T IM machine (ENGEL U.K. Ltd, UK) was used for gear manufacturing. The details of gear and injection mould design are shown in chapter 3.4.

As per the manufacturer's recommended material preparation, the material was predried for 4 hours at 100 °C. It was then IM as per recommended processing conditions, which can be found in Table 5.1. IM parameters were optimised in the middle of recommended ranges [170, 171]. However, the holding time was determined by weighing the sample until the sample weight reached its maximum as per good moulding practice, allowing the system to reach a steady state. To apply changes to the IM process parameters on the samples, two complete material purging trials were carried out and the first 25 manufactured gear samples were discarded on each setting. The average shrinkage of the material was 1.7%, this was offset by designing a slightly larger mould cavity. After the plastic sprue bar was removed, and the location hole and pinholes cut, the polymer gears were ready for testing.

Table 5.1 IM procedure parameters.

Parameters	POM-C Gear	POM-H Gear
Melt Temperature (°C)	200	205
Mould Temperature (°C)	100	50
Injection Speed (mm/s)	45	45
Hold Pressure (MPa)	70	70
Holding time (s)	35	35
Cooling time (s)	75	75

5.2.2 Wear performance and material characterisation

To test the real-time wear performance of polymer gear pair, the test rig shown in chapter 4.3.3 was applied for the wear testing.

The morphology of the worn surface of the gear teeth was observed using a scanning electron microscope (SEM) ZEISS Sigma (Carl Zeiss AG, Germany). To reduce surface charging during SEM imaging, a thin film of gold was deposited onto the samples using an Au/Pd evaporation system. The images were captured using either secondary electron (SE) mode or the in-lens detector. The gun voltage was set to 5.00 kV and the high current set to OFF to avoid burning the plastic sample.

In order to compare the elastic properties of POM-H and POM-C, dynamic mechanical analyses of the polymers were performed using a dynamic mechanical analyser (DMA 242 E Artemis, Netzsch, Inc, Selb, Germany). Flat specimens (16 mm in gauge length, 8 mm in width, and 2 mm in thickness) were heated from 20 to 180 °C. The tests were performed in single cantilever mode at a frequency of 16.67 Hz, maximum dynamic force of 10 N, and static force of 2 N, displacement of 0.05 mm, and a heating rate of 20 °C/min.

While DMA analysis can reveal the mechanical properties related to the temperature, a FLIR C2 (Flir Systems, Inc, USA) thermal camera was used to generally monitor the gear teeth surface temperature in the linear phase (the steady-state constant wear rate phase of operation) during gear meshing. While the temperature was monitored, only

one point was recorded which was the point when the temperature stabilised during the linear phase.

5.3 Results and discussion

5.3.1 Wear performance

The wear and fatigue performance of the POM gears were evaluated using the rig shown in Fig. 4.3. In this study, all the tests were set at a rotation speed of 1000 rpm (16.67 Hz) and no misalignments were set for the gear meshing. In each test, a pair of the same type of gears meshed against each other. Those tested gears operated at a centre distance of 60 mm. The load was 9 N m and the test was kept running until the teeth broke. Further analysis revealed that both types of acetal gears had a relatively high endurance, which was reflected by a very low wear rate. As the driver gears usually broke first, they were regarded as the focus of polymer gear failure. Thus, all the research was focused on the driver gears in this study.

The smoothed results of the two types of acetal gears can be seen in Fig. 5.2, this was calculated from the mean values of 6 experiments, with the error shown as the shaded regions until gears broke. The end of gear service life was recorded when the gear teeth broke or when a tooth jumped out from the mesh point. This end of service life is illustrated as the steep rise in Fig. 5.2. The POM-H gears had an average of 35% longer service life than POM-C gears. For the POM-H gears, the wear could be divided into three phases: running-in, linear wear, and finally high wear. The gear pair failed to work as the gear teeth became softer and jumped out from meshing under high temperatures. This matched the conclusion in other studies [69]. POM-C gears show a similar pattern to POM-H gears, with running-in and linear wear phases, however, the POM-C gears had a relatively higher wear rate in both phases. When it came to the final phase, the curve of the POM-C gears steepens near the teeth breakpoint. The part 3 of the curve had a very short range on the horizontal axis. When comparing it to the curve of the POM-H gears, the curve shape of the POM-C gears showed a much more rapid wear increase before the breaking point. At this point a crack formed, making the LVDT (Fig. 4.3) display a sudden increase in readings. This final part of the curve can be called a crack phase rather than a final massive wear phase, as the gear failed.

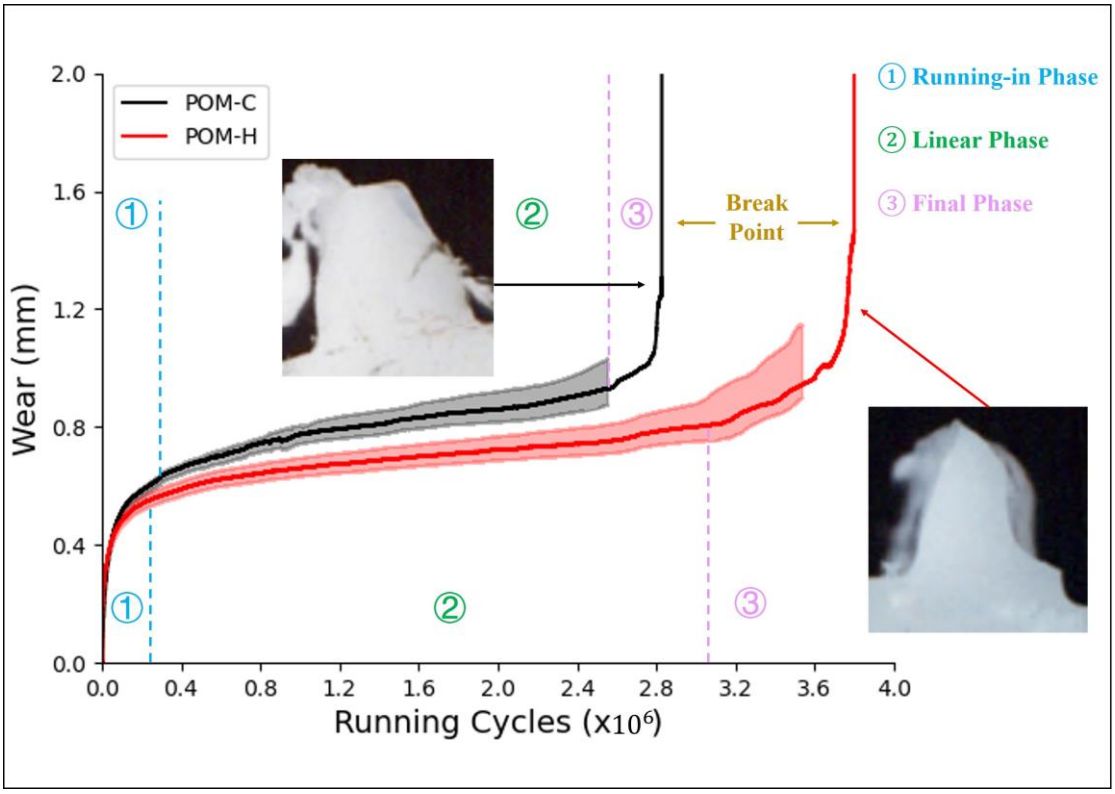

Fig. 5.2 Wear degradation of POM gears.

5.3.2 Dynamic mechanical property

To compare the two polymers and support the wear results, single cantilever mode dynamic mechanical analysis (DMA) was used to characterise the mechanical properties of POM-H and POM-C. The average storage modulus (E'), is the energy stored by the material through elastic deformation [172]. This is higher in POM-H than POM-C from 20 °C to 160 °C, which covers working conditions from room temperature to POM melting temperature (Fig. 5.3(a)). A thermal camera was used to check the gear surface temperature with an emissivity value of 0.92 [173]. Similar results were provided in other research [12], in the linear wear phase, the surface temperatures of both POM-H and POM-C gears at the contact area was stabilised at about 110 °C (Fig. 5.3(b)), meaning that the gear pair operated under this temperature for most of the time. The characterisation of elastic properties with DMA helps to support the results of wear from Fig. 5.2, because previous studies had established a correlation between elastic properties and wear properties of engineering polymers. For instance, Lancaster [174] showed a set of relationships between wear resistance on a polymer-metal system of polymers and other mechanical properties. Their study, covering a wide range of polymers, including commercial POM-H and polyamides, suggested that polymers with

higher elastic modulus tend to perform better in wear applications. Similar correlations between elastic properties and wear have been shown in other previous studies [174-176]. Also, POM-H maintains a higher loss modulus than POM-C throughout the whole testing temperature range (Fig. 5.3(c)). This means POM-H has generally better impact resistance. As the loss modulus represents the viscous part of the sample [175, 176], the increase of the loss modulus value of POM-H from around 105 °C leads to a more viscous performance and resultant higher crack resistance, which means at the stabilised working temperature (around 110 °C), there is a relatively big difference on viscous performance between POM-H and POM-C gears. This results in the final breaking format of gear tooth softening rather than gear tooth break. At the same time, the loss modulus value of POM-C reduces with temperature, which leads to crack formation and direct gear tooth breakage due to cracks.

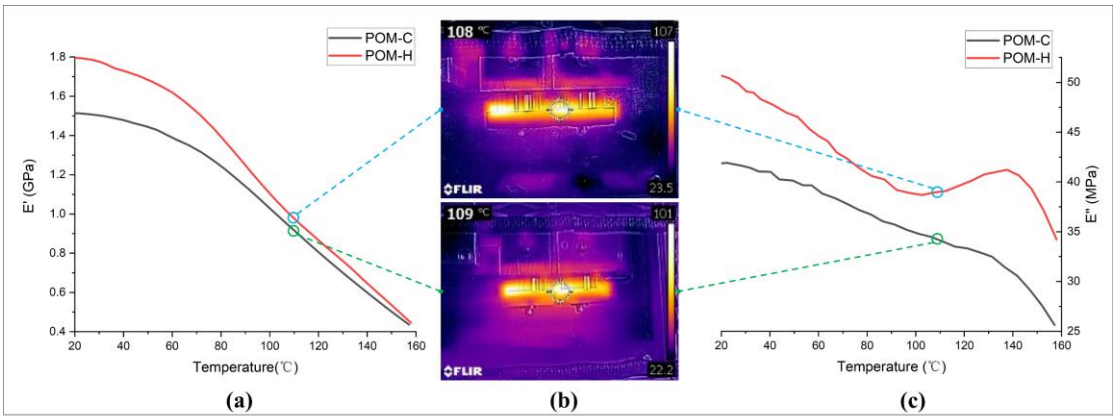

Fig. 5.3 DMA results of POM-C and POM-H: (a) Average storage modulus; (b) Thermal image; (c) Loss modulus.

The significant difference in elastic properties and wear properties of the homo- and co-polymer material grades here is likely due to the differences in their molecular structures, highlighted in Fig. 5.1. Given that the structure of POM-H presents a more uniform backbone, it is likely to have more stable, organised crystalline domains as the polymer solidifies after IM [177, 178]. Also, the uniform structure of POM-H allows for higher entanglement between crystalline domains. Correspondingly, the acetic acid molecules along the backbone of the POM-C are detrimental to the formation of crystalline structures. This difference in structure ultimately leads to higher elastic and wear properties in POM-H compared to POM-C [177, 178].

5.3.3 Failure mechanism

To investigate the failure mechanisms of the gears, a high-resolution scanning electron microscope (SEM) was used. Differences existed between each area (tip, root, and pitch line) of the gear teeth contact surface of the two acetals.

At the tip area, the POM-H gear teeth look smooth at relatively low magnification of 189 times (Fig. 5.4(a)). Little wear can be seen on the surface. Alternatively, when looking at the POM-C gear teeth under the same magnification, the tip area is deformed showing large flaw regions (Fig. 5.4(c)). The POM-H gear teeth only display clearly as a rough and melted worn surface when viewing at a higher magnification such as 2.99k times (Fig. 5.4(b)).

The root area also shows different patterns. For the POM-H gear teeth, the surface is relatively smooth with the melted material flow (Fig. 5.4(d)). For the POM-C gear teeth, the grooves are visible with lots of debris (Fig. 5.4(e)).

The most significant difference happens around the pitch line, marked as the blue double-sided arrows in Fig. 5.4(f)–(h). For the POM-H gear teeth, the pitch line area is clean without much wear (Fig. 5.4(f)). As in the theory of gear meshing, at the pitch lines of the meshing gears, the gears have no sliding but only rolling against each other [106]. In this experiment, due to the relative low Young's modulus character of POM, the teeth generate deformation during meshing, thus the pitch line is extended to a piece of area instead of a critical line. The two sides surrounding the pitch line area have much more melted debris than other areas, as shown in Fig. 5.4(g). This is because, on each side of a pitch line area, the gears slide against each other, with friction leaving more melted debris. The motion of the gears during meshing makes gears have an S-shaped profile, as stated by other authors [106]. In the pitch line area image of the POM-C gear teeth, there exists abrasive wear all around the pitch line as pitting [179] and a crack occurs there (Fig. 5.4(h)). Finally, the gear breaks because a crack develops on any one of the gear teeth.

In general, there are no cracks visible beneath the surface of POM-H gear teeth, and the pasted debris demonstrates the polymer deformation (Fig. 5.4(i)). As also stated by other researchers [180, 181], the polymer becomes softer first, then is stretched and finally detached. The main cause of wear is adhesion (Fig. 5.4(k)). While for the POM-

C gear, the smear is the most noticeable on the teeth (Fig. 5.4(j)), indicating the wear mechanism when the polymer wears away from the gear. The smear occurs when the gears start running and then are stretched and become more noticeable during the gear meshing. Finally, it reaches a point that the polymer breaks and peels off the leading edge of the smear (Fig. 5.4(l)). Similar results were found by others [167, 182]. A possible reason could be that the POM-H and POM-C have different microstructures after the injection moulding process, and it leads to the variety of failure mechanisms similar to the other researchers discussed in [111]. Further research to study this mechanism is reported in the next chapter.

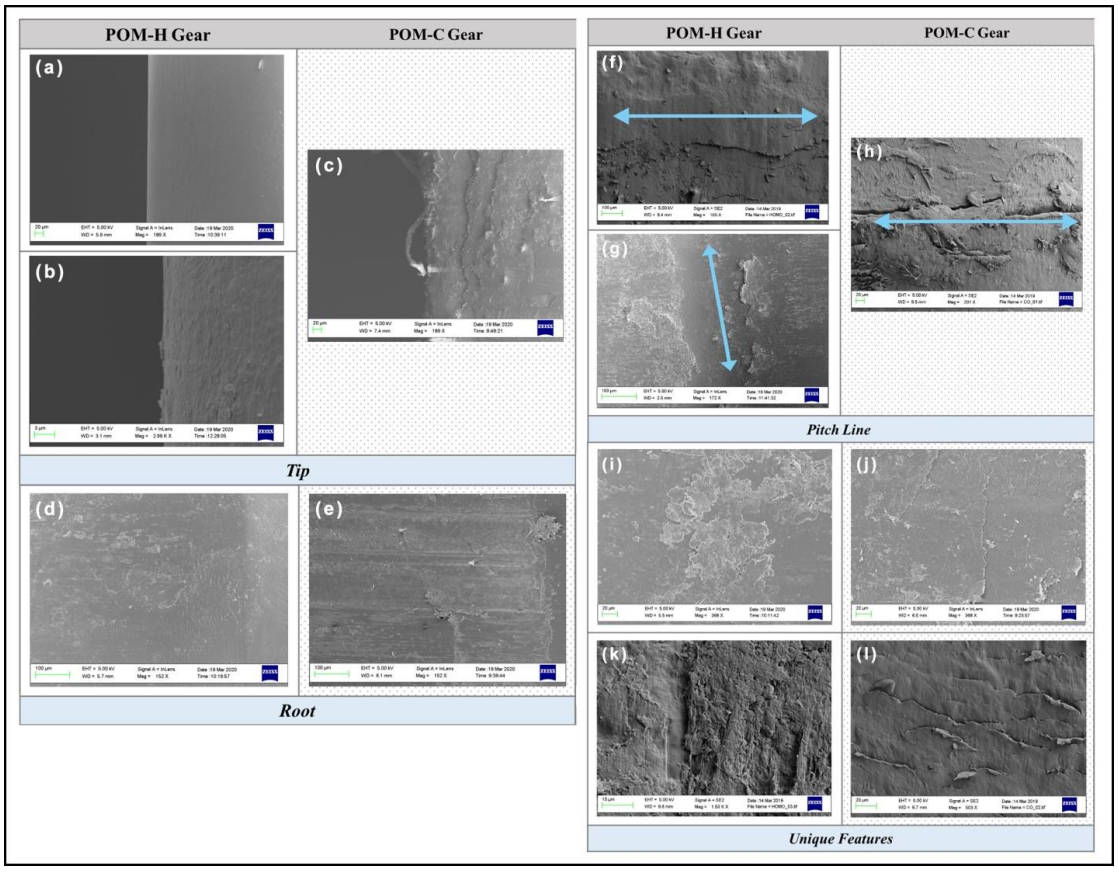

Fig. 5.4 Comparison on different gear teeth areas between POM-C and POM-H through SEM.

5.3.4 Performance analysis

The wear rate from the acetal gear test results can be expressed as the ratio of change in geometry of the worn gear (in terms of length) to the number of revolutions (cycles) the gear undertook in the test.

Wear rates under specific value of torque was studied by Friedrich [183], providing an equation of wear rate k_s as $k_s = \frac{V_w}{Fs}$, with V_w as the wear volume, F as the normal force and s as the sliding distance. By adapting the spur gear tooth profile, this equation can be further expressed as

$$k_s = \frac{Qbd}{2TN} \tag{5.19}$$

with Q as the wear depth, b as the gear face width, d as the gear pitch circle diameter, T as the torque, and N as the number of cycles the gear takes.

In previous research [69], it has been discovered that the critical value of k_s, above which the wear rate grows much faster, is related to the maximum gear contact surface temperature θ_{max}, consisting of ambient temperature θ_a, body temperature θ_b and flash temperature θ_f. This can be further expressed as

$$\theta_{max} = \theta_a + \theta_b + \theta_f = \theta_a + k_1 T + k_2 T^{3/4} \tag{5.20}$$

where

$$k_1 = \frac{c_r \mu}{bc\rho Z(r_a^2 - r^2)} \text{ and } k_2 = \frac{1.11\mu\left(V_1^{1/2} - V_2^{1/2}\right)}{rb(2k\rho ca)^{1/2}} \tag{5.21}$$

with T as the transmitted torque, ρ as the specific gravity, k as the thermal conductivity, c as the specific heat, a as the half contact width, r_a as the outside radius, r as the reference radius, b as the tooth face width, V_1 and V_2 as the sliding velocities of the two contact gears [49].

c_r is a constant relating to the contact ratio of the two gears, as

$$c_r = \frac{1 + \text{contact ratio}}{4} . \tag{5.22}$$

For Hertzian line contact [12], k_2 can be further expressed as a more basic form

$$k_2 = \frac{1.11\mu\left(V_1^{1/2} - V_2^{1/2}\right)}{2r^{3/4}b^{3/4}(k\rho c)^{1/2}}\left(\frac{\pi E}{R}\right)^{1/4} \tag{5.23}$$

where E is the effective elastic modulus and R is the relative radius.

With gear information k_1 and k_2 given after tests along with temperatures recorded, the critical value of torque T, beyond which the wear rate shall increase rapidly, could be calculated. Then the corresponding wear rate k_s at the critical torque could also be observed using Equation (5.1). Then the prediction of gear performance below the critical torque can be interpreted using k_s.

For the current experiment that the maximum surface temperatures reaching the melting point were 178 °C for POM-H and 166 °C for POM-C respectively, similar to the previous research [69], using Equations (5.2–5.5), the corresponding predicted loading capacities were 11.5 N m for POM-H and 10.3 N m for POM-C gear respectively. As the incremental step loading method was approved to reveal the wear rate of various loads efficiently [12, 69], it was applied for the two types of acetal gears at 1000 rpm from 6 N m with a step load increment of 1 N m until the gear broke. The results were calculated by the mean values of 6 repetitive experiments. The errors were plotted as shaded regions in Fig. 5.5(a), and error bars in Fig. 5.5(b). The wear curves were shown in Fig. 5.5(a) and it could be seen that the POM-C gear broke at 11 N m and the POM-H gear failed at 12 N m. The wear rates were calculated using Equation (5.1) and the wear rate against load plot is shown in Fig. 5.5(b). Similar to the pattern of the POM-H gear from 6 to 9 N m, the POM-C gear kept a relatively stable low wear rate at the load of 6 to 8 N m, and then wore more quickly until breaking. These tests prove that the above equations could offer good prediction on the gear transition torque for both POM-C and POM-H gears. It is found that the wear rate of POM-H gears tested at the load of 7 N m was lower than the value at 6 N m. We believe this is simply down to the inherent experimental error at this stage of the process because there are rapid changes of temperature and wear in the first cycles of the test which are all difficult to control and introduce variability.

For POM-H, it is possible to use Equation (5.1) to work out the wear rate k_s, and then the gear wear. However, for POM-C gears, before the factor of temperature, fatigue owns a more noticeable influence on the breakage of the gear teeth. In this situation, it might not be very useful to use k_s for gear wear prediction.

From previous studies on fatigue propagation [156], the stress intensity factor played a key role in monitoring fatigue crack growth. As a complex and material-shape-dependent property, the stress intensity factor contains information on both the load

applied to the cracking point and geometry influence. The growth rate of fatigue crack of gear teeth could be measured using the Paris–Erdogan equation

$$\frac{\mathrm{d}a}{\mathrm{d}N} = C(\Delta K)^m \tag{5.24}$$

with a as the crack length, N as the load cycle, K as the stress intensity factor. C and m are two experimentally obtained material-dependent coefficients. $\mathrm{d}a/\mathrm{d}N$ is the crack growth and ΔK is the stress intensity factor range for one cycle given as $\Delta K = K_{\max} - K_{\min}$.

In past, there had been a variety of studies on gear fatigue related quantities, especially the stress intensity factor. A typical solution of stress intensity factor for gear fatigue [184] was shown as

$$K = \frac{6FLY}{bS^2}\sqrt{\pi a}\,, \tag{5.25}$$

where

$$Y = \left(\cos\phi - \frac{C}{L}\sin\phi\right) Y_{\mathrm{m}}(\alpha) - \frac{S}{6L}\sin\phi\, Y_{\mathrm{t}}(\alpha)\,. \tag{5.26}$$

F is the load applied; L, S, b and C are length quantities including gear specimen dimensions; a is the crack length; $\phi = \arctan F_{\mathrm{y}}/F_{\mathrm{x}}$; $Y_{\mathrm{m}}(\alpha)$ and $Y_{\mathrm{t}}(\alpha)$ are shape factors where $\alpha = a/S$.

By extending K and F to a range for a cycle, it could be seen that $\Delta K = \frac{6\Delta FLY}{bS^2}\sqrt{\pi a}$, where ΔK is the stress intensity factor range and ΔF is the load range for a cycle.

With a pre-set F, it is possible to produce a logarithmic graph showing fatigue crack growth as a function of $\mathrm{d}a/\mathrm{d}N$ against ΔK[156]. With a sufficient number of tests, a more accurate pattern of fatigue could be obtained, helping to determine when and where the crack would occur, which could be further studied. This could be used in future predictions in the performance of POM-C gears. In this study, the fatigue approach analysis was not conducted due to the insufficient experiment data. It could be applied in future research on crack development in polymer gears.

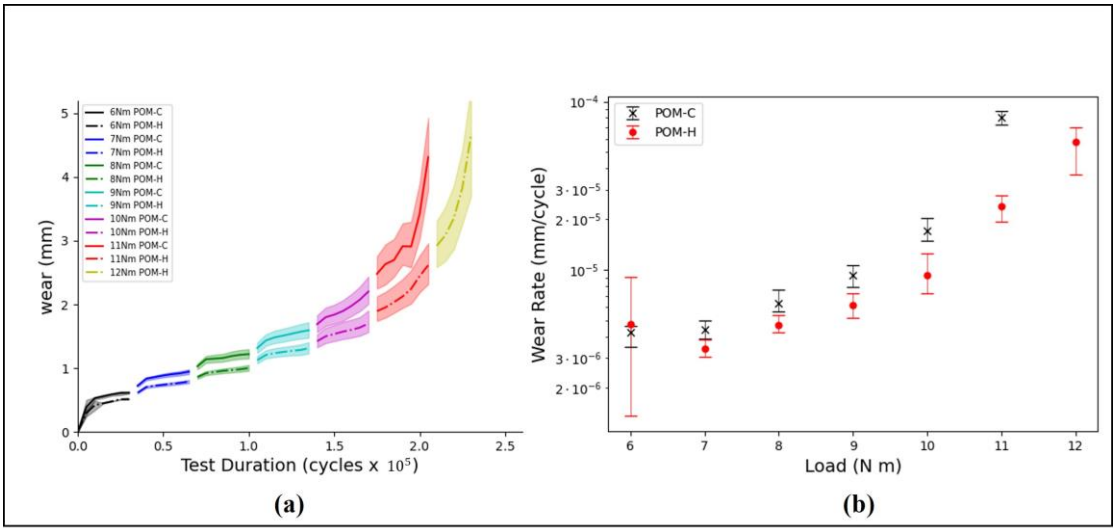

Fig. 5.5 Step loading tests results for acetal gears (a) Wear curve. Step changed per 3×10^4 cycles. (b) Wear rate.

5.4 Conclusions

Two types of commercial grade POM (POM-H and POM-C) gears were manufactured to compare the wear performance. The tests found a significant difference in the wear performance. POM-H gears had three wear phases, namely running in, linear wear, and final massive wear. The final massive wear was due to the temperature reaching the material melting point, and the teeth were therefore too soft to keep normal meshing, namely thermal failure. And similar results have been concluded in other references [12, 73]. In contrast, POM-C gears have better performance in thermal aging, which lead to a finding that the POM-C gears shared the same first two phases with POM-H ones, but also had the third one as the crack phase rather than exhibiting thermal failure. This finding also matched with the conclusions in [155, 156]. The final breakpoint was due to the fatigue cracks around the pitch lines of the gear teeth. DMA tests supported the above findings in the aspect of energy dissipation between the two materials. SEM images illustrated differences in the material failure mechanism, of which the most obvious one was that the POM-H illustrated material adhesion while the POM-C revealed mainly smearing. More tests were carried out with various loads from 6 N m until reaching their corresponding transition torque values and similar results were found in the above aspects. In general, the POM-H gear wear performance could be estimated with Equation (5.1) while the POM-C gear wear performance should refer to Equation (5.6). It can be concluded that the transition torque prediction for both POM-

H and POM-C gears was still applicable using Mao's method [12]. In this study case, the POM-H gears performed about 35% better in service life on average than the POM-C gears. Considering the mechanics studied above, the polymer formulation based on the homopolymer had a better performance than the copolymer formulation for injection moulded polymer gears. This is a physical phenomenon due to differences in the molecular structure of POM-H and POM-C which leads to very different mechanical performances and failure modes. Even though the POM-C performs better in thermal aging when it comes to the gear application tested here, the crack and wear resistance play more important roles. Consideration on a case-by-case application basis may be applicable here.

6 Polymer gear analysis using a revised procedure

6.1 Introduction

Following an introduction to gears (Chapter 3) and IM (Chapter 3), as well as initial moulding experiments (Chapter 4), it seems clear that typical procedures currently used in polymer gear analysis often pay insufficient attention to some significant materials issues. Thus, this chapter has parallel, interleaved themes that propose, develop and evaluate a revised, systematic but still practically plausible analysis procedure and report on its use in further experiments which covered the entire process including gear manufacturing, characterisation and sample analysis. Computerised Tomography (CT) scanning was used to ensure gear quality. Then wear testing was carried out to reveal the wear performance during the whole meshing process. Later, further analysis was undertaken to determine hardness and crystallinity, utilising scanning electronic microscopy (SEM), dynamic mechanical analysis (DMA), optical microscopy (OM) and SAXS/WAXS applications to give an insight into gear sample structure. The experimental suite forms a whole set of procedures to progressively study the engineering performance and material science behind polymer gears. The aim is to further investigate the challenge which was found in Chapter 2.4, namely that there is a gap between the study of polymer science and polymer gear performance.

As the POM gears have been studied in Chapter 5 and differences were found between POM-H and POM-C gears, this procedure was undertaken on the POM gears.

6.2 Experimental procedure

6.2.1 Gear injection moulding

The sample preparation methods were detailed in Chapter 5.2. As an extra process, a CT scan (Nikon XT H 225/320 LC, Nikon Metrology, UK) was applied to check the gear quality for any voids present inside the gear body to improve the holding time parameter setting. If the voids found such as Fig. 6.1, the gears will be defined as defective and the IM process needs to be adjusted such as increasing holding time parameter (one of the IM settings) or re-design the gate system. This method was recommended because it helped to find out the defects inside the gear body effectively.

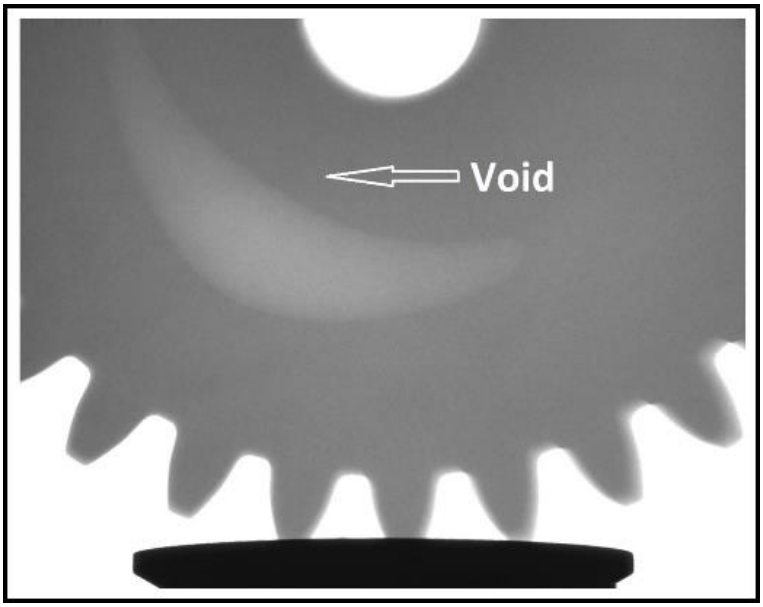

Fig. 6.1 A sample of CT scan.

6.2.2 Gear wear testing

This work uses the same data (and samples) from the tests reported earlier and the details of gear wear testing were included in Chapter 5.

6.2.3 Hardness measurement

Superficial Rockwell hardness (HR15W) was measured on the outer surface and the core of the gears. A Rockwell Hardness Tester (Wilson Rockwell 574, Buehler, Coventry, UK), equipped with a 1/8 in diameter hardened steel ball indenter, was used. The material surface was preloaded with a force of 3 kg. Following this, a major force of 15 kg was applied. While HR15W of the outer surface was measured directly, the measurements on the core were done on the cross-section face of the gear, with pre-treated samples.

This test was undertaken by Dr A. Lopera Valle, WMG, University of Warwick.

For the pre-treatment of gear teeth samples, first, they were mounted in clear epoxy. Then they were roughly sectioned using a precision cutter (IsoMet High Speed Pro, Buehler, USA). Then the section surfaces were polished using a polishing machine (AutoMet 300 Pro, Buehler, USA) with the grit size gradually reduced from 35 μm to no greater than 9 μm. The details of the whole process can be found in refs [185, 186], they offered specific treatment methods for polymers including sample cutting,

mounting and polishing thus following the procedures would be safe enough without significantly altering the materials properties.

6.2.4 Crystallinity and thermal properties

The thermal properties of the composites were measured using a thermogravimetric analyser and differential scanning calorimeter (TGA/DSC 3+, Mettler Toledo, Leicester, UK), equipped with the ultra-micro balance cell and differential thermal analysis (DTA) sensors, under a nitrogen flow of 10 mL/min. Typical sample mass was 20 mg. Analysis was performed in open Al_2O_3 pans. Samples were initially equilibrated at 25 °C for 10 minutes, heated to 220 °C at 10 °C/min, and held at that temperature for 10 minutes. Following this, the samples were cooled to 25 °C, at a cooling rate of 10 °C/min. A final heating to 650 °C at 10 °C/min was performed. From the DSC heating scans, melting temperature T_{m}, and enthalpy of fusion ΔH_{m} were determined. The degree of crystallinity of the polymer matrix, χ_C was determined as a function of melting peak area using equation:

$$\chi_C = \frac{\Delta H_{\mathrm{m}}}{\Delta H_{\mathrm{m}}^0} \times 100 \tag{6.1}$$

where ΔH_{m}^0 is the melting heat associated with pure crystalline material, 250 J/g [187-189] and 326 J/g [190-192] for POM-H and POM-C, respectively. The ΔH_{m} was measured from the DSC results of the first melting peak, in the heating cycles described above, using an integral tangential baseline setting in the Mettler Toledo STARe thermal analysis software (Mettler Toledo, Leicester, UK).

The crystallinity was evaluated in samples extracted from the most outer layer and the core of the gear. This was done by cutting 3–5 mm thick slices from the gears and selectively cutting material from these two regions.

This test was undertaken by Dr A. Lopera Valle, WMG, University of Warwick.

6.2.5 Microscopy

The surface of worn gear teeth was checked by SEM to evidence any differences between POM-H and POM-C gears.

Worn gear cross sections were examined by polarised light microscopy (Nikon Eclipse LV150N with DIC, Nikon Inc., Japan). For the gear teeth sample pre-treatment, it was

same as the process explained in chapter 6.2.3 and the only difference was the final grit size was no greater than 3 μm.

For examination of new gear teeth samples, they were thin-sliced with a microtome (Cryo-ultramicrotome, Leica Microsystems, Germany) to a thickness from 10 to 20 μm and then placed on the glass slide and immersed into Nujol.

6.2.6 SAXS/WAXS analysis

Cross sections of POM prepared by the author were taken to Diamond Synchrotron, (Harwell, UK) for SAXS/WAXS testing as part of a wider composite analysis beam time grant obtained by Dr V. Goodship, WMG, University of Warwick.

6.3 Results

6.3.1 Wear performance

The results showed as Fig. 6.2 are a replotting of Fig. 5.2 but it has been divided into more phases in this study. It showed that the wear of POM-C gear can be divided into running-in, linear and broken phases. While for the POM-H gear, it can be regarded as four phases, namely running-in, linear, massive wear and broken.

It was noted that the wear performance of POM-H and POM-C gears was similar but has evident differences. The differences between those two types of POM were widely researched in material science [193-195]; but in polymer gear studies, most of the literature only stated the material as POM.

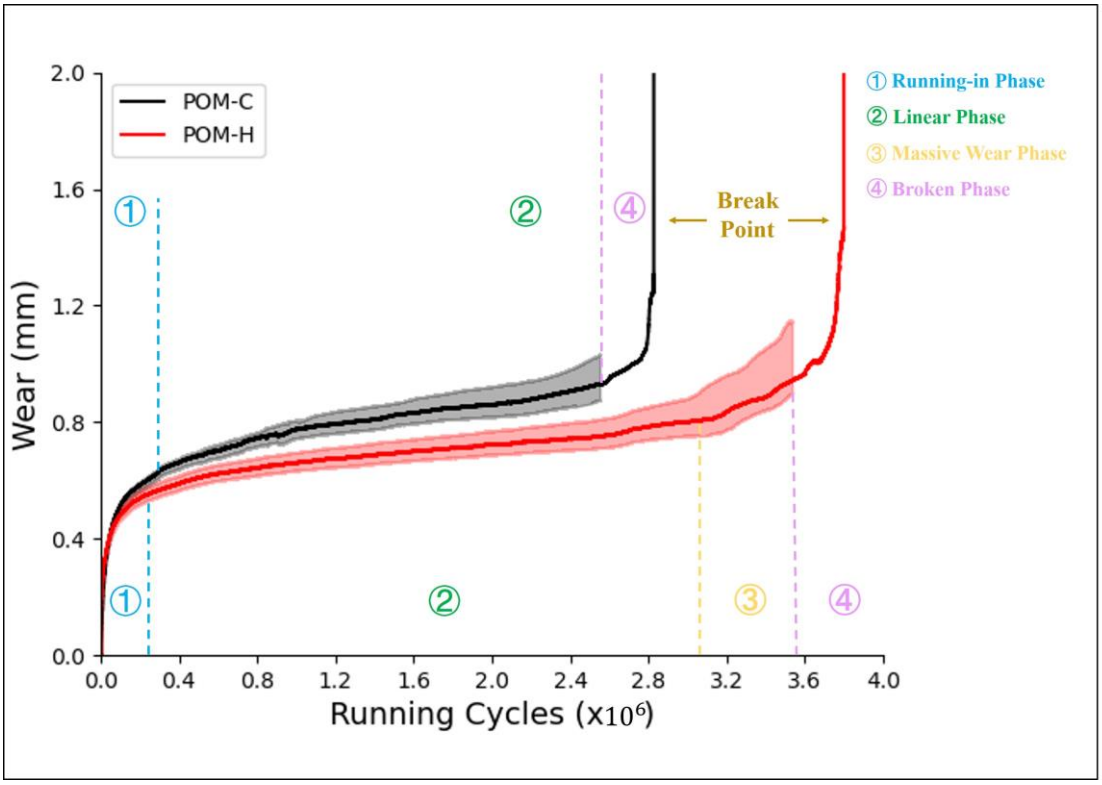

Fig. 6.2 Wear performance of POM gears.

6.3.2 Hardness Test

The HR15W hardness of the surface and core of the gears was measured. These measurements may provide information on the wear and fatigue response of the two materials. The results for HR15W hardness are summarised on Table 6.1. While the hardness of the POM-C outer surface and core were found to be the same, around 70 HR15W, there was a small difference between those of POM-H. The hardness of this material's core was found to be slightly higher than that of the surface. The cause for this may be linked to the formation of more crystalline regions in the core of the gears during injection moulding. Given that cooling rate of the gears is higher in the surface than in the core, the formation of an amorphous skin is likely. With lower cooling rate, the polymer in core of the POM-H gears had enough time and temperature (kinetic energy) to grow semi-crystalline regions. These regions may not have developed in the POM-C as this material tends to be less crystalline that POM-H. The thermal characterisation discussed below will shine light on whether crystallinity is linked to the differences in hardness and, in consequence, in wear and fatigue.

This higher hardness may be linked to the higher performance of POM-H seen in the wear tests. Once the skin layer of the gears has been worn out, it may be the higher resistance to plastically deform under a localised load, in addition to a potentially higher resistance to fatigue, of POM-H may lead to a lower wear, as shown in Fig. 6.2.

Table 6.1 Hardness measurement

	POM-H [HR15W]	POM-C [HR15W]
Surface	69.73 ± 1.27	70.76 ± 0.83
Core	75.56 ± 1.14	70.52 ± 1.48

6.3.3 Thermal properties

The melting point and crystallinity of the surface and core of POM-H and POM-C gears were estimated and summarised in Table 6.2. Two cycles of melting were carried in the DSC. The first cycle, Fig. 6.3(a), provides information about the thermal properties of the materials as injection moulded, and the second cycle, Fig. 6.3(b), shows the inherit behaviour of the materials under the same cooling conditions of 10 °C/min.

Table 6.2 Melting point and crystallinity measurements

Material	Tm1 (°C)	X1 (%)	Tm2 (°C)	X2 (%)
POM-H Edge	183 ± 0.6	46.4 ± 1.9	176 ± 0.5	48.1 ± 0.2
POM-H Core	183 ± 0.2	53.6 ± 0.6	177 ± 0.2	46.2 ± 1.3
POM-C Edge	173 ± 1.6	42.3 ± 2.1	170 ± 0.9	57.6 ± 1.0
POM-C Core	175 ± 1.6	44.2 ± 1.4	171 ± 2.2	58.0 ± 1.1

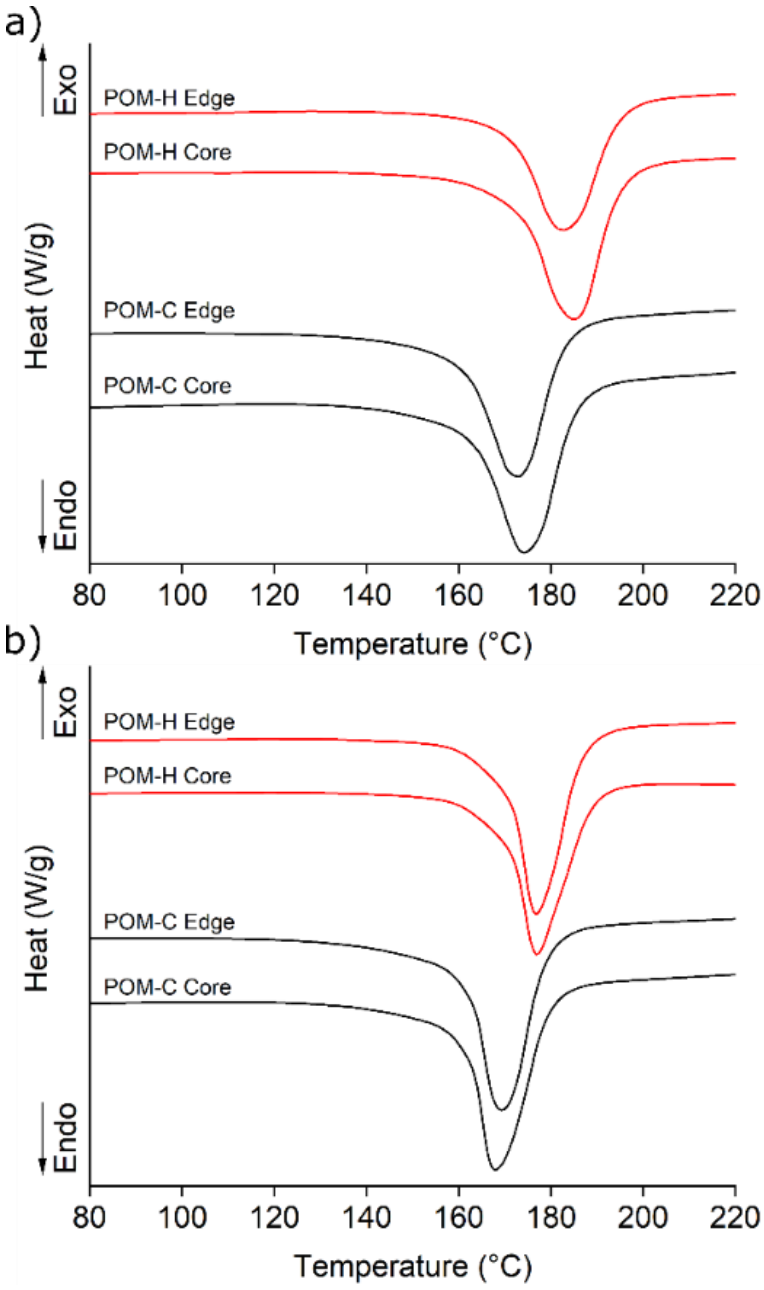

Fig. 6.3 DSC measurement of POM gears. (a) First cycle. (b) Second cycle.

With a well-defined single melting peak, the melting process was consistent throughout all POM materials. However, there were some differences in the values of melting point and crystallinity between POM-C and POM-H. The first DSC melting cycle of POM-C did not change between the surface and core. The melting point and crystallinity were around 174 °C and 43 % respectively. On the other hand, a significant difference in the crystallinity was found in the first melting cycle of POM-H. The crystallinity of the surface material close to 8% lower than in the core of the gear. The lower crystallinity in the surface is likely to be associated with the more amorphous skin in the outer region

of injection moulded semi-crystalline polymers. No significant differences in the melting point of the core and surface for POM-H was found.

In the second melting event, in Fig. 6.3(b), the crystallinity of surface and core for both materials was the same. This is because the cooling cycle was done at the same rate. The crystallinity of POM-H was found to be roughly 10% lower than that of POM-C. This means that the intrinsic crystallinity of POM-C is higher than that of POM-H. This result suggests that the differences in crystallinity between the core and surface of POM-H in the first DSC melting cycle was associated with the cooling rate of the gears during injection moulding and not with the materials themselves.

A slight variation in the melting point of POM was observed between the first and second DSC melting cycles.

6.3.4 Dynamic mechanical analysis (DMA)

The results of DMA were stated in chapter 5.3.2 and proved to be effective to reveal the mechanical properties regarding the changing of temperature. Thus, the DMA method was recommended as part of polymer gear analysis procedure as well.

6.3.5 Scanning electronic microscopy (SEM)

The results of SEM were detailed in chapter 5.3.3 and proved to be effective to explain the surface characters of polymer gear teeth. Thus, the SEM method was recommended as part of polymer gear analysis procedure.

6.3.6 Cross Section Analysis

As gear teeth undergo working conditions mainly during the linear phase (Fig. 6.2), the gear teeth samples are viewed after sectioning, mounting and polishing on the section surface. The wear process inside the gear teeth is demonstrated clearly during this phase using this technique.

For the POM-H (Fig. 6.4(a)), the interactions of the meshing teeth cause internal changes to the material, seen as thin layers with the width of less than 100 μm separated from the teeth. Not only lead to wear, those layers were extended to the non-contact side of the gear surface which brought in cracks of the gear. A similar but thicker separated layer was found around the engagement point but with an opposite cutting direction with the ones around the tip. This result perfectly matches the gear sliding

mechanism (Fig. 6.5) that the friction direction of gear changes at the pitch line. For the driver gear, the friction directions are away from the pitch line. This wear process continues during the whole linear wear phase.

For the POM-C, it was found that the wear varied as the linear phase progressed (Fig. 6.4(b)-(c)). Similar findings were reported, which were believed to be related to the change of friction direction [12]. Towards the end of the linear phase (Fig. 6.4(c)), the gear tooth was largely deformed and most of the tip area was worn. The wear behaviour, e.g. the sliced thin layers in Fig. 6.4(a), was not found in the pictures of POM-C gears during the whole linear wear phase.

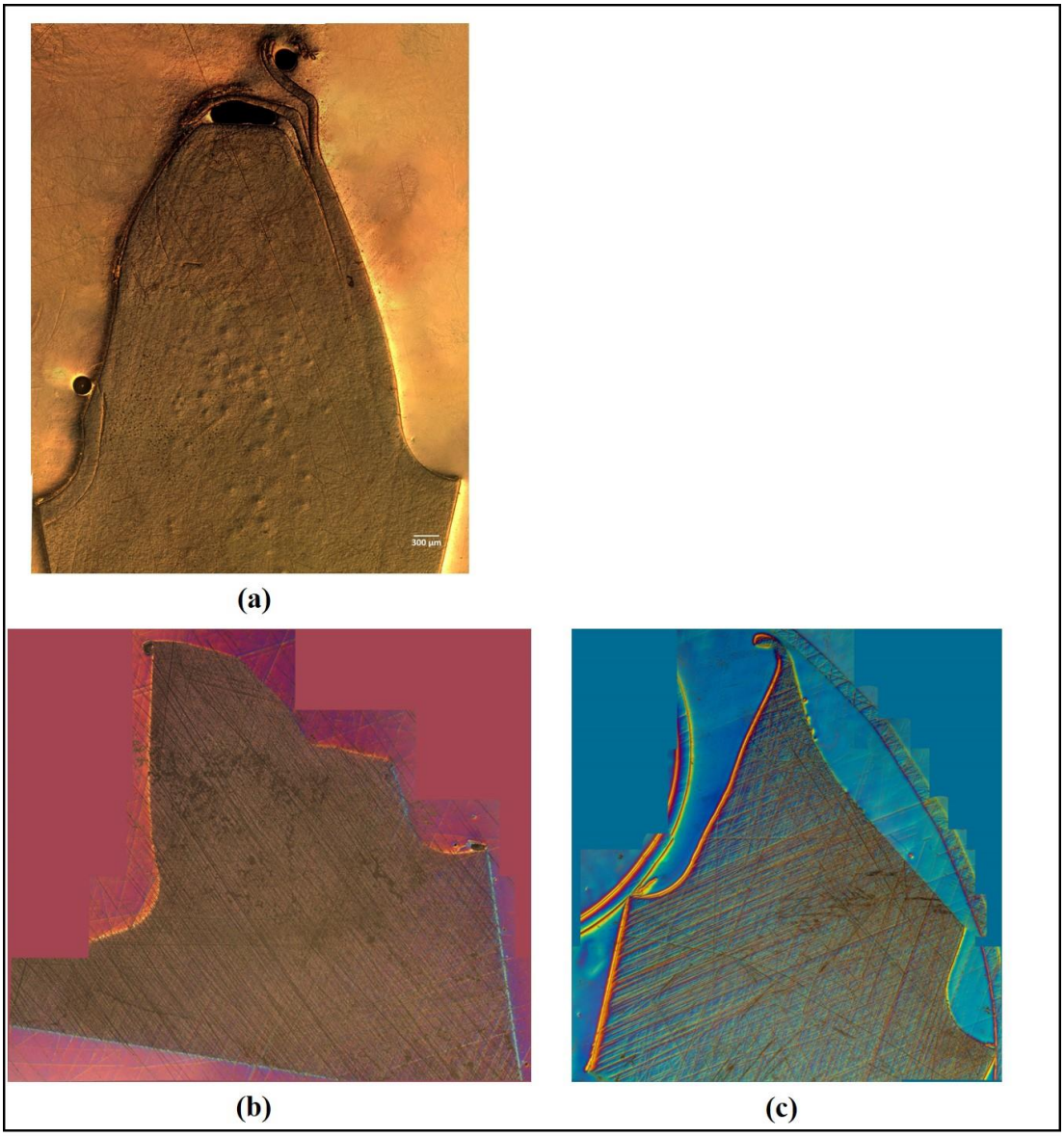

Fig. 6.4 Comparison of crossing section. (a) Linear phase of POM-H gear tooth. (b) Middle of linear phase of POM-C gear tooth. (c) End of linear phase of POM-C gear tooth.

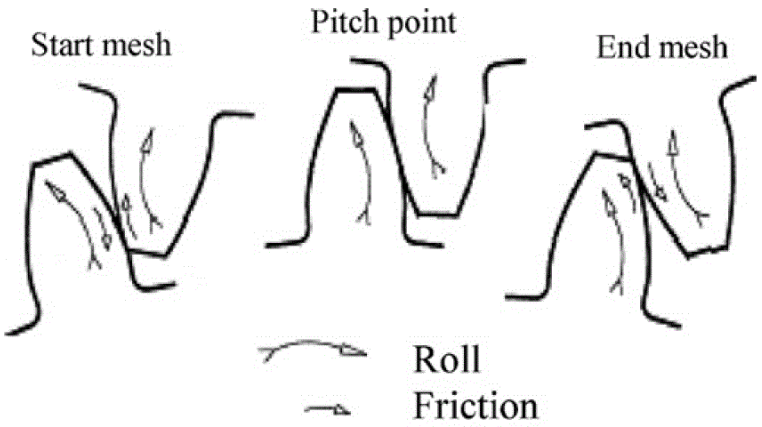

Fig. 6.5 Gear meshing mechanism[12].

6.3.7 Thin-section microtomy for microscopic analysis

The sections of gear teeth were sliced using a microtome and then examined using polarised microscopy.

The polarised microscopic images brought an insight of material structure of POM-H and POM-C gear teeth, which had not been revealed previously in the literature. Fig. 6.6(a) shows that the POM-H gear tooth has a three-layer structure: the outer transparent skin, the middle layer and the inner core. The structure corresponds to the wear phases shown in Fig. 6.2. During gear meshing, the wear progressed through the outer surface and the skin area during the running-in phase. Then the middle layer matched with the linear phases. After that, the wear enormously increased when encountering the crystalline area. Finally, it led to a jump-out of softened gear teeth from meshing. For the POM-C gear picture, the tooth exhibited a universally material structure, but it can be further divided into two layers as seen in Fig. 6.6(b). There are a thin skin area on the surface and a core area inside. What is more, this is also reflected in Fig. 6.2, showing that the wear started from a running-in, then went through a continuous linear phase and then followed by a sudden crack when the linear phase ended.

Similar to the conclusion in chapter 6.3.3, the reason for these differences may be relevant to the IM process. As shown in Table 5.1, the recommended mould temperature setting for POM-H (50 °C) was much lower than that of POM-C (100 °C). It may lead to the conclusion that the skin is highly aligned in POM-H as it was the result of fountain flow and then rapid cooling as it hit the cold mould wall. The middle layer would develop as the mould fills and is more crystalline as it was insulated from the mould

wall and has more time to cool and therefore develop higher levels of crystallisation. And the core would be able to cool slowest and therefore exhibit the highest crystallinity. It is also noted that in Fig. 6.6(a), the thickness of the skin and middle layer area is approximately equal to the total wear length of the running-in and linear phases. This suggests that the thickness of the skin and middle layer of POM-H gear teeth strongly relate to the endurance of the gear teeth, under the aspect of material science. Fig. 6.6(b) shows that POM-C gear teeth do not have this material property therefore have a different failure mechanism. The above findings in the polarised microscopic pictures well match the wear testing results in Fig. 6.2.

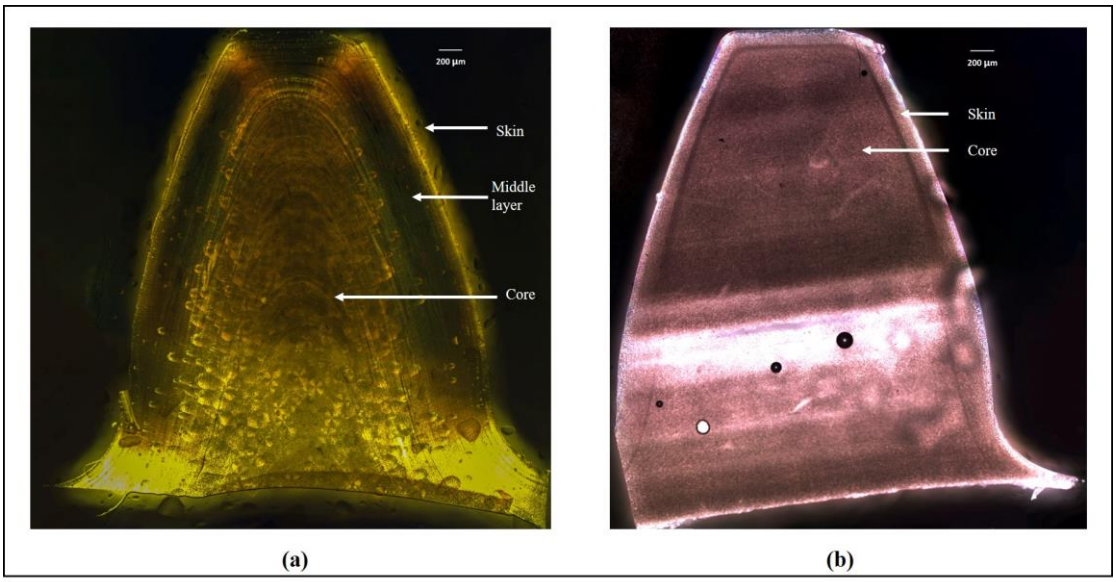

Fig. 6.6 Polarised microscope on Thin-section of gear teeth. (a) POM-H gear tooth. (b) POM-C gear tooth.

6.3.8 SAXS/WAXS analysis

As SAXS/WAXS result analysis is complex and beyond the scope of the author's remit, the subsequent analysis of the results was performed on the authors's behalf by Mr Neil Reynolds, WMG, University of Warwick who confirmed that there was no change of crystallinity across the surface of the POM-CO cross section.

6.4 Discussion

The polymer gear analysis procedure applied in this chapter helped discover the reason for the wear performance difference between POM-H and POM-C gears, in the aspect

of the inherent differences in the materials. The entire process was captured through the stages of initial manufacturing, characterisation, and analysis.

A traditional manufacturing procedure was applied to produce polymer gears. CT scanning was introduced to detect gear defects and ensure only structurally sound mouldings were carried into the testing phase. This technique also helped optimise the holding time parameter (one of the IM settings) in the process.

Previous researchers in POM gears ignored any potential differences in the performance of POM-H and POM-C gears. Gear testing focused on the wear behaviour of the two different polymer grades, reflected by different wear patterns in the polymer gear meshing.

Successive sample analyses were applied following wear tests. First, hardness and crystallinity measurements were applied to provide material diagnosis information on the two polymer grades. These measurements detailed the differences between the measured parameters of the two polymer gears, by taking data at discrete points on the core and the surface of the gear teeth. To discover if these results would affect the wear behaviours of the two polymer gears, SEM and cross section analysis using OM were taken to view the characteristics on both the surface and cross sections of the two polymer gears. And DMA analysis linked the connection between the mechanical behaviour and the temperature changing of gear teeth. The visual difference presented in the mainly focused on the wear behaviour. Further analysis by thin-section microtomy, extended the analysis into a deeper investigation of the material structure revealing the two-layer material structure of POM-H gears which was found to match phases of its wear behaviour. POM-C gears did not exhibit a complex structure; in this case further analysis was carried out using high resolution SAXS/WAXS. This confirmed there were no significant crystallinity changes occurring through the gear tooth structure, explaining the differences in wear behaviour.

As the procedure successfully helped understand the wear mechanisms of polymer gears and showed a good potential in revealing the characters of material in this study, it is therefore recommended as a coherent set of investigative procedure for studies on polymer gears. Even though those techniques are widely applied in material science, few have been used specifically on the study of polymer gears. Most of the current publications about polymer gears are limited on study methods such as surface

observation using SEM and OM. The set of the recommended extra procedure as well as their benefits are listed in Table 6.3. Future research on gears made by various polymers may try with any of those techniques.

Table 6.3 Set of extra procedure recommended for polymer gear study

Techniques	Benefits
CT scanning	Detecting defects inside gears.
Hardness measurements	Checking material homogeneity.
Crystallinity measurements	Checking material homogeneity.
Cross section analysis using OM	Investigating failure mechanisms.
DMA analysis	Studying the viscoelastic behaviour.
Thin-section microtomy	Revealing material structure.

7 A potential cloud base Internet of Things (IoT) approach for polymer gear data and analysis

7.1 Introduction

While recognising that some of the required technologies are not currently mature enough to deliver all the concepts discussed, this chapter explores and speculates on how some ‘big data’ approaches might aid our understanding of polymer gear behaviour under a wide range of practical conditions. It considers whether they might soon be able to enhance international collaboration between major research centres, with prospects of eventual wider use.

As detailed in chapter 2, there are many methods to predict the service life of polymer gears. Most of them are transferred from the standards of metal gears but they lack accuracy because of the unique character of polymers compared to metals. As a pioneer, Mao contributed to the design method specifically for polymer gears regarding the polymer temperature [12], making the polymer gears more reliable in design and more accurate in service life prediction. However, to accurately predict the service life of polymer gears using some specific equation is a real challenge. This is because the performance of polymer gears is influenced by many factors such as the material, wear, load, running speed, fatigue, crack condition, temperature and manufacturing methods. What is more, due to the character of polymer, when the temperature changes, many of the other temperature dependant properties will be influenced as well. In practice, software such as Abaqus and Ansys using computer-aided engineering (CAE) technology has helped to predict the working condition of polymer gears [196-198] but it was time consuming in modelling and the result was limited to specific cases without general applicability. In summary, there are no accurate standards to value the rating life of polymer gears. To contribute to this research, gaining more experimental data of polymer gears is essential, which was also mentioned in chapter 2.

Until now, each method studying polymer gears has its limitation such as low accuracy in life prediction and low general applicability. This chapter tries to introduce another potential method to help gain more testing data efficiently from polymer gears in application based on the technology of IoT and cloud. As any similar solution was not

yet found in polymer gear publications, this idea using practical technologies was regarded as new contribution to the polymer gear research.

7.2 Design of the solution

The infrastructure is shown in Fig. 7.1. It was shown in previous chapters that the test rig (Fig. 4.3) can obtain data about gear performance efficiency. If the concepts of test rigs were transferred into real applications such as cars and motorbikes, with the help of incoming 5G, each application becomes a test rig and can continuously send real time measurement data to a cloud platform. If the measured data were highly formatted such as time against wear and time against temperature and the relational database was designed for storing the formatted datasets, the measured data could be stored in databases for future analysis. It would also support customised real-time data processing. For example, when the temperature of the polymer gears is higher than some pre-set value or the wear is higher than the limit, the driver of the cars or motorbikes would receive a warning message immediately.

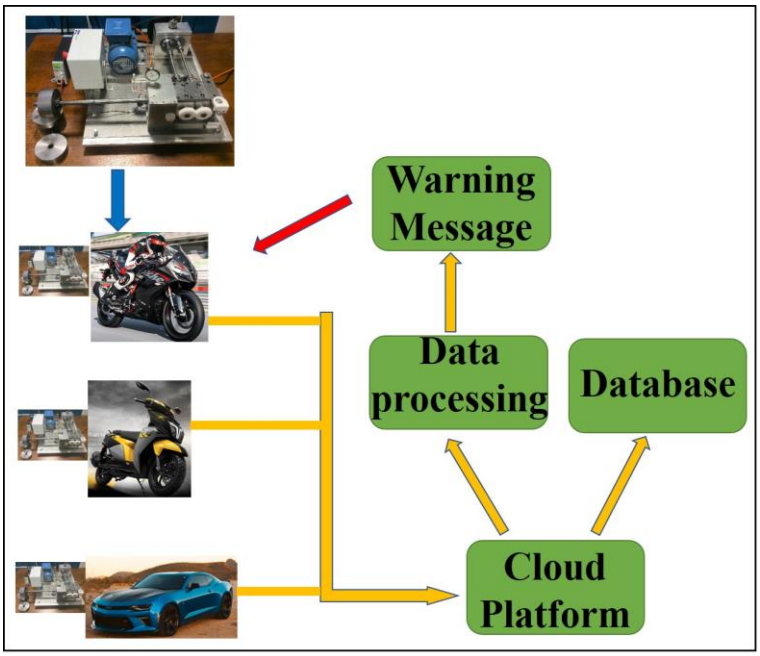

Fig. 7.1 The structure of a real-time polymer gears testing solution

7.3 Infrastructure deployment

To deploy this infrastructure, the electrical components used are listed in

Table 7.1. Those components can be divided into two groups, the sensors and the development boards. The sensors are for the measurement of the characters such as

distance and rpm and transferring them into digital signals. And the development boards are used to process the data and make them readable to the users through interfaces such as for monitoring. For the connection step, the sensors are connected to either the Arduino nano board or to the Raspberry pi 4b. Both the Arduino nano and the Raspberry pi are connected with each other as an integrity system for data processing. The information for setting up methods and the accuracy of components can be found in the references [199-203]. The finally built hardware system would look like Fig. 7.2. As this work was more focused on the whole infrastructure of the design, the components applied will be different regarding individual projects and it should be noted the process such as the calibration and the error calculation are needed when the system is applied into real applications. It also means the example that installing this design on motorbikes showing in Fig. 7.1 has not been realised yet while it is believed to be a future possibility.

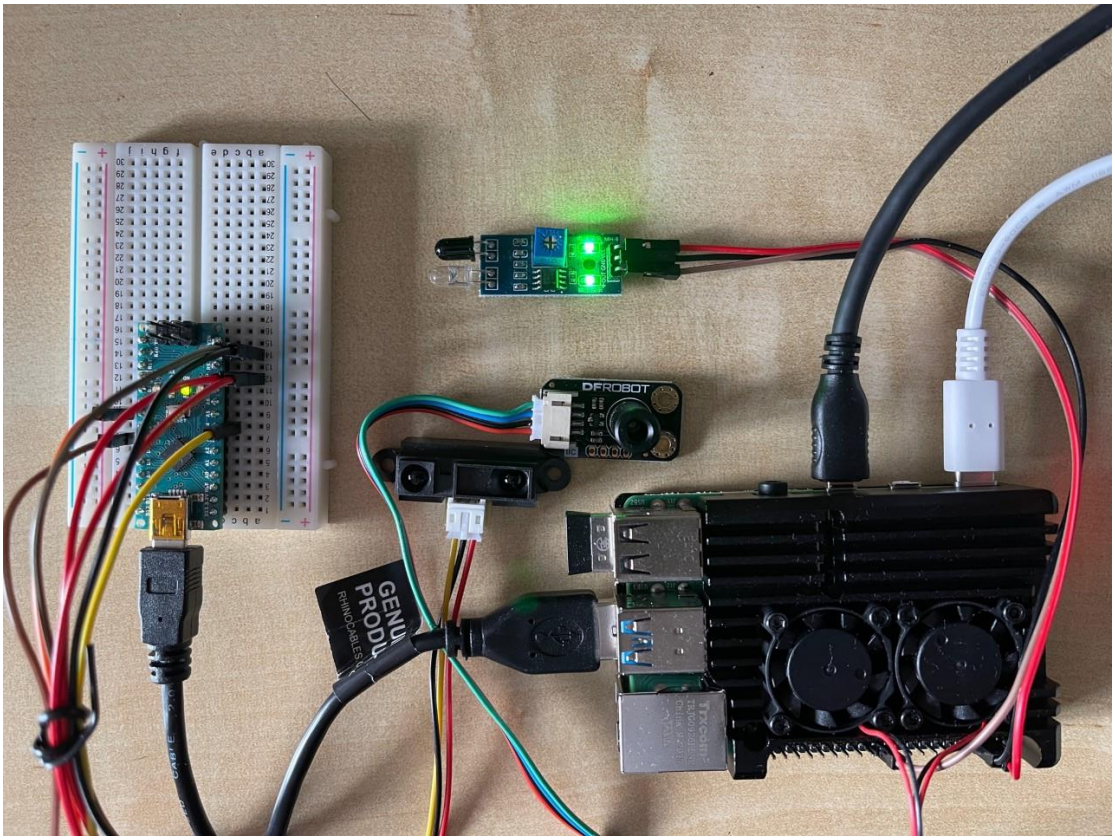

Fig. 7.2 IoT hardware set

Table 7.1 Key components used in testing solution

Key Component
Single board computers Raspberry pi 4 model b
Arceli GP2Y0A21YK0F sharp IR analog distance sensor
Arduino AVR nano V3 development board
Youmile IR infrared obstacle avoidance sensor
DFRobot SEN0263 temperature sensor development tools

In this project, python was used as the programming language for data processing in Raspberry pi 4b. First, python scripts were written to design data collection from the sensor, such as sampling frequency, sampling accuracy, data format etc. Following the collection, some of the raw data needs post-processing to present valuable information. For example, the obstacle avoidance sensor cannot count RPM directly, while it does count how many times a marked point on the gear passed, and the time duration is collected as well, then RPM could be calculated from these data by running the below equation in python scripts:

$$\mathrm{RPM} = \frac{\text{cycles}}{\text{duration}} \times 60\,, \tag{7.1}$$

where cycles = count number – 1, and

duration = end time – start time, measured in seconds.

After the data was processed, it was transferred to the cloud via the internet. As the 5G network does not yet cover the living area of the author, in this study, Wi-Fi was used as an alternative. The Wi-Fi connection was a built-in function on the Raspberry pi. Once the 5G become more popular in the future, any add-on 5G module [204] which is compatible with Raspberry pi can be used to upgrade.

For the transmission of the data, the Message Queuing Telemetry Transport (MQTT) protocol was chosen. It is a kind of publish-subscribe network protocol to transport messages between devices. It has the advantages of low requirement of bandwidth, operates with small amounts of codes and fulfils the ISO standard. Unlike the protocols using “request” and “response” for communication, the MQTT uses the “publish” and

“subscribe” methods, which means it does not require the interaction between the message sender and the receiver. There can be more than one message senders as well as receivers in a single message transmission case. What is more, the sender and the receiver can be the same device, namely the device can receive the data which is generated by itself. For communication, the devices only need a broker to manage the MQTT service, and it was Amazon Web Services (AWS) in this project.

To undertake the process using AWS, an AWS account was first created, which gained access to the AWS services such as data storing, data analysis and bill management. Then the AWS IoT Core service was chosen which is based on the MQTT protocol and provided further services such as the user interface and real-time status monitoring. After setting up the procedures such as the licences and the security policies, some python codes were created to deploy the subscribe and the publish process. The Raspberry pi acted as the publisher and sent the data to the subscriber, namely the AWS IoT Core. The interface of the AWS IoT Core can display the real-time data received from the Raspberry pi (Fig. 7.3).

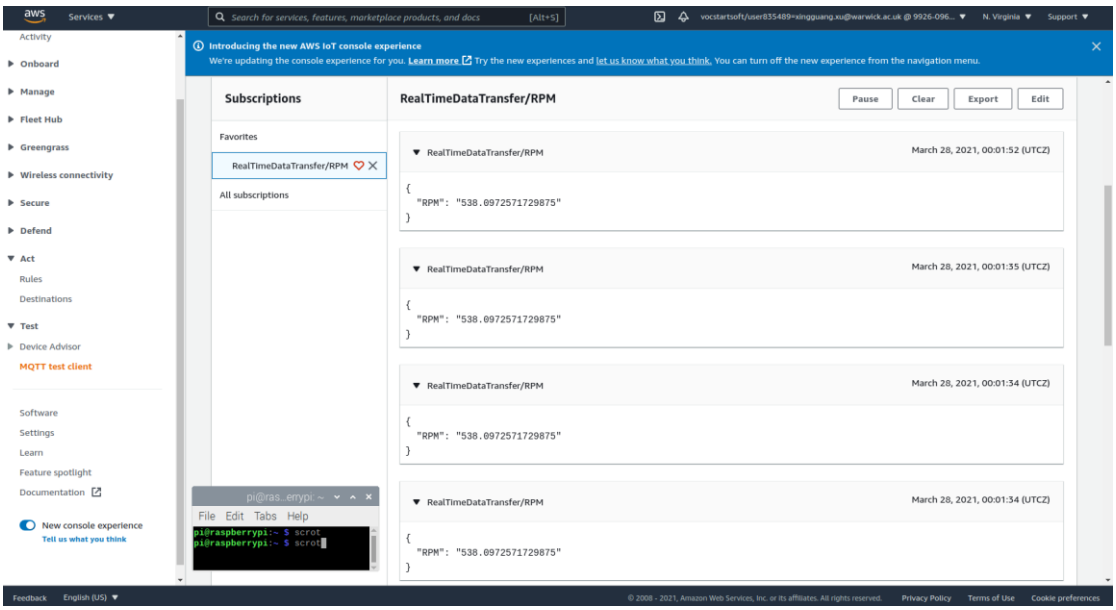

Fig. 7.3 Display of real-time received data on AWS IoT Core

The AWS IoT Core offered the cloud platform for the data transportbetween devices, which realised the fundamentals of the IoT. However, it can only check the real-time data without the abilities of processing such as data storing and analyzing. Thus, another AWS service named Amazon DynamoDB was used for data storage. It is a database service and can store the formated data into a cloud platform. In this case, once the data

is received from the Raspberry pi, it is stored into the database (Fig. 7.4). Then the data can be used anytime in the future for any purpose.

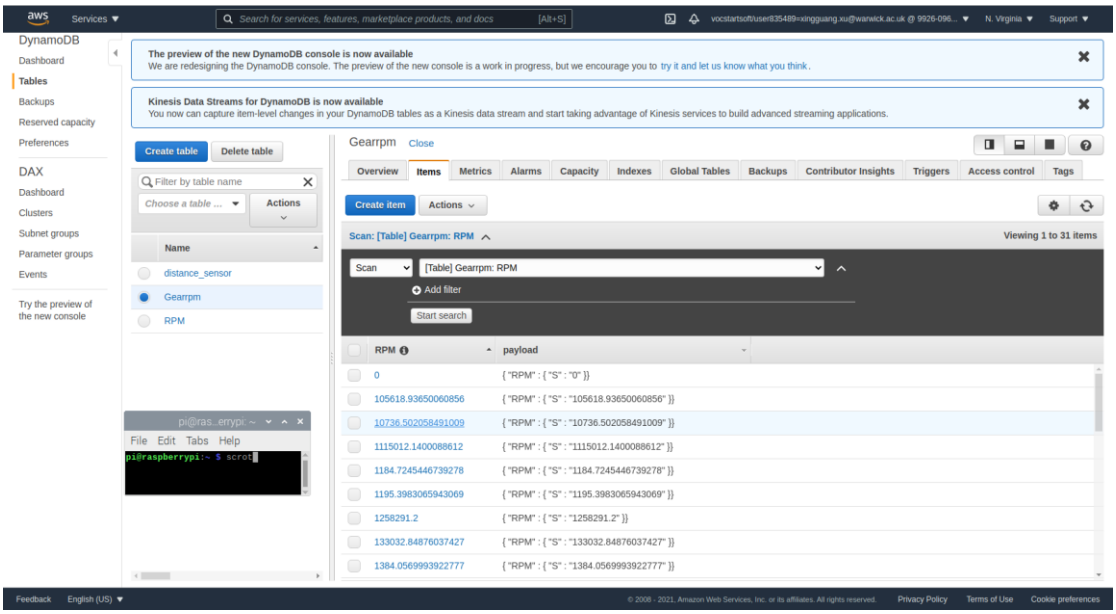

Fig. 7.4 Display of real-time received data stored on Amazon DynamoDB

Besides storing the data into the database for future analysis, another function focusing on the analysis of streaming data was designed. Another service named AWS Lambda was applied. It provided a platform to deploy the customed python code to analyse the data. The connection between AWS IoT Core and AWS Lambda was built. Each time the AWS IoT Core received the data, it triggered the function on AWS Lambda. If it fulfils the designed condition in the script such as temperature or the wear was higher than the limit values, the warning message will be returned.

Until now, the subscriber was still the cloud platform and there were no communications between the sensors and the other physical devices in the real world. To undertake this communication process, the amazon Simple Notification Service (SNS) was applied. It is a fully managed messaging service for both application-to-application (A2A) and application-to-person (A2P) communication. In this project, the AWS Lambda service was regarded as the application, then the messages were sent to persons directly with the methods of email address and short message service (SMS).

The component design showed in Fig. 7.1 was deployed. First, data such as gear RPM, amount of wear and surface temperature were collected by sensors. The Raspberry pi and the Arduino deployed the data collecting methods such as the data collecting

frequency then sent the data to the AWS IoT core, a cloud platform. The received data can not only be stored in database (Amazon DynamoDB) but also analysed through designed function in AWS Lambda. Which means both the database and the designed function are subscribers of the data collected from the sensors. The function will return the message such as “Gears are broken” once the conditions are met such as the gears are too hot or they wore too much on the teeth. Then the Amazon SNS service was used as the subscriber of the designed function. Once the warning messages were returned, they will be sent to the persons directly through both the email (Fig. 7.5 (a)) and SMS (Fig. 7.5 (b)).

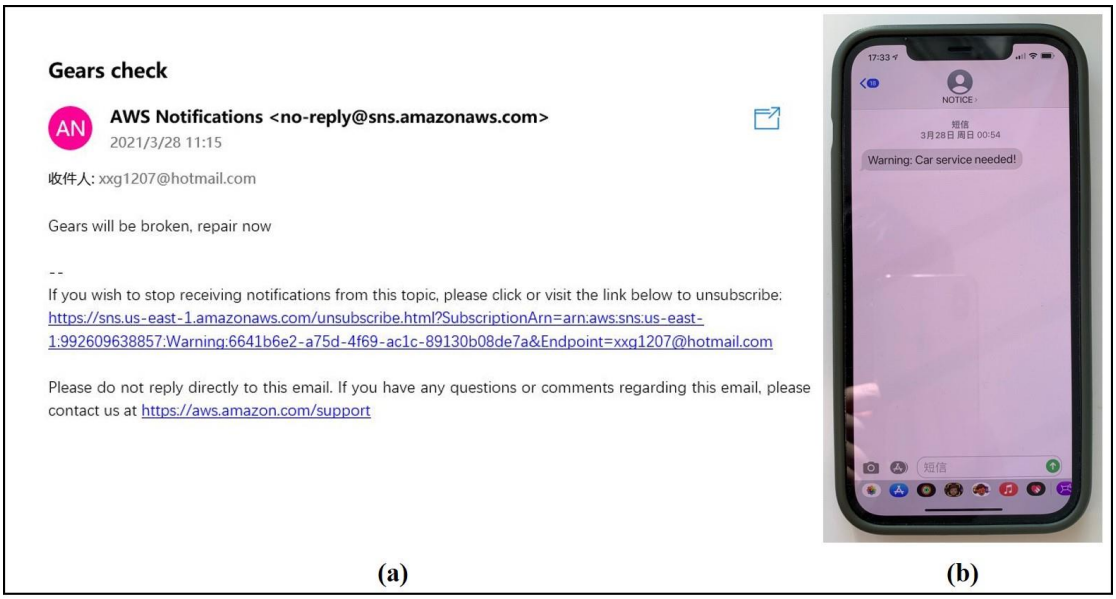

Fig. 7.5 Warning message sent through: (a) email address (b) SMS

This design realised real-time communication between polymer gears and other objects (such as people), and it offered high flexibility to the content they communicated not only the value of wear. Many other kinds of data such as the temperature, the level of noise and the RPM of polymer gears can be extracted with the help of related add-in sensors. It will help gain more effective testing data as well as better data management for polymer gears in various scenarios such as cars, motorbikes and different gear research labs. Data can be collected and gathered promptly then analysed on one platform.

When it comes to the cost, one application such as a car and a motorbike only needs one set of this design. Different gear boxes can share this design by simply adding more sensors. Compared to the cost of test rigs, it’s cost-efficient. What is more, the author

believes the data will become the actual asset in the near future. A design that brings in more data will definitely deserve a try.

8 Conclusions and discussion

8.1 General conclusions

At the end of the research a number of achievements have been made. First, customed polymer gears have been designed and manufactured using injection moulding (IM). A full control of the gears manufacturing was obtained by material selection and IM parameter setting. Secondly, the relationship between the IM parameter settings and the performance of polymer gears have been studied and some practical suggestions were raised to help manufacture better quality polymer gears. Thirdly, as one of the most prevalent polymer gear materials, POM gears have been studied and inherent differences between the performance of homopolymer acetal (POM-H) and copolymer acetal (POM-C) were found, which cannot be ignored. The findings provide more insight for the future applications of POM gears. Fourthly, a new polymer gears analysis procedure was introduced. It placed more emphasis on the material science by applying several advanced characterisation methods to gear materials. The process was proven effective as it successfully explained the real reason why the POM-H and POM-C gears performed differently. Finally, a new polymer gear testing solution based on the IoT and cloud technology was innovated to monitor polymer gears status in real-time.

For the gears manufacturing, different kinds of gear shapes as well as IM mould designs were compared. Following trials and upgrades, the best quality design among them was finally chosen. Instead of purchasing polymer gears from the market directly, taking charge of gears design as well as manufacturing brought many advantages to research such as lower material cost and more flexibility during the manufacturing process. What is more, it not only offered polymer gears with good quality such as symmetry in shrinkage but also kept the gear teeth profile design the same as with the previously studied polymer gears in the author's research team. This meant the current study kept the continuity and compatibility of the research findings on polymer gears.

The relationship between the IM parameter settings and the wear performance of polymer gears were studied. It was found that the IM parameter settings can influence the performance of polymer gears and an approximately 44% disparity in service life length between the best and the worst performances was recorded in this study. The

ranking of these influential factors from high to low is melting temperature, holding pressure, injection speed, cavity temperature.

POM gears are one of the most prevalent polymer gears in industry and they were frequently studied by academic research. In this study, two commercial grades of acetal based on POM-H and POM-C were injection moulded into gears respectively and their wear performance were compared as a further research on POM gears. The results showed that not only the POM-H gears had about 35% better service life than POM-C ones, but also other noticeable differences were discovered in failure mechanism, thermal and mechanical characteristics as well in this study.

As a conclusion generated from the big data of research publications about polymer gears, polymer science and polymer gear performance are two of the most important topics, but they have not been strongly connected yet, which means it was lack of evidence to explain the polymer gear performance from the material science aspect. This research not only targeted the issue but also offered some suggestions, which was a new gear analysis procedure focusing on the material science aspect. The procedure was proved effectively in this research as it successfully revealed the reason why the POM-C and POM-H gears performed differently which was spotted previously. A series of material analysis techniques were applied such as CT-scan, microtome, samples sectioning and X-Ray at the Diamond synchrotron facility (Harwell, UK). This analysis procedure was applied to investigate the reasons for performance differences between POM-H and POM-C gears. Findings illustrated the reason behind the differences was the crystallinity status of POM gears and the resultant failure modes.

Finally, a real-time status recording solution for polymer gears was created utilising sensor technology. It was based on the IoT and the cloud technology, which offered the ability to transport related data of polymer gears including but not limited to the wear, temperature and RPM to the cloud platform. The data were stored in a relational database; thus, it will be convenient for future usage. What is more, specific design functions were created via python to enable the real-time gear status monitoring. Once the wear or surface temperature exceeded the set values, the warning messages will be sent to the users automatically through both email and SMS. This solution helps gain more experimental data of polymer gears. In theory, any equipment using gears with an internet connection can deploy this design and real working conditions can be

transported to the cloud platform. This design has the advantages of low cost, high mobility and high customisation and is highly suited to incoming demands and application in connected autonomous vehicles (CAV). Another prominent advantage of this design is that instead of a separate testing on polymer gears in the laboratory, it is able to collect the performance data directly during the implementation from any device using gears including printers and motorbikes. Last but not least, it also contributes to the application of polymer gears as the design is a real-time monitor on performance. Once the abnormality is detected, or a minimum wear point reached, maintenance can be deployed. This could potentially extend both service life and replace routine wear checks.

8.2 Contribution to new knowledge

- Literature Review Design

A bibliometrics method was applied to review the big picture in polymer gears. This revealed the weak link between polymer gears and material science. Further, the author created a novel python script to automatically summarise the papers to examine previous research more efficiently.

- Methodology

Full control of all aspects in polymer gears manufacturing was attempted including the material, manufacturing process: tool design and IM parameter settings, gear testing and characterisation. This enables new finding on POM to be realised.

- IoT

This thesis reports a new design for an IoT cloud-based solution to help gain more experimental data of polymer gears. This design breaks the limitation of testing data about polymer gears coming from laboratory research and opens a field for in-service application monitoring.

In summary, this research is data driven and evidence based. The challenges of the polymer gear study and implementation were identified from big data analysis and solved with the help of experimental data. The findings and this data driven method are highly valuable to the knowledge of polymer gears.

8.3 Recommendations for future work

8.3.1 Effect of IM parameter settings on gear performance

It was concluded that the IM parameter settings had an influence on the performance of polymer gears but the physical phenomenon behind that was not studied in depth. It is recommended to explore this link further.

8.3.2 POM-H and POM-C gear comparison

The comparison between POM-H and POM-C based gears was undertaken, but as it was focused on industrial applications, commercial material was used in this study. A comparison between pure POM-H and POM-C manufactured gears is therefore recommended.

8.3.3 Implementation of IoT Polymer gear analysis

The newly created polymer gear analysis procedure was successfully applied on a study case in this research. More studies referring to this procedure are recommended to see whether more useful information can be obtained for the polymer gears IoT solution in real applications.

The proposed architecture of the cloud based IoT solution for polymer gears is recommended for deployment to test this design on real applications such as motorbikes and improve upon the concept in practice.

8.3.4 Other recommendations

There are other wider areas to be investigated as the outcomes of this research. For example, a comparison could be taken between IM and 3D printing polymer gears using the methods described here. Further, finding material formulas which are specifically designed for polymer gears which can bring better gear performance. There is a need to create more general simulation models which can predict the gear performance in advance without the need for experiments. And finally, there continues to be a need for reliable standards for polymer gears to guide gear design and operation in future years.

References

1. de Solla Price, D.J., *On the origin of clockwork, perpetual motion devices, and the compass*. 2019: Good Press.
2. Lewis, M., *Gearing in the ancient world.* Endeavour, 1993. **17**(3): p. 110-115.
3. White, J., Walton, D., and Weale, D. *The beneficial effect of tip relief on plastic spur gears*. in *Technical papers of the annual technical conference-society of plastics engineers incorporated*. 1998. Society of plastics engineers inc.
4. Gear, S. and Committee, S.T., *Gear design, manufacturing, and inspection manual*. Vol. 15. 1990: SAE International.
5. Hertz, H., *Ueber die beruehrung elastischer koerper (on contact between elastic bodies).* Gesammelte werke (Collected works), 1895. **1**(1): p. 156-160.
6. Avery, J., *Injection molding alternatives: a guide for designers and product engineers*. 1998: Hanser Verlag.
7. Bozdana, A.T. and Eyercioğlu, Ö., *Development of an expert system for the determination of injection moulding parameters of thermoplastic materials: EX-PIMM.* Journal of Materials Processing Technology, 2002. **128**(1-3): p. 113-122.
8. Yousef, S., et al., *Wear characterization of carbon nanotubes reinforced polymer gears.* IEEE transactions on nanotechnology, 2013. **12**(4): p. 616-620.
9. Dearn, K., Kukureka, S., and Walton, D., *Engineering polymers and composites for machine elements.* Handbook of Polymer Tribology, 2018: p. 441-479.
10. Yelle, H.J., *Design of thermoplastic gears with an involute tooth profile.* 1978.
11. BS, B.S., *Specification for non-metallic spur gears.* 1987.
12. Mao, K., *A new approach for polymer composite gear design.* Wear, 2007. **262**(3-4): p. 432-441.
13. Association, A.G.M., *Standard Nomenclature-Gear Tooth Wear and Failure.* AGMA, Pub, 1951. **110**: p. 43-55.
14. Halling, J., *A contribution to the theory of mechanical wear.* Wear, 1975. **34**(3): p. 239-249.
15. Marshek, K.M. and Chan, P.K., *Qualitative analysis of plastic worm and worm gear failures.* Wear, 1981. **66**(3): p. 261-271.
16. Häger, A. and Davies, M., *Short-fibre reinforced, high-temperature resistant polymers for a wide field of tribological applications*, in *Composite materials series*. 1993, Elsevier. p. 107-157.
17. Durand, J., Vardavoulias, M., and Jeandin, M., *Role of reinforcing ceramic particles in the wear behaviour of polymer-based model composites.* Wear, 1995. **181**: p. 833-839.
18. Arkles, B., Goodhue, R., and S, G. *Wear characteristics of fluoropolymer composites*. in *Abstracts of papers of the american chemical society*. 1974. Amer chemical soc 1155 16th ST, NW, Washington, DC 20036.
19. Nak-Ho, S. and Suh, N.P., *Effect of fiber orientation on friction and wear of fiber reinforced polymeric composites.* Wear, 1979. **53**(1): p. 129-141.
20. Cirino, M., Friedrich, K., and Pipes, R., *The effect of fiber orientation on the abrasive wear behavior of polymer composite materials.* Wear, 1988. **121**(2): p. 127-141.
21. Yu, J., et al., *Study on the toughening mechanism of POM/NBR blends.* Acta Polymerica Sinica, 2000. **1**.

22. Bahadur, S. and Gong, D., *The role of copper compounds as fillers in the transfer and wear behavior of polyetheretherketone.* Wear, 1992. **154**(1): p. 151-165.
23. Legocka, I., et al., *Preliminary study on application PE filler modified by radiation.* Radiation Physics and Chemistry, 2000. **57**(3-6): p. 411-416.
24. Hilarius, K., et al., *Influence of shear deformation on the electrical and rheological properties of combined filler networks in polymer melts: Carbon nanotubes and carbon black in polycarbonate.* Polymer, 2013. **54**(21): p. 5865-5874.
25. Friedrich, K., Zhang, Z., and Schlarb, A.K., *Effects of various fillers on the sliding wear of polymer composites.* Composites science and technology, 2005. **65**(15-16): p. 2329-2343.
26. Friedrich, K., Reinicke, R., and Zhang, Z., *Wear of polymer composites.* Proceedings of the Institution of Mechanical Engineers, Part J: Journal of Engineering Tribology, 2002. **216**(6): p. 415-426.
27. Voort, J.V. and Bahadur, S., *The growth and bonding of transfer film and the role of CuS and PTFE in the tribological behavior of PEEK.* Wear, 1995. **181**: p. 212-221.
28. Xue, Q.-J. and Wang, Q.-H., *Wear mechanisms of polyetheretherketone composites filled with various kinds of SiC.* Wear, 1997. **213**(1-2): p. 54-58.
29. Lancaster, J.K., *Composites for aerospace dry bearing applications*, in *Composite Materials Series*. 1986, Elsevier. p. 363-396.
30. Briscoe, B., *The tribology of composite materials: a preface*, in *Composite Materials Series*. 1993, Elsevier. p. 3-15.
31. Stachowiak, G. and Stachowiak, G., *The effects of particle characteristics on three-body abrasive wear.* Wear, 2001. **249**(3-4): p. 201-207.
32. Biron, M., *Thermoplastics and thermoplastic composites*. 2018: William Andrew.
33. Friedrich, K., Fakirov, S., and Zhang, Z., *Polymer composites: from nano-to macro-scale*. 2005: Springer Science & Business Media.
34. FRIEDRICH, K., *Wear of reinforced polymers by different abrasive counterparts*, in *Composite Materials Series*. 1986, Elsevier. p. 233-287.
35. Xing, X. and Li, R., *Wear behavior of epoxy matrix composites filled with uniform sized sub-micron spherical silica particles.* Wear, 2004. **256**(1-2): p. 21-26.
36. Rong, M.Z., et al., *Structure–property relationships of irradiation grafted nano-inorganic particle filled polypropylene composites.* Polymer, 2001. **42**(1): p. 167-183.
37. Wang, Q., et al., *The effect of particle size of nanometer ZrO2 on the tribological behaviour of PEEK.* Wear, 1996. **198**(1-2): p. 216-219.
38. Zhao, Q. and Bahadur, S., *The mechanism of filler action and the criterion of filler selection for reducing wear.* Wear, 1999. **225**: p. 660-668.
39. Rao, M., *An investigation of the tribological behaviour of polymeric materials in rolling-sliding contacts*. 1997, University of Birmingham.
40. Ikegami, K., Kikushima, K., and Shiratori, E., *Effects of material constitutions on the strength of fiber reinforced plastic gears.* Composites science and technology, 1986. **27**(1): p. 43-61.
41. Gurunathan, C., Kirupasankar, S., and Gnanamoorthy, R., *Wear characteristics of polyamide nanocomposite spur gears.* Proceedings of the Institution of

Mechanical Engineers, Part J: Journal of Engineering Tribology, 2011. **225**(5): p. 299-306.
42. Senthilvelan, S. and Gnanamoorthy, R., *Damping characteristics of unreinforced, glass and carbon fiber reinforced nylon 6/6 spur gears.* Polymer testing, 2006. **25**(1): p. 56-62.
43. Senthilvelan, S. and Gnanamoorthy, R., *Influence of reinforcement on composite gear metrology.* Mechanism and machine theory, 2008. **43**(9): p. 1198-1209.
44. Kurokawa, M., Uchiyama, Y., and Nagai, S., *Performance of plastic gear made of carbon fiber reinforced poly-ether-ether-ketone.* Tribology International, 1999. **32**(9): p. 491-497.
45. Kurokawa, M., et al., *Performance of plastic gear made of carbon fiber reinforced polyamide 12.* Wear, 2003. **254**(5-6): p. 468-473.
46. SHALYGIN, V., *PRODUCTION OF HIGH-CAPACITY PLASTICS GEARS USING A ROLLING METHOD.* RUSSIAN ENGINEERING JOURNAL-USSR, 1970. **50**(4): p. 53-&.
47. Tsukamoto, N., *Investigation about the Strength of Plastic Gears: 1st Report, The Strength of Nylon Gears which have Counter-Crowning.* Bulletin of JSME, 1979. **22**(173): p. 1685-1692.
48. Tsukamoto, N., *Investigation about the strength of plastic gear. II: abrasion of the nylon gear for power transmission, meshing with the steel gear.* 1981.
49. Mao, K., *A numerical method for polymer composite gear flash temperature prediction.* Wear, 2007. **262**(11-12): p. 1321-1329.
50. Mao, K., Chetwynd, D., and Millson, M., *A new method for testing polymer gear wear rate and performance.* Polymer Testing, 2020. **82**: p. 106323.
51. Walton, D., et al., *The efficiency and friction of plastic cylindrical gears Part 2: Influence of tooth geometry.* Proceedings of the Institution of Mechanical Engineers, Part J: Journal of Engineering Tribology, 2002. **216**(2): p. 93-104.
52. Walton, D. and Goodwin, A., *The wear of unlubricated metallic spur gears.* Wear, 1998. **222**(2): p. 103-113.
53. Liu, H., et al., *Starved lubrication of a spur gear pair.* Tribology International, 2016. **94**: p. 52-60.
54. Liu, H., et al., *Tribological evaluation of a coated spur gear pair*. Tribology International, 2016. **99**: p. 117-126.
55. Zhu, C., et al., *Research on dynamical characteristics of wind turbine gearboxes with flexible pins.* Renewable Energy, 2014. **68**: p. 724-732.
56. Tang, J.-y., Chen, S.-y., and Zhong, J., *A improved nonlinear model for a spur gear pair system.* Engineering mechanics, 2008. **25**(1): p. 217-223.
57. Tang, J.-y., et al., *Effect of static transmission error on dynamic responses of spiral bevel gears.* Journal of Central South University, 2013. **20**(3): p. 640-647.
58. Terashima, K., Tsukamoto, N., and Shi, J., *Development of plastic gears for power transmission: Power Transmission Mechanism of Plastic Gears.* Bulletin of JSME, 1984. **27**(231): p. 2061-2068.
59. Tsukamoto, N., Yano, T., and Sakai, H., *Noise and transmission efficiency under deformation of tooth form of nylon gear.* Bulletin of JSME, 1982. **25**(207): p. 1465-1473.
60. Small, H., *Co‐citation in the scientific literature: A new measure of the relationship between two documents.* Journal of the American Society for information Science, 1973. **24**(4): p. 265-269.

61. Chen, C., *CiteSpace: a practical guide for mapping scientific literature*. 2016: Nova Science Publishers Hauppauge, NY.
62. Chen, C. and Leydesdorff, L., *Patterns of connections and movements in dual‐map overlays: A new method of publication portfolio analysis.* Journal of the association for information science and technology, 2014. **65**(2): p. 334-351.
63. Chen, C., Ibekwe‐SanJuan, F., and Hou, J., *The structure and dynamics of cocitation clusters: A multiple‐perspective cocitation analysis.* Journal of the American Society for information Science and Technology, 2010. **61**(7): p. 1386-1409.
64. Brown, R., *Handbook of polymer testing: physical methods*. 1999: CRC press.
65. Grellmann, W., Seidler, S., and Anderson, P.I., *Polymer testing*. 2007: Hanser Munich.
66. Li, W., et al., *An investigation on the wear behaviour of dissimilar polymer gear engagements.* Wear, 2011. **271**(9-10): p. 2176-2183.
67. Mao, K., et al., *The wear resistance improvement of fibre reinforced polymer composite gears.* Wear, 2019. **426**: p. 1033-1039.
68. Mao, K., Hooke, C., and Walton, D., *The wear behaviour of polymer composite gears.* Journal of Synthetic Lubrication, 1996. **12**(4): p. 337-345.
69. Mao, K., et al., *The wear and thermal mechanical contact behaviour of machine cut polymer gears.* Wear, 2015. **332**: p. 822-826.
70. Gauvin, R., Patrick, G., and Henry, Y., *Maximum surface temperature of the thermoplastic gear in a non-lubricated plastic/steel gear pair*. Ecole Polytechnique de Montreal. J Manuf Process, 1984: p. 20-27.
71. Hooke, C.J., et al., *Measurement and Prediction of the Surface Temperature in Polymer Gears and Its Relationship to Gear Wear*. Journal of Tribology, 1993. **115**(1): p. 119-124.
72. Kansal, G., Rao, P., and Atreya, S., *Study: temperature and residual stress in an injection moulded gear.* Journal of Materials Processing Technology, 2001. **108**(3): p. 328-337.
73. Mao, K., et al., *Polymer gear surface thermal wear and its performance prediction.* Tribology International, 2010. **43**(1-2): p. 433-439.
74. Dearn, K., et al., *Applications of dry film lubricants for polymer gears.* Wear, 2013. **298**: p. 99-108.
75. Yu, G., et al., *Examination on the wear process of polyformaldehyde gears under dry and lubricated conditions.* Friction, 2020: p. 1-13.
76. Chen, J., Juarbe, F., and Hanley, M., *Factors affecting fatigue strength of nylon gears.* 1981.
77. Senthilvelan, S. and Gnanamoorthy, R., *Effect of rotational speed on the performance of unreinforced and glass fiber reinforced Nylon 6 spur gears.* Materials & design, 2007. **28**(3): p. 765-772.
78. Mao, K., et al., *Friction and wear behaviour of acetal and nylon gears.* wear, 2009. **267**(1-4): p. 639-645.
79. Yakut, R., Düzcükoğlu, H., and Demirci, M., *The load capacity of PC/ABS spur gears and investigation of gear damage.* Archives of Materials Science, 2009. **42**: p. 42.
80. Zorko, D., et al., *Durability and design parameters of a Steel/PEEK gear pair*. Mechanism and Machine Theory, 2019. **140**: p. 825-846.

81. Evans, S. and Keogh, P., *Efficiency and running temperature of a polymer–steel spur gear pair from slip/roll ratio fundamentals.* Tribology International, 2016. **97**: p. 379-389.
82. Indurkhya, N. and Damerau, F.J., *Handbook of natural language processing*. Vol. 2. 2010: CRC Press.
83. Tremblay, T., *Injection Modeling Part Design for Dummies*. 2011: John Wiley & Sons.
84. Buffat, P. and Borel, J.P., *Size effect on the melting temperature of gold particles.* Physical review A, 1976. **13**(6): p. 2287.
85. Harper, C.A., *Handbook of plastic processes*. 2006: John Wiley & Sons.
86. Li, X.-P., Zhao, G.-Q., and Yang, C., *Effect of mold temperature on motion behavior of short glass fibers in injection molding process.* The International Journal of Advanced Manufacturing Technology, 2014. **73**(5-8): p. 639-645.
87. Siegmann, A., Buchman, A., and Kenig, S., *Residual stresses in polymers III: The influence of injection‐molding process conditions.* Polymer Engineering & Science, 1982. **22**(9): p. 560-568.
88. Bryce, D.M., *Plastic injection molding: manufacturing process fundamentals*. 1996: Society of Manufacturing Engineers.
89. Lu, X. and Khim, L.S., *A statistical experimental study of the injection molding of optical lenses.* Journal of Materials Processing Technology, 2001. **113**(1-3): p. 189-195.
90. Jansen, K., Van Dijk, D., and Husselman, M., *Effect of processing conditions on shrinkage in injection molding.* Polymer Engineering & Science, 1998. **38**(5): p. 838-846.
91. Trotignon, J. and Verdu, J., *Effect of the holding pressure on the skin‐core morphology of injection‐molded polypropylene parts.* Journal of applied polymer science, 1990. **39**(5): p. 1215-1217.
92. Yu, C.J. and Sunderland, J., *Determination of ejection temperature and cooling time in injection molding.* Polymer Engineering & Science, 1992. **32**(3): p. 191-197.
93. Goodship, V., *ARBURG practical guide to injection moulding*. 2017: Smithers Rapra.
94. Hu, Z. and Mao, K., *An investigation of misalignment effects on the performance of acetal gears.* Tribology International, 2017. **116**: p. 394-402.
95. Goodship, V., *Injection Moulding: A Practical Guide*. 2020: De Gruyter.
96. Goodship, V.D., Middleton, B., and Cherrington, R., *Design and manufacture of plastic components for multifunctionality: structural composites, injection molding, and 3D printing*. 2015: William Andrew.
97. Hsu, C.-M., *Improving the electroforming process in optical recordable media manufacturing via an integrated procedure.* Engineering Optimization, 2004. **36**(6): p. 659-675.
98. Erzurumlu, T. and Ozcelik, B., *Minimization of warpage and sink index in injection-molded thermoplastic parts using Taguchi optimization method.* Materials & design, 2006. **27**(10): p. 853-861.
99. Ozcelik, B. and Erzurumlu, T., *Comparison of the warpage optimization in the plastic injection molding using ANOVA, neural network model and genetic algorithm.* Journal of Materials Processing Technology, 2006. **171**(3): p. 437-445.

100. Tang, S.H., et al., *The use of Taguchi method in the design of plastic injection mould for reducing warpage.* Journal of Materials Processing Technology, 2007. **182**(1-3): p. 418-426.
101. Fischer, J., *Handbook of molded part shrinkage and warpage*. 2012: William Andrew.
102. Li, K., et al., *Warpage optimization of fiber-reinforced composite injection molding by combining back propagation neural network and genetic algorithm.* The International Journal of Advanced Manufacturing Technology, 2017. **90**(1-4): p. 963-970.
103. Chiang, K.-T. and Chang, F.-P., *Application of grey-fuzzy logic on the optimal process design of an injection-molded part with a thin shell feature.* International Communications in Heat and Mass Transfer, 2006. **33**(1): p. 94-101.
104. Pareek, R. and Bhamniya, J., *Optimization of injection moulding process using Taguchi and ANOVA.* International Journal of Scientific & Engineering Research, 2013. **4**(1): p. 1-6.
105. Chen, W.-C., et al., *A neural network-based approach for dynamic quality prediction in a plastic injection molding process.* Expert systems with Applications, 2008. **35**(3): p. 843-849.
106. Breeds, A., et al., *Wear behaviour of acetal gear pairs.* Wear, 1993. **166**(1): p. 85-91.
107. Xu, G. and Yang, Z., *Multiobjective optimization of process parameters for plastic injection molding via soft computing and grey correlation analysis.* The International Journal of Advanced Manufacturing Technology, 2015. **78**(1-4): p. 525-536.
108. Gong, G., Chen, J.C., and Guo, G., *Enhancing tensile strength of injection molded fiber reinforced composites using the Taguchi-based six sigma approach.* The International Journal of Advanced Manufacturing Technology, 2017. **91**(9): p. 3385-3393.
109. Hooke, C., et al., *Wear and friction of nylon-glass fibre composites in non-conformal contact under combined rolling and sliding.* Wear, 1996. **197**(1-2): p. 115-122.
110. Kukureka, S., et al., *The effect of fibre reinforcement on the friction and wear of polyamide 66 under dry rolling–sliding contact.* Tribology International, 1999. **32**(2): p. 107-116.
111. Apichartpattanasiri, S., Hay, J., and Kukureka, S., *A study of the tribological behaviour of polyamide 66 with varying injection-moulding parameters.* Wear, 2001. **251**(1-12): p. 1557-1566.
112. Mao, K., *The performance of dry running non-metallic gears*. 1993, The University of Birmingham.
113. Mao, K., et al., *Friction and wear behaviour of acetal and nylon gears.* Wear, 2009. **267**(1-4): p. 639-645.
114. Mao, K., et al., *Polymer gear surface thermal wear and its performance prediction.* Tribology International, 2010. **43**(1-2): p. 433-439.
115. Mao, K., et al., *The wear and thermal mechanical contact behaviour of machine cut polymer gears.* Wear, 2015. **332-333**: p. 822-826.
116. Taguchi, G., *Quality engineering in Japan.* Communications in Statistics-Theory and Methods, 1985. **14**(11): p. 2785-2801.

117. Taguchi, G., *Introduction to quality engineering: designing quality into products and processes*. 1986.
118. Taguchi, G., *System of experimental design; engineering methods to optimize quality and minimize costs*. 1987.
119. Selden, P.H., *Sales process engineering: a personal workshop*. 1996: ASQ Quality Press.
120. Rao, R.S., et al., *Xylitol production by Candida sp.: parameter optimization using Taguchi approach.* Process Biochemistry, 2004. **39**(8): p. 951-956.
121. Rao, R.S., et al., *The Taguchi methodology as a statistical tool for biotechnological applications: a critical appraisal.* Biotechnology Journal: Healthcare Nutrition Technology, 2008. **3**(4): p. 510-523.
122. Rosa, J.L., et al., *Electrodeposition of copper on titanium wires: Taguchi experimental design approach.* Journal of materials processing technology, 2009. **209**(3): p. 1181-1188.
123. uz Zaman, U.K., et al., *Impact of fused deposition modeling (FDM) process parameters on strength of built parts using Taguchi's design of experiments.* 2018: p. 1-12.
124. Ealey, L.A., *Quality by design: Taguchi methods and US industry*. 1988: ASI Press Dearborn, Michingan.
125. Sadeghi, B., *A BP-neural network predictor model for plastic injection molding process.* Journal of materials processing technology, 2000. **103**(3): p. 411-416.
126. Lau, H., et al., *Neural networks for the dimensional control of molded parts based on a reverse process model.* Journal of Materials Processing Technology, 2001. **117**(1-2): p. 89-96.
127. Li, E., Jia, L., and Yu, J., *A genetic neural fuzzy system-based quality prediction model for injection process.* Computers & chemical engineering, 2002. **26**(9): p. 1253-1263.
128. He, F. and Zhang, L., *Mold breakout prediction in slab continuous casting based on combined method of GA-BP neural network and logic rules.* International Journal of Advanced Manufacturing Technology, 2018. **95**.
129. Khadilkar, A., Wang, J., and Rai, R., *Deep learning–based stress prediction for bottom-up SLA 3D printing process.* The International Journal of Advanced Manufacturing Technology, 2019. **102**(5): p. 2555-2569.
130. Looney, C.J.N.Y., *Pattern recognition using neural networks: Oxford University Press.* 1997.
131. Basma, A.A., Kallas, N.J.G., and Engineering, G., *Modeling soil collapse by artificial neural networks.* 2004. **22**(3): p. 427-438.
132. Hornik, K., *Approximation capabilities of multilayer feedforward networks.* Neural networks, 1991. **4**(2): p. 251-257.
133. Leshno, M., et al., *Multilayer feedforward networks with a nonpolynomial activation function can approximate any function.* Neural networks, 1993. **6**(6): p. 861-867.
134. Battiti, R., *First-and second-order methods for learning: between steepest descent and Newton's method.* Neural computation, 1992. **4**(2): p. 141-166.
135. Liang, Y., et al., *Successive approximation training algorithm for feedforward neural networks.* Neurocomputing, 2002. **42**(1-4): p. 311-322.
136. Shepherd, A.J., *Second-order methods for neural networks: Fast and reliable training methods for multi-layer perceptrons*. 2012: Springer Science & Business Media.

137. Liu, W. and Dai, Y., *Minimization algorithms based on supervisor and searcher cooperation.* Journal of Optimization Theory and Applications, 2001. **111**(2): p. 359-379.
138. Garson, D.G., *Interpreting neural network connection weights.* 1991.
139. Sha, B., et al., *Investigation of micro-injection moulding: Factors affecting the replication quality.* Journal of Materials Processing Technology, 2007. **183**(2-3): p. 284-296.
140. *Hostaform C 9021 GV1/20 datasheet*. 19.03.2021]; Available from: https://tools.celanese.com/products/datasheet/SI/HOSTAFORM%C2%AE%20C%209021%20GV120.
141. Rutherford, A., *Introducing ANOVA and ANCOVA: a GLM approach*. 2001: Sage.
142. Fine, T.L. and Mukherjee, S., *Parameter convergence and learning curves for neural networks.* Neural Computation, 1999. **11**(3): p. 747-769.
143. Finnoff, W. *Diffusion approximations for the constant learning rate backpropagation algorithm and resistence to local minima*. in *Advances in Neural Information Processing Systems*. 1993.
144. Gori, M. and Maggini, M., *Optimal convergence of on-line backpropagation.* IEEE transactions on neural networks, 1996. **7**(1): p. 251-254.
145. Kursun Bahadir, S., Sahin, U.K., and Kiraz, A., *Modeling of surface temperature distributions on powered e-textile structures using an artificial neural network.* Textile Research Journal, 2019. **89**(3): p. 311-321.
146. Altan, M., *Reducing shrinkage in injection moldings via the Taguchi, ANOVA and neural network methods.* Materials & Design, 2010. **31**(1): p. 599-604.
147. Snyder, L., *At the "PEEK" of the polymer food chain.* Gear Technol, 2010: p. 26-28.
148. Tajima, Y. and Itoh, T., *Creep rupture properties of homopolymer, copolymer, and terpolymer based on poly (oxymethylene).* Journal of applied polymer science, 2010. **116**(6): p. 3242-3248.
149. Jiao, T., Chang, T., and Caputo, A., *Load transfer characteristics of unilateral distal extension removable partial dentures with polyacetal resin supporting components.* Australian dental journal, 2009. **54**(1): p. 31-37.
150. Savion, Y., et al., *The use of Dental D (polyacetal resin) as an alternative for chrome-cobalt removable partial denture: a case report.* Refu'at ha-peh veha-shinayim (1993), 2001. **18**(3-4): p. 30-1, 108.
151. Starr, J.B., *Acetal resins.* Kirk‐Othmer Encyclopedia of Chemical Technology, 2000.
152. Collins, G.L., Wissbrun, K.F., and Kim, H., *Elastomeric acetal polymers*. 1990, Google Patents.
153. Ibeh, C.C., *Thermoplastic materials: properties, manufacturing methods, and applications*. 2011: CRC Press.
154. McKeen, L.W., *10 - High-Temperature/High-Performance Polymers*, in *The Effect of Long Term Thermal Exposure on Plastics and Elastomers*, L.W. McKeen, Editor. 2014, William Andrew Publishing: Oxford. p. 209-238.
155. Archodoulaki, V.M., Lüftl, S., and Seidler, S., *Degradation behavior of polyoxymethylene: Influence of different stabilizer packages.* Journal of applied polymer science, 2007. **105**(6): p. 3679-3688.
156. Hertzberg, R., Skibo, M., and Manson, J., *Fatigue crack propagation in polyacetal.* Journal of Materials Science, 1978. **13**(5): p. 1038-1044.

157. Stohler, F.R. and Berger, K., *Stabilization of polyacetals.* Die Angewandte Makromolekulare Chemie: Applied Macromolecular Chemistry and Physics, 1990. **176**(1): p. 323-332.
158. Ghazali, W.M., et al. *A review on failure characteristics of polymer gear*. in *MATEC Web of Conferences*. 2017. EDP Sciences.
159. Jain, M., Patil, S., and Ghosh, S. *A review on failure characteristics of polymeric gears*. in *AIP Conference Proceedings*. 2019. AIP Publishing LLC.
160. Singh, A.K., Siddhartha, and Singh, P.K., *Polymer spur gears behaviors under different loading conditions: A review*. Proceedings of the Institution of Mechanical Engineers, Part J: Journal of Engineering Tribology, 2018. **232**(2): p. 210-228.
161. Tsukamoto, N., *Argument on plastic gears for power transmission.* JSME international journal. Ser. C, Dynamics, control, robotics, design and manufacturing, 1995. **38**(1): p. 1-8.
162. Singh, P.K. and Singh, A.K., *An investigation on the thermal and wear behavior of polymer based spur gears.* Tribology International, 2018. **118**: p. 264-272.
163. Goriparthi, B.K., et al., *Mechanical, wear and fatigue behavior of functionalized CNTs reinforced POM/PTFE composites.* Materials Research Express, 2019. **6**(6): p. 065051.
164. Yousef, S., et al., *Wear characterizations of polyoxymethylene (POM) reinforced with carbon nanotubes (POM/CNTs) using the paraffin oil dispersion technique.* JOM, 2016. **68**(1): p. 288-299.
165. Černe, B., et al., *Influence of temperature-and strain rate-dependent viscoplastic properties of polyoxymethylene on the thermo-mechanical response of a steel-polyoxymethylene spur gear pair.* Materials Today Communications, 2020. **25**: p. 101078.
166. Cerne, B., et al. *Flash temperature analysis method for polymer gears with consideration of deviations in meshing kinematics*. in *ASME 2019 International Design Engineering Technical Conferences and Computers and Information in Engineering Conference*. 2019. American Society of Mechanical Engineers Digital Collection.
167. Evans, S. and Keogh, P., *Wear mechanisms in polyoxymethylene spur gears.* Wear, 2019. **428**: p. 356-365.
168. Trobentar, B., et al., *Experimental failure analysis of S-polymer gears.* Engineering Failure Analysis, 2020: p. 104496.
169. Singh, A.K. and Singh, P.K., *Noise Emission from ABS, POM and HDPE Spur Gears-A Comparative Study*. Materials Today: Proceedings, 2018. **5**(9): p. 18038-18044.
170. *Hostaform C 9021 datasheet*. 19.03.2021]; Available from: https://tools.celanese.com/products/datasheet/SI/HOSTAFORM%C2%AE%20C%209021.
171. *Delrin 500T BK602 datasheet*. 19.03.2021]; Available from: https://dupont.materialdatacenter.com/en/products/datasheet/SI/Delrin%C2%AE%20500T%20BK602.
172. Menard, K.P. and Menard, N., *Dynamic mechanical analysis.* Encyclopedia of Analytical Chemistry: Applications, Theory and Instrumentation, 2006: p. 1-25.
173. Kalin, M. and Kupec, A., *The dominant effect of temperature on the fatigue behaviour of polymer gears.* Wear, 2017. **376**: p. 1339-1346.

174. Lancaster, J. *Relationships between the wear of polymers and their mechanical properties*. in *Proceedings of the Institution of Mechanical Engineers, Conference Proceedings*. 1968. SAGE Publications Sage UK: London, England.
175. Huang, Y.-F., et al., *Self-reinforced polyethylene blend for artificial joint application.* Journal of Materials Chemistry B, 2014. **2**(8): p. 971-980.
176. Abdelbary, A., *Wear of polymers and composites*. 2015: Woodhead Publishing.
177. Jarvis, D.L., *Polyacetals*, in *Brydson's Plastics Materials*. 2017, Elsevier. p. 513-526.
178. McKeen, L.W., *Fatigue and tribological properties of plastics and elastomers*. 2016: William Andrew.
179. Doll, N.P., *Modeling thermomechanical behavior of polymer gears*. 2015, University of Wisconsin--Madison.
180. Harrass, M., Friedrich, K., and Almajid, A., *Tribological behavior of selected engineering polymers under rolling contact.* Tribology International, 2010. **43**(3): p. 635-646.
181. Samyn, P. and De Baets, P., *Friction and wear of acetal: A matter of scale.* Wear, 2005. **259**(1-6): p. 697-702.
182. Evans, M., Akehurst, S., and Keogh, P. *Wear mechanisms in polyoxymethylene (POM) spur gears*. in *5th World Tribology Congress, WTC 2013*. 2014. University of Bath.
183. Friedrich, K., *Friction and wear of polymer composites*. 2012: Elsevier.
184. Aberšek, B. and Flašker, J., *Stress intensity factor for cracked gear tooth.* Theoretical and applied fracture mechanics, 1994. **20**(2): p. 99-104.
185. *Buehler Polishing Application Guide*. 2021 02.02.2021]; Available from: https://www.buehler.com/assets/Brochures/English/Consumables/FN01465_0216_Polishing_Application_Guide_WEB.pdf.
186. *Buehler Mounting Application Guide*. 2021 02.02.2021]; Available from: Mounting Application Guide.
187. Jebawi, K.A., et al., *Hot compaction of polyoxymethylene, part 1: Processing and mechanical evaluation.* Journal of applied polymer science, 2006. **102**(2): p. 1274-1284.
188. Berer, M., et al., *Fatigue fracture properties and morphology of Polyoxymethylene (POM) plates produced under moderate processing conditions.* International Journal of Polymer Science, 2018. **2018**.
189. Plummer, C., Béguelin, P., and Kausch, H.H., *The temperature and strain‐rate dependence of mechanical properties in polyoxymethylene.* Polymer Engineering & Science, 1995. **35**(16): p. 1300-1312.
190. Li, J., et al., *Crystalline Characteristics, Mechanical Properties, Thermal Degradation Kinetics and Hydration Behavior of Biodegradable Fibers Melt-Spun from Polyoxymethylene/Poly (l-lactic acid) Blends.* Polymers, 2019. **11**(11): p. 1753.
191. Pielichowska, K., *The influence of molecular weight on the properties of polyacetal/hydroxyapatite nanocomposites. Part 1. Microstructural analysis and phase transition studies.* Journal of polymer research, 2012. **19**(2): p. 1-16.
192. Andrzejewski, J., Skórczewska, K., and Kloziński, A., *Improving the Toughness and Thermal Resistance of Polyoxymethylene/Poly (lactic acid) Blends: Evaluation of Structure–Properties Correlation for Reactive Processing.* Polymers, 2020. **12**(2): p. 307.

193. Zsidai, L., et al., *Friction and thermal effects of engineering plastics sliding against steel and DLN-coated counterfaces.* Tribology Letters, 2004. **17**(2): p. 269-288.
194. Marsavina, L., et al., *Experimental determination and comparison of some mechanical properties of commercial polymers.* Mater. Plast, 2010. **47**(1).
195. Arp, H.P.H., et al., *Review of polyoxymethylene passive sampling methods for quantifying freely dissolved porewater concentrations of hydrophobic organic contaminants.* Environmental toxicology and chemistry, 2015. **34**(4): p. 710-720.
196. Langlois, P., *Tooth Contact Analysis—Off Line of Action Contact and Polymer Gears.* Gear Technology, 2017: p. 84-91.
197. Naikwadi, S. and Lonare, G., *Design & Analysis of Helical Gear of Washing Machine Transmission System.* 2018.
198. Winkler, A., *Concerning the Structural Assessment of Metal/Polymer Gear Wheels Using the Finite Element Method.*
199. *The manual of GP2Y0A21YK0F distance measuring sensor*. 05.04.2021]; Available from: https://www.pololu.com/file/0J85/gp2y0a21yk0f.pdf.
200. *The manual of Infrared obstacle avoidance sensor*. 05.04.2021]; Available from: https://www.rhydolabz.com/documents/26/IR_line_obstacle_detection.pdf.
201. *The manual of DFRobot SEN0263 temperature sensor*. 05.04.2021]; Available from: https://media.digikey.com/pdf/Data%20Sheets/DFRobot%20PDFs/SEN0263_Web.pdf.
202. *The manual of Raspberry pi*. 05.04.2021]; Available from: https://www.raspberrypi.org/magpi-issues/MagPi84.pdf.
203. *The manual of Ardunio nano*. 05.04.2021]; Available from: https://www.mouser.com/pdfdocs/Gravitech_Arduino_Nano3_0.pdf.
204. *SIM8200EA-M2 5G HAT for Raspberry Pi*. 2021.04.05]; Available from: https://www.waveshare.com/sim8200ea-m2-5g-hat.htm.

Appendix A Results of automatic literature review

Title	Year;Author	Abstract	SUMMARY
Life and damage mode modeling applied to plastic gears	2015 Alencar Bravo a, Demagna Koffi a, Lotfi Toubal a,*, Fouad Erchiqui b	There is a need to correctly dimension gears for an application with an understanding of how the gear will deteriorate until final failure. However, this task has been difficult because engineers must consider the complexity of gear meshing phenomena combined with the gear material- specific properties and application particularities to determine the critical failure and maintenance points. This article provides a review of the multiple damage modes of plastic gears, including both general and plastic gear-exclusive modes. This article reviews the different branches of the damage problem, performs a combined solution of finite element analysis (FEA) and validated analytical equations for plastic gears. With this knowledge, a unique system of analysis of gear utilization perspectives that evaluates all possible damaging processes is built. By applying a range of normal loads on a plastic gear, it was verified that the damage mode depends highly on the applied load. The identification of the proper damage mode allows preventive actions to be taken because the limits of plastic gears and the optimal usage are identified. With this damage modeling strategy, the designer can skip several steps in reaching a decision regarding plastic gear applicability. This synthesis represents significant progress for plastic gear damage modeling because the major factors of plastic gear functioning and the damage factors are observed. © 2015 Elsevier Ltd. All rights reserved. 1.	Conclusions The simulation of plastic gear meshing and damage is complex but important to correctly dimension gears for an application with the understanding of how the gear will deteriorate until final failure. With this strategy of damage modeling, the results will enable the designer to skip many steps of the decisions based on the field of plastic gear applicability. Although the combination of various equations and literature datasets imposes some limits on the model utilization, this strategy demonstrates significant progress for plastic gear damage modeling because all major factors of plastic gear functioning and damage are observed. This consideration allows the software to drastically increase the simulation speed, allowing for results in a reasonable amount of time. The general simulation results are shown in Table 5. The result is a dimensionless number that is the opposite of the safety factor definition, meaning that the gear will be damaged if it is higher than 1.The results show that the gear continues to fail due to generalized temperature damage until 37,500 N/m.5E-07 99 50.1860 Table 5 Results in terms of the normal load.08E+06 Wear [cycles] Bold results represent the damage mode according to load conditions. The general simulation results are shown in Table 5. A graphical representation of the damage modes as a function of the normal load is shown in Fig.The results show that the gear continues to fail due to generalized temperature damage until 37,500 N/m. 12 shows the range of all damage modes related to the normal force. 13 shows the root fatigue life and wear life in detail. In this article, different branches of the plastic gear damaging problem were reviewed, and a toolbox was developed to be used together with a FEA and Matlab software to enable a designer to accurately forecast the behavior of plastic gears. Tests continued using the same 1000 N/m, but the step was increased to 2500 N/m after 20,000 N/m because actions can be easily taken to improve the gear performance against thermal damage (by improving the convection coefficient). The gear first suffered a static surface failure, which means that, from the first turn, significantly decreasing the gear performance and accelerating very much the degradation with damage model synergy leading to catastrophic failure.91% of the flexural strength, it supports the maximum normal load with the minimal relative decrease in performance. The second and third lines provide the root stress by the flexural resistance and the contact stress by the compression stress, Fig. The next lines provide the bulk and surface temperatures. It is preferable to use the actual stress by the strength as a reference because it is a generalization and provides an estimate of how much stress the root can support.
1 Introduction	Error	Error	Error
Efficiency and running temperature of a polymer–steel spur gear pair from slip/roll ratio fundamentals	2016 S.M. Evans a,b,n, P.S. Keogh a	a r t i c l e i n f o A new methodology to predict the transient operational temperature of a polymer–steel gear pair under Article history: Received 24 November 2015 loaded running is presented. For the involute gear form, rolling and sliding leads to a loss of gear effi- Received in revised form: ciency and generation of heat in the contact zone. The power dissipated is used to set the conditions for a 29 January 2016 series of rod on disc experiments. The rod-on-disc data are processed in a time averaging procedure, Accepted 31 January 2016 which allows prediction of the complete gear temperature. This is assessed with analytical and finite Available online 6 February 2016 element models to validate the predicted temperature rise against the experimental data. The sig- Keywords: nificance is that the experimental procedures may be used to assess gear thermal performance without Gear efficiency testing full gear pairs. Polymer gear temperature & 2016 Elsevier Ltd. All rights reserved. Slip/roll ratio Temperature prediction 1.	error
Finite element method model to predict bulk and flash temperatures on polymer gears	2018 Carlos M.C.G. Fernandes a,*, Diogo M.P. Rocha c, Ramiro C. Martins a, Luis Magalh˜aes b,	A R T I C L E I N F O A FEM thermal model was implemented to predict the bulk and flash temperature of gears in general and polymer Keywords: gears in particular. Bulk temperature Flash temperature Using the capabilities of a gear power loss model previously validated, a solution for the temperature rise and Polymer gears distribution along the tooth is suggested. The accuracy of the power loss model is decisive for the prediction of FEM gear temperature field by FEM model. The FEM model was validated with experimental results from the literature. The model allows to predict the bulk temperatures for oil jet, dip lubrication or non-lubricated conditions. The FEM model allows an higher accuracy on the calculation of the load carrying capacity of polymer gears, whose mechanical properties are critically dependent on the bulk temperature. 1.	Conclusions The present work allows to verify that: (cid:4) combining a well calibrated power loss model [14,54,55] with a thermal FEM model produces accurate results; (cid:4) the FEM thermal model is able to predict bulk temperatures both for oil jet, dip lubrication or non-lubricated conditions; (cid:4) a transient FEM thermal model was implemented.4 Nm of input torque presented a higher discrepancy from the experimental result, no matter the rotational speed. Experimental results vs. A value higher than zero would result in very high bulk temperature predictions, which are not observed in the experiments. Both experimental results as well as FEM model results are presented in Fig. Temperature field result for 95 Nm load torque. Table 5 Difference [%] between current FEM model and experimental results [7]. The mesh was created in the same way as described previously and the resulting mesh is presented in Fig. The temperature results along the path of contact are presented in Fig. Results discussion The simulations carried on using polymer gears, i. Such results were achieved considering that the coefficient of friction for POM is lower than for any metallic gear considered. The results show that Aluminium presents similar heat conductivity capacity to copper but with a lower material density. 12 shows the influence of speed on the temperature field. in order to implement the FEM model, Heaviside functions and polynomials were used to describe the behaviour of power loss, Hertz half width and contact radius along the path of contact (or meshing time) as shown in Appendix C. The time steps show that the heat source is moving towards the tooth tip and the maximum temperature predicted are 187 (cid:7)C and 34 (cid:7)C, respectively. The results show that Aluminium presents similar heat conductivity capacity to copper but with a lower material density. In order to solve the coefficient of friction problem, "low-loss" gear tooth geometries should be implemented since it is a good way to improve the efficiency and decrease the heat gener- ation as shown in previous studies [2,13,14,52,53]. Equation (25) shows that the lower the gear loss factor (HVL) is, the lower the heat flux on the meshing tooth will be. under 10 Nm and 1000 rpm show that the maximum surface temperature of 187 (cid:7)C surpasses the melting point of the material which is usually around 175 (cid:7)C. The algorithm implementation can be resumed with the flowchart shown in Fig.17 shows the heat flux generated locally. is 200 times higher than the average heat flux applied for a steady-state condition. Bulk temperature on dip lubricated FZG type A gears.A standardized FZG back-to-back scuffing test according to DIN 51534 whose bulk temperatures were measured can be found in Ref.11 and were tested for the operating conditions found in Table 4. ΔT ¼ T bulk (cid:3) T bulk (37) max min The temperature gradient found for the POM gear tooth is quite high compared to the other materials due to the fact that POM's thermal conductivity is very low. However, analyzing in the current model the values pre- dicted for 17. However, the bulk temperature was almost independent of the rotational speed. However, the heat transfer on the gear sides is lower under dry lubrication conditions than for oil lubricated conditions because the ambient air has very low density and viscosity,' s work [25] focuses on the analysis of the flash temperature with Blok's solution provided for the quasi-steady approximation and flash temperature estimation.4 Nm of input torque presented a higher discrepancy from the experimental result, no matter the rotational speed. The current FEM simulation used the material properties presented in Table B. The mesh was also created in Gmsh® with 51142 nodes and 282834 elements, as presented in Fig. Both experimental results as well as FEM model results are presented in Fig. T5 ¼ TA þ TB þ TF (36) Equation (34) predicts a bulk temperature of 109 (cid:7)C for the operating conditions presented in Table B. The mesh was created in the same way as described previously and the resulting mesh is presented in Fig. The temperature results along the path of contact are presented in Fig. 14, the characteristics presented in Table B. The mesh was created in the same way as described previously and the resulting mesh is presented in Fig. The temperature results along the path of contact are presented in Fig. 14, the initial temperature solution is presented in Fig. 14a and the flash temperature distribution is presented for each meshing position in Fig.21 Tribology international 120 (2018) 255–268 The difference between the maximum and minimum temperatures achieved within the gear tooth are presented in Fig. Improve thermal behaviour on polymer gears To understand the influence of gear material on the operating tem- perature, steel, POM, copper and aluminum were considered, whose properties are presented in Table 8. A type C14 FZG gear with the geo- metric characteristics presented in Table B.5 Material 16MnCr5 The mechanical properties as well as the thermal characteristics of the gear materials are presented in Table 8.8 Specific heat, c [J/(kg K)] 493 The physical properties of lubricating oils are presented in Table B. The approximations of the contact radius and the Hertz half-width is presented in Figs. Tribology international 120 (2018) 255–268 Take for instance, the heat flux applied for the meshing time t ¼ 3.4898-10(cid:3)3 s at contact radius r ¼ 28.9102 mm, which is represented in Fig. In order to solve the coefficient of friction problem, "low-loss" gear tooth geometries should be implemented since it is a good way to improve the efficiency and decrease the heat gener- ation as shown in previous studies [2,13,14,52,53]. To solve the low thermal conductivity problem of polymer materials as well as the heat transfer by convection to air, the hybridization of the gear material, combining different materials can be a good path to follow.

Title	Year;Author	Abstract	SUMMARY
Friction and wear behaviour of acetal and nylon gears	2009 K. Mao a,*, W. Li b, C.J. Hooke c, D. Walton c	a r t i c l e i n f o The current paper will present an extensive investigation of polymer gear (acetal and nylon) friction Article history: Received 25 August 2008 and wear behaviour. First, a unique test method for polymer gear wear will be described in brief and Received in revised form 27 October 2008 later used in the extensive investigation of acetal and nylon gear wear. Initial tests were performed using Accepted 27 October 2008 acetal pinions with acetal gears, and nylon pinions with nylon gears, with further investigation carried out using dissimilar polymer gears. In this case the driver and driven effects on the gear wear behaviour Keywords: was also considered when dissimilar materials were used. For acetal against acetal gears, it was found Wear rate that the acetal gear wear rate increased dramatically when the load reached a critical value for a specific Polymer gear geometry and the gear surface showed slow wear, with a low specific wear rate if the gear was loaded Gear surface temperature below this critical value. It was found that the surface temperature was the dominant factor influencing Gear mesh and contact path the wear rate and an initial relationship between gear surface temperature and gear load capacity has been established and further developed. Experimental investigation on nylon gears was also carried out and different failures have been found compared to acetal gears, such as gear root and pitch fractures. The most interesting observation from the experimental work is the significant difference in wear behaviour when running acteal against nylon gears, especially the low wear rate when acetal is used as the driver gear. Crown Copyright © 2009 Published by Elsevier B.V. All rights reserved. compare the design standards with test data [4]. The only known attempt to compare various polymer composite gear design stan- dards was carried out by Walton and Shi [5] and their results are sufficient to show that wide discrepancies between standards exist. These standards were developed from metal gear practice in which the rating of a gear tooth is determined by either bending strength or surface durability, often referred to as wear. However, none of those standards correlated well with the test results [6,7] and the polymer composite gears' potential use in power transmission is limited due to the lack of understanding of their behaviour under load as well as physical limits created by the low strength of poly- mer. A great number of experimental works involved meshing poly- mer gears with steel pinions, e.g. nylon against steel [8,9]. Since accurate moulded gears are now available, it is necessary to learn more about the performance of these gears under different operating conditions. The study of moulded gear performance is important for economic reasons because these can be mass pro- duced at a fraction of the cost compared to machined gears. In general, the available information on polymer composite gear wear is still limited and the existing gear surface temperature predic- tions require further study to be used for practical applications. For instance, Hachman and Strickle's equation [10] was based on the assumption that a lubricant does not contribute significantly 1.	A new method for acetal performance prediction Test results show that the form of failure for acetal gears is pre- dominately wear. For comparison of the theory and test results, ambient temperature and speed effects on the transition torque have been investigated. A theoretical analysis of the effect of running speeds on the transition torque was also carried out and the results are shown in Fig. Sliding is away from the pitch line on the driver resulting in a wear 'trough' and toward the pitch line on the driven resulting a wear 'pip', giving rise to the particular wear pattern. Comparison of experimental and predicted results. This approach of critical load for acetal gear has been applied to the experimental applications and good agreements have been achieved between the prediction and test results.shown to be close to those found using a semi-analytical method assuming no internal hysteresis and constant material properties. It is shown that Blok's solution can be used to provide a quasi-steady approximation for mean flash temperature estimation as shown in Fig. A new method for acetal performance prediction Test results show that the form of failure for acetal gears is pre- dominately wear. Essentially the gears are operating in the same manner as a gear pump and this situation is shown schematically in Fig. A theoretical analysis of the effect of running speeds on the transition torque was also carried out and the results are shown in Fig. It may also be noted that the pitch circle diameter is identical (60 mm) for all the tested gears shown in Fig. That the fracture only occurred on the driving gear may be related to the tooth wear as shown in Fig. It is very interesting to see the different wear and failure behaviour when running dissimilar material, especially when acetal as driver against nylon showing better performance compared with the sit- uation reversed. It may be noted that, because of the low thermal conductivity of acetal, conduction through the gear teeth will not raise the temperature of the co-contacting surface. It may also be noted that the pitch circle diameter is identical (60 mm) for all the tested gears shown in Fig. (9), the torque required to cause surface melting, termed the transition torque, can be found. This could provide a new design method of rating gears in which the gear trains are first designed according to the speed ratios required and the transmissible power, estimated on the basis of operating below the transition torque.shown to be close to those found using a semi-analytical method assuming no internal hysteresis and constant material properties. However, if the gear teeth start and end meshing posi- tions are considered, Blok's solution is inaccurate and the current approach should be used. However, if the gear teeth start and end meshing positions are considered, Blok's solution is inaccurate and the current approach should be used [21]. A new method for acetal performance prediction Test results show that the form of failure for acetal gears is pre- dominately wear. The nylon gear friction and wear performances are completely different when compared to that of acetal gear and the gear fail- ures are mainly root and pitch fractures instead of surface wear. It is very interesting to see the different wear and failure behaviour when running dissimilar material, especially when acetal as driver against nylon showing better performance compared with the sit- uation reversed.927(cid:3)T a – r2) c(cid:7)Zb(r2 Blok's solution can be used to provide a quasi-steady approx- imation that is for mean flash temperature estimation. However, if the gear teeth start and end meshing positions are considered, Blok's solution is inaccurate and the current approach should be used [21]. It is shown that Blok's solution can be used to provide a quasi-steady approximation for mean flash temperature estimation as shown in Fig. It can be seen that there is good agreement between the predicted and measured val- ues. This approach of critical load for acetal gear has been applied to the experimental applications and good agreements have been achieved between the prediction and test results.
E-mail: fzg@fzg.mw.tum.de Potential of oil-lubricated cylindrical plastic gears Christian HASL*, Christopher ILLENBERGER*, Peter OSTER*, Thomas TOBIE* and Karsten STAHL* *Gear Research Centre (FZG), Technical University of Munich (TUM), Faculty of Mechanical Engineering, Boltzmannstr. 15, 85748 Garching, GERMANY Received: 14 April 2017:		Bending strength of injection molded polyacetal test gears is investigated in back-to-back testing using oil- lubrication. To validate state of the art calculation methods, tooth geometries with a variable number of teeth are investigated, maintaining a constant center distance and transmission ratio. To enable testing on a constant level of tooth temperature for variable torque loads and speeds, occurring tooth temperatures are measured and considered in latter testing. Test results show that bending strength of tooth geometries with a higher number of teeth stand higher tooth root stresses acc. to VDI 2736, as the calculated tooth root stress is too high due to negligence of load-induced deflections. A modified method for calculating tooth root stress considers load- induced deflections, allowing to trace back the failures of the different tooth geometries to a common stress level. Therefore, a possible approach to consider the actual contact ratio for tooth root stress calculation of steel- plastic spur gear pairings is proposed. Keywords : Cylindrical thermoplastic gears, Bending strength, Actual contact ratio, Polyacetal (POM) 1.	Consequently, it can be concluded, that the method is adequate to consider the effect of the load-induced deflections of steel-POM pairings based on a standard rack profile (DIN 867, 1986). Outlook Considering the results of further experimental tests, the aim is to derive a modified method to calculate bending strength of highly loaded (= oil-lubricated) thermoplastic gears. This includes the validation of existing fatigue strength yet contained in (VDI 2736, 2014). to the herein proposed, modified approach results in a common tooth root stress level for all investigated test gear geometries. Potential and Challenges Regarding the evaluation of the test results, it is shown that the prediction of the sustainable torque acc. If the in this way determined bending strength data are subsequently used to design gears with lower numbers of teeth compared to the test gears, the results acc. The test results confirm that load-induced deflections are a significant factor. Recalculating the root stresses of all performed gear tests, based on this approach, results in a common stress level for all examined tooth geometries. Potential and Challenges Regarding the evaluation of the test results, it is shown that the prediction of the sustainable torque acc. He shows that a conventional steel-polyamide tooth geometry can transmit a maximum power of about 4 kW without instant thermal damage. Acknowledgements FZG would like to thank German Research Foundation (DFG, Deutsche Forschungsgemeinschaft, HO 1339/47-1) for their kind sponsorship of this research project focusing on bending strength of thermoplastic gears. If the in this way determined bending strength data are subsequently used to design gears with lower numbers of teeth compared to the test gears, the results acc. This, however, can cause that feasibility checks of considered plastic gear applications with higher numbers of teeth, on the basis of (VDI 2736, 2014), may be negative due to the negligence of elasto-kinematic potential of certain tooth geometries regarding bending strength. This geometrically induced effect causes the power density of plastic gear pairs to rise with higher numbers of teeth due to the stronger tendency to load-induced increase in contact ratio. corresponding to the cycles at failure of the test gears However, analog recalculation acc. to (VDI 2736, 2014) significantly vary for each investigated tooth geometry although the same material is used. Recalculating the root stresses of all performed gear tests, based on this approach, results in a common stress level for all examined tooth geometries. Using oil-lubrication (and 'cooling') most herein presented tests took place at a test gear revolution speed of 2200 to 3000 rpm meaning a continuous power of up to almost 30 kW which is e. Hence, the good correlation of tolerable tooth root stress acc.

Title	Year;Author	Abstract	SUMMARY
Study of rolling contact fatigue behavior of a wind turbine gear based on damage-coupled elastic-plastic model	2018 , Caichao Zhu, Peitang Wei, Zhangdong Sun	i n f o a r t i c l e Keywords: Gear contact fatigue has a significant influence on the reliabilities of heavy-duty gear-driven machines such Elastic-plastic as wind turbines. In the present work, an elastic-plastic contact fatigue model in conjunction with damage is Kinematic hardening developed to study the fatigue performance of a megawatt wind turbine gear. In this model, damages caused by Rolling contact fatigue (RFC) both elasticity and plasticity are considered based upon the continuous damage mechanics (CDM) in the frame of Continuous damage mechanics (CDM) ABAQUS using a user material subroutine. Damage accumulation and the evolution of the material mechanical Crack initiation properties are recorded during the fatigue crack initiation life. The contributions of elastic damage and plastic Wind turbine gear damage are distinguished. The effect of applied load on the contact fatigue life is studied and the stress–life curve is fitted based upon the numerical data. Results show that under a wide range of load conditions, the contact fatigue of the gear is always dominated by the elastic damage. analytically investigated the deformation behaviour of carburized steels, and found cyclic softening phenomenon under both axial and torsional loading conditions. The evolution of rolling contact fatigue displays as the gradual dete- rioration of mechanical properties of critical material points. Damage continuously accumulates within the high-stressed region till a criti- cal damage value is reached as the crack initiates. Hence the contin- uous damage mechanics (CDM) may provide a potential way to explore the mechanism of rolling contact fatigue. Ringsberg [13] developed a crack initiation prediction model considering the damage summation, but only limited to low-cycle fatigue and ratcheting failure. A crystal finite element method coupled with CDM was used to analyse the ini- tiation of subsurface fatigue cracks in rolling bearings by Raje et al. [14] , but this method did not consider the damage caused by plastic deformation. Very recently Zhan et al. [15] derived damage-coupled elastic-plastic constitutive equations to calculate the fatigue damage of a fuselage structure. However, this loading condition is quite different compared with the gear rolling contact state. Applications of continu- ous elastic-plastic damage theory on gear contact fatigue crack initiation problems are rarely reported. In the current work, a damage-coupled elastic-plastic numerical model is developed to analyse the contact fatigue crack initiation of a heavy-duty wind turbine gear. Elastic and plastic damage evolution equations are considered simultaneously. We aim to figure out the de- tailed evolution of the fatigue damage and the mechanical properties during repeated gear meshing process, and distinguish the contribution of the shear stress amplitude and the plastic deformation on the contact fatigue life, respectively. 1.	Main conclusions can be summarized as follows: (1) The increment of the cumulative plastic strain is quite small dur- ing the first 1. (3) Under an elastic load, no plastic damage generates at early load- ing cycles, but plastic damage finally appears because the gradual accumulation of damage results in the deterioration of the mate- rial mechanical properties and eventually leads to plastic defor- mation. Simulation results of effect of load on fatigue life are in good agreement with previous work reported by others. Acknowledgments This work is financially supported by the National Natural Science Foundation of China (Grant Nos. However, as the first crack initiates, the distribution of the material properties in the horizontal direc- tion is no longer uniform and the critical damage appears only on certain local material points.
An investigation of misalignment effects on the performance of acetal gears	2017 Zedong Hu *, Ken Mao	A R T I C L E I N F O This paper concentrates on the effects of misalignment on meshing behaviour of acetal gears as hardly any Keywords: Acetal spur gear misalignment investigations on polymer gears in the existing literature. The experimental results show that the Misalignment wear of acetal gears is insensitive to radial and axial misalignments but sensitive to yaw and pitch mis- Wear debris morphology alignments which degrade the conjugate contact action. Yaw misalignment leads to 'scoop' wear marks near Micro cracks tooth pitch points. Pitch misalignment causes 'superimposed palisade' wear marks and micro cracks near tooth roots. Compared with metal gears, the effects of small pitch angle on acetal gears are insignificant which may be linked closely to polymer's low elastic modulus. Strikingly different wear striations and various debris morphologies are observed by using scanning electronic and optical microscope (SEM, OM) and misalignment effects can be noted. 1.	Some possible causal wear mechanisms, and general conclusions are presented in this paper. General conclusions The wear behaviours of machine cut acetal gears subject to radial, axial, yaw and pitch misalignments have been investigated. A number of conclusions may be drawn from this work. Experimental results and discussions The wear phenomena of a nominally properly aligned gear pair is described in Section 3.1, and the results compared with those of misalignment tests outlined in Sections 3. Test results on axial misalignment and discussions AM test results presented in Fig. Taking the results of alignment (see Fig. 4(b) demonstrates that AM leads to edge loading, resulting in a contact area reduction, subsequently contact pressure increase. Test results on radial misalignment and discussions RM has two cases that actual centre distance (CD) is less than and greater than the nominal CD. The RM test results are shown in Fig. The later results in an increase in the gear profile contact ratio, which could be proved by Fig. Test results on yaw misalignment and discussions Three different sets of acetal gear tests subjected to YM were con- ducted, at yaw angles α of 0. Test results on pitch misalignment and discussions Three different sets of pitch misalignment (PM) experiment were carried out respectively at pitch angles of β ¼ 0. PM test results are presented in Fig. This will reduce the tooth strength resulting in gears failing prematurely. It results in an increase in local CS and hence the initial wear rate in- creases greatly. Detailed experiment results are presented and discussed. b) An increase in axial gap, pitch and yaw angles results in an increase in wear rate. 11(b) shows that initial wear rate approaches a linear relationship with PM angle. However, linear wear rate increases as PM angle in- creases within 0. There are four main categories of misalignment for gear engagement under imperfect conditions shown in Fig. Experimental method A unique gear test rig shown in Fig. Perfect alignment test In the alignment test, two regimes of debris shown in Fig. SEM examinations of the driving and driven teeth shown in Fig. 5(b) shows that the wear rate tends to increase as axial gap increases. In addition to powdery wear debris, handful of long strip-like wear debris shown in Fig. Noticeable load distribution shift could be seen from SEM micrographs of worn tooth surfaces shown in Fig. The RM test results are shown in Fig.45 mm) shown in Fig. 7(a) is parallel to that of alignment, and its initial wear rate is close to that of alignment but linear wear rate is slightly lower than that of alignment as shown in Fig.3 mm) shown in Fig. 7(a) are steep in initial phase, and their initial wear rates shown in Fig. Long strip-like debris shown in Fig. 8(a) dropped instantly once initiated and needle-like debris shown in Fig. SEM micrographs of worn tooth surfaces are shown in Fig. 9(a) shows that the wear curves with yaw angles of 0. 9(b) shows that wear rates increase as yaw Tribology International 116 (2017) 394–402 angle increases.3 mm), spindly needle-like wear debris shown in Fig. 11(a) shows that PM wear curves are similar to that of alignment when pitch angle does not exceed a threshold value. However it still shows the wear trend. 12 shows the OM micro- graphs of snowflake-like wear debris. 13 shows the pitting over driving root, the intersection of 'superimposed palisade' wear marks and micro cracks on tooth root respectively. d) Uneven wear is shown in the SEM micrographs of axial misalignment tests due to edge loading. It is noted that the initial wear rate is directly proportional to the axial gap and the linear wear rate appears slightly less linear to the axial gap. Note: CD is nominal centre distance 60 mm, CD' is the actual centre distance, d presents radial gap, thus CD' ¼ CD þ d alignment d ¼ 0 mm. It is inter- esting to note that the worn tooth surfaces (Fig. Note that when a yaw angle α ¼ 1. Note: the plot of yaw angle α ¼ 0. As with alignment test, almost no visible differences of debris morphology was found when actual CD increases (d ¼ þ0. The snowflake like debris is found solely in Appendix A. The superimposed layers of 'palisade' wear striations tend to trap powdery Supplementary data related to this article can be found at http://dx. Experimental method A unique gear test rig shown in Fig. Of the four categories of misalignment, acetal gears are most sensitive to pitch misalignment in view of its unique wear marks-superimposed 'palisade', micro cracks near tooth roots and steep initial wear gradient. 2, was designed and manufac- tured at the University of Warwick with a capacity to continuously measure the gear surface wear, and also conduct the test in both align- ment and misalignment modes. To continuously measure and record the wear in real-time, a bespoke data-logging system was designed and made, consisting of a displacement measurement de- vice and a data-logging software. The non-contact displacement mea- surement device was designed by applying the principle that output voltage of Hall Effect sensor varies in response to an applied magnetic field. However their linear wear rates are not greater than that of alignment. However when actual CD diminishes, a strikingly different debris regime was observed. Copious debris scatters over driving tooth roots and driven tooth tips, however, not much as AM test (Fig. However it still shows the wear trend. There were no wood-shavings-like wear debris and large snowflake-like wear debris mentioned in tests of AM and PM, although the load was increased to 12NM. A slight increase in CD almost does not greatly impact acetal gears' performance, but a reduction in CD does affect significantly. Some possible causal wear mechanisms, and general conclusions are presented in this paper. The assembly photos of gear test rig and its wear mechanism are presented in detail in Ref. All the test data presented in this paper are obtained from machine cut acetal gear pairs running at a speed of 1000 rpm and a torque of 7. Test results on axial misalignment and discussions AM test results presented in Fig. PM test results are presented in Fig. Detailed experiment results are presented and discussed.

Title	Year;Author	Abstract	SUMMARY
A tribo-dynamic contact fatigue model for spur gear pairs	2017 ⇑	Article history: This study proposes a contact fatigue model for spur gears operating under the high speed condition Received 20 October 2016 where the dynamic behavior is evident. Realizing the tight relationship between the gear dynamics Received in revised form 12 January 2017 and the gear tribology, a six degree-of-freedom discrete dynamics model and a mixed elastohydrody- Accepted 17 January 2017 namic lubrication model for spur gears are bridged through an iterative numerical scheme to determine Available online 18 January 2017 the surface normal pressure and tangential shear under the tribo-dynamic condition, where the gear dynamics and the gear tribology interact. The resultant multi-axial stress fields (from these surface trac- Keywords: tions) on and below the surface are then used to assess the fatigue damage. A comparison between the Gear tribo-dynamic and quasi-static life predictions is performed to demonstrate the important role of the Tribo-dynamics gear tribo-dynamics in the fatigue damage. The impacts of the input torque, surface roughness and lubri- Contact fatigue cant temperature on the gear contact fatigue under the tribo-dynamic condition are also investigated. (cid:1) 2017 Elsevier Ltd. All rights reserved. model that incorporates the influence of the tribo-dynamic behav- ior for spur gear pairs. As a gear pair rotates in mesh, the periodic mesh stiffness and the transmission error are the main excitations that dictate the LOA vibrational motion. The alternating number of the tooth pairs in contact and the time-varying compliances (associated with the base rotation, the tooth bending and shear deflections, and the contact deformation) determine the former, and the manufactur- ing and mounting errors, the intentional micro-geometry modifi- cations, and the deformations due to loading define the latter. A massive number of studies have been carried out focusing on the modeling of the noise and vibration aspect of gears [13,14], using either a discrete lumped-parameter description [8–12,15,16] or a deformable finite element description [17–19]. These works pointed to the significant gear dynamic responses, especially in the vicinity of the resonances. Realizing the important role of the gear dynamic behavior in the lubrication performance of gear con- tacts, Wang and Cheng [20] evaluated the minimum film thickness under the dynamic loading condition, while assuming Hertzian pressure distributions. Employing the more sophisticated mixed elastohydrodynamic lubrication (EHL) formulation and a two degree-of-freedom (DOF) discrete dynamic description of a general spur gear pair, Li and Kahraman modeled the hydrodynamic film thickness and contact pressure distributions [8] as well as the gear mesh damping [12], demonstrating the tight relationship between the gear dynamics and the gear tribology. Coupling the gear dynamic response and the lubrication behavior in an iterative way, Li [10] and Li and Anisetti [11] examined the mechanical power loss and the flash temperature rise, respectively. Paouris 1.	However, it is noted, the large magnitudes of the LOA dynamic bearing force at the resonances may cause the bearing fatigue failure and then results in the gear failures indirectly even when the nonlinear tooth separation occurs. Employing an example unity ratio spur gear pair, the fatigue lives under the tribo-dynamic and the quasi-static conditions are compared to show large deviations, especially in the vicinities of the resonances where the RMS dynamic mesh force either peaks or drops (because of the tooth separation due to the nonlinear gear dynamics) abruptly. It is shown the quasi-static assumption can be valid only when the rotational speed is far away from the resonances, pointing to the necessity of the inclusion of the tribo-dynamic description in the high speed gear contact fatigue modeling. The lubricant temperature is shown to be able to lengthen the life evidently only when the input torque is relatively low. The surface roughness ampli- tude reduction is an effective method to improve the fatigue performance. The converged normal pressure and tangential shear are then used to determine the multi-axial stress fields on and below the surface, provided which, the contact fatigue crack nucleation life is then determined accord- ing to a multi-axial fatigue criterion.
The wear and thermal mechanical contact behaviour of machine cut polymer gears	2015 K. Mao n, P. Langlois 1, Z. Hu, K. Alharbi, X. Xu, M. Milson, W. Li, C.J. Hooke, D. Chetwynd	a r t i c l e i n f o The present paper will concentrate on an extensive investigation of machine cut acetal gear wear and Article history: Received 2 September 2014 thermal mechanical contact behaviour. The results for machine cut acetal gears will be compared to Received in revised form previously published results obtained for polymer gears manufactured through injection moulding. The 29 January 2015 machine cutting manufacturing process can be economical for small batch runs due to the expense of Accepted 30 January 2015 the mould for injection moulding. Injection moulding becomes economical for larger batches. A new and unique polymer gear test rig has been employed to investigate the polymer gear wear behaviour. The Keywords: unique test rig design allows the effect of misalignment on polymer gear engagement to be considered Polymer gears and the gear surface wear to be recorded continuously. Extensive experimental tests have been carried Wear out to investigate machine cut acetal gear wear performance. Further examinations have been carried Wear rate out using a scanning electron microscope to understand the gear wear mechanisms. An equation has Friction been presented to predict polymer gear flank temperature and correlated well with the tests. Surface temperature & 2015 Elsevier B.V. All rights reserved. Tip relief 1.	It can be concluded that machine cut acetal gears can be designed using the existing methods for injection moulded acetal gears. The test rig has been used to test the wear behaviour of machine cut acetal gears and the results compared with those previously published by the authors for acetal gears manufactured by injection moulding. Correlation between the predicted transition torque and the test results is good. The tests show that the wear rates for the machine cut and injection moulded acetal gears tested are independent of the manufacturing process. The tests further show therefore that the polymer gear wear rate for machine cut acetal gears will be increased dramatically when the load reaches a critical value for a specific geometry.A unique polymer gear test rig with the capabilities to include assembly misalignments and to continuously measure wear has been presented. Mao, A new approach for polymer composite gear design, Wear 262 (2007) 432–441. Mao, The Performance of Polymer Composite Gears (Ph. Nagai, Performance of plastic gear made of carbon fiber Int. Nagai, Performance of plastic gear made of carbon fiber reinforced poly-ether-ether-ketone: Part two, Tribol. Nagai, Performance of plastic gear made of carbon fiber reinforced polyamide 12, Wear 254 (2003) 468–473. Correlation between the predicted transition torque and the test results is good.

Title	Year;Author	Abstract	SUMMARY
An accelerated multilevel test and design procedure for polymer gears	2015 Aljaž Pogačnika, Jože Tavčar b,fl	Article history: This paper presents a new accelerated testing procedure for plastic gears that is based on several different Received 15 July 2014 levels of testing. The iterative testing procedure fulfils requests from the product development process. Accepted 3 October 2014 The following criteria are considered for testing: reduced number of tests, shorter test time and reliable Available online 13 October 2014 results for different applications. The proposed method was applied over the full range on a gear pair made from polyacetal (POM) and polyamide 6 (PA6). Different rotational speeds and torque loads, and Keywords: therefore different transferred powers, were used for testing. During testing, gear temperature and cycles Plastic gear to failure were monitored. The paper also includes a comparison between the measured and theoretically Accelerated testing calculated gear temperatures. A prediction of the life span on the basis of statistical methods is a part of Lifetime the proposed test procedure. The presented procedure enables testing within acceptable cost and time Failure modes consumption limits. The testing method can be reproduced and applied to plastic gears from different Temperature materials. Testing has shown that polymer gears fail in two typical ways: by fatigue and by sudden melting. The wear fail mode can be avoided by using an appropriate material pair. Fatigue can be measured by life span tests and is predictable. However, the melting of gears, which is a consequence of high gear temper- atures, is not easily predictable. In most cases, melting failure mode occurs during the first few hours of gear testing. For reliable and optimal gear design, gear testing cannot be avoided because the tribological interaction between gears is specific for each combination of materials. (cid:2) 2014 Elsevier Ltd. All rights reserved. 1.	Our conclusion is that the tribological characteristics of the polymer materials pair can be detected using preliminary tribolog- ical tests or standard gear test [21]. Preliminary step test results (first-level test) Preliminary step tests were conducted at 1176 rpm. The results of the step test are used as entry data for the second-level life span test. Cycles to failure The load level during life span testing is defined using the step test results and the target life span. (2) can be used for load determination during the life span test and was derived from the POM/PA6 test results. (2) to make direct connec- tion with step test results. According to the test results, the load level is then increased or decreased (Table 2) in a way that the testing condi- tions and expected life span are closer to the working conditions in application. The results of three life span tests of POM/PA6 gears at load 45. If the results of life span tests are plotted as points into Weibull probability form, an estimation of the parameter b can be seen as slope of the line through the points [31]. The distribution of the result of the life span test parameter b depends also on the material pair combination: for example, the PA6/PA6 gear pair distribution is wider. At least two life span tests results are needed for this calculation. By applying the regression data to the results from Table 6, the life span (in relation to the load and speed) can be calculated, as shown in Eq. Calculated results from Eq. (5) and (6) are the result of several iterations in Minitab software. Better results were achieved by using the third square root of life span, the sec- ond square root of load and the first square root of speed. Matching the life span in the prediction model to the test results is reliable, especially at speeds below 1. Based on these results, eight of the nine predicted life span values were shorter than the life span test values. Our test results using PA6 and PA6-30 show that glass fibre reinforcement improves the robustness of the gears towards strength over time. A larger difference reduces the reliabil- ity of the test results. The results from the test are the material data (rF and rH) for a spe- cific number of loads and bulk gear temperatures. The results are then transferred to the new application geometry based on the VDI 2736 root stress calculation and the bulk temperature model. There is an open question about the reliability of the test results if the gear modules and number of teeth in the applications are 100% higher or smaller than the test gears. Application of the test data The example demonstrates how to apply the test data result to a new gear pair design. The matrix life span test results for POM/PA6 gear pair (Fig. Based on results from Eq. This paper presents detailed results of the life span matrix test for the POM/PA6 material pair. The result is increased gear life span and temperature calculation accuracy and reliability. Typical gear bulk temperatures for different torque levels and material combinations are shown in Figs. The measured gears temperature is the bulk temperature in the “thermal view”, as shown in Fig. By applying the regression data to the results from Table 6, the life span (in relation to the load and speed) can be calculated, as shown in Eq. Our test results using PA6 and PA6-30 show that glass fibre reinforcement improves the robustness of the gears towards strength over time. Life span testing has shown that the PA6/PA6 gear pair (mod- ule = 1 mm) can transfer 36 W of power. Engineers are typically inter- ested in the life span with at least a 90% survival rate, which is often denoted B10 and indicates the number of cycles at which 10% of population will fail. Tavčar / Materials and Design 65 (2015) 961–973 967 Table 5 Calculated (according to VDI 2736) and measured gear bulk temperatures for the POM/PA6 gear pair at different load levels and speeds during the life span test; COF l = 0. Tavčar / Materials and Design 65 (2015) 961–973 Fig. Tavčar / Materials and Design 65 (2015) 961–973 969 4. Discussion and application Advanced gear drive design requires data on the mechanical and tribological properties of the materials. The presented accelerated testing procedure demonstrates a pragmatic approach of how to obtain the needed material data for optimised gear design. Tavčar / Materials and Design 65 (2015) 961–973 970 Table 7 Typical gear failure modes and mechanisms. Application of the test data The example demonstrates how to apply the test data result to a new gear pair design. There is a request to design a gear pair for a Fig. Tavčar / Materials and Design 65 (2015) 961–973 Fig. Design constraints Power = 4. Tavčar / Materials and Design 65 (2015) 961–973 speed of rotation. At higher tan- gential speeds, the calculated temperatures are in general lower than the measured values (Table 5), however at lower tangential speeds, the calculated temperatures are higher compared to the measured ones. For the first iteration, logarithmic model was used, however it did not pass the correlation criteria. A lower coef- ficient of friction and a lower temperature are key factors for better performance. Performing at least 6 tests from Table 2 is recommended: three speeds of rotation at two load levels. If the life span of the two tests differen- tiates by more than 30%, an additional test was performed. The existing models for temperature calculations can give a rough estimate, but they do not provide reliable calculations. The coefficients of friction for different pairs of materials are presented in Table 4. Temperatures The bulk temperature of the gears calculated according to VDI 2736 is presented in Table 5. according to the test conditions presented in Table 2. The cal- culated life span values for POM/PA6 gears with a 90% survival rate are presented in Table 6. (6) in a linear scale of cycles to failure are graphically presented in Fig. Typical gear failure modes are presented in Table 7. The presented accelerated testing procedure demonstrates a pragmatic approach of how to obtain the needed material data for optimised gear design.41 m/s is presented in Eq. The presented accelerated test model is an upgrade to existing models using data gathered with testing. The suggested testing and calculation procedure is presented using an example for a small appliance. There are several typical modes of running in the temper- ature increase of the gears: (A) After a gradual increase in the temperature at a specific level, the temperature stabilises (typical for gear made from glass-reinforced materials and gear pair with good matching POM/PA6-30). When forming equation for lifespan in relation to load and speed, the main criteria was good regression correlation and also simple form. There is a good match between the test gears and the test in application (between 20% and 30% of the life span).

Title	Year;Author	Abstract	SUMMARY
Review Article Polymer spur gears behaviors under different loading conditions: A review Akant Kumar Singh, Siddhartha and Prashant Kumar Singh Proc IMechE Part J: J Engineering Tribology 2018, Vol. 232(2) 210–228 ! IMechE 2017 Reprints and permissions: sagepub.co.uk/journalsPermissions.nav DOI: 10.1177/1350650117711595 journals.sagepub.com/home/pij		The significance of polymer gears to transmit power and motion is increasing continuously due to their inherent characteristics. Polymer gears have established themselves as attractive alternatives to traditional metal gears in plethora applications. They are light in weight, have lower inertia, and run noiseless than their metal counterparts. This article presents a comprehensive review of the research on polymer spur gears operating under low (0–8 Nm) and moderate (>8 and 417 Nm) loading conditions. Different polymers and polymer composites used till date for the fabrication of such gears are included along with different operating conditions. Various design features of polymer gears and tooth modification techniques for the improvement of the performance and durability of these gears have also been included in this review. The aspects of the modeling and simulation studies of the polymer gears are also emphasized in this paper for completeness of the review. The concept of hybrid gears is discussed along with their tribological properties. Various methods of manufacturing of polymer gears and their failure modes are discussed so as to make the article useful for researchers. Keywords Polymer gears, gear tooth wear, tooth modifications, performance improvements, modeling and simulation Date received: 12 October 2016; accepted: 28 April 2017	65 In it is concluded that the generated another study, sound power level is proportional to operating speed and load for most of the polymers except POM.107 They concluded that only melt tem- perature and packing time had a significant effect on Singh et al. Results concluded that optimizing the polymer gear tooth geometry could reduce the slip-ratio at the pitch point resulting in the improved service life of gears. It was concluded that when the cooling started, the stresses were max- imum at the teeth corner and when the cooling pro- gressed, the stresses were maximum at the root of the gear teeth. Conclusion and future scope The article has provided a review on various design features and performance characteristics of polymer and polymer composite gears. A hypothesis was made that using a hybrid (polymer injection molded metal) gear; a strong adhesion might occur between the coated polymer and the tooth surface resulting in an improved performance of gear. This hypothesis was verified in a further study. Results indicated a considerable reduction in the noise during the operation.71 A higher torque causes a higher amount of rotational lag that result in excessive wear in the dedendum region of polymer gears.72 The increase in rotational speed of gear results in less wear due to the decrease in single tooth contact period. The fibers aligned along the gear tooth involute profile restrict shrinkage of similar gear pair, the wear on the tooth surface is that results in less total profile deviation.89 Reinforcing the polymer matrix with nano-size The orientation of fibers in a direction parallel to sliding direction results in a low wear resistance. The values of these stres- ses showed satisfactory results. The simulated results of these gears showed improved load sharing and lower bend- ing and contact stresses compared to the standard gears. Results showed that the bending stresses decreased with increase in a number of teeth, module, and pressure angle. Also, the results of the numerical simu- lation revealed that amorphous polymer composites offered better resistance to warpage and shrinkage in comparison to crystalline polymer composite. The simulated results showed that the path of contact extended at the beginning and end of the meshing cycle due to the large tooth deflections of polymer gear teeth. Simulation results showed that the cumulative sliding wear had a significant effect on contact load due to the variation of tooth profile. Results concluded that optimizing the polymer gear tooth geometry could reduce the slip-ratio at the pitch point resulting in the improved service life of gears. The calculated results showed that the temperature, rotational speed, and humidity had a significant effect on the load sharing due to the varying viscoelastic properties. The results obtained by this method were compared with those obtained using existing method for steel spur gears. Results showed that the springs model used for steel spur gears were suitable for plas- tic spur gears. The results obtained by the proposed method were compared with those obtained experimentally. The proposed calculation results had less than 4% deviation that was more accurate than that obtained by DuPont's method. The modeling results showed that the carbon fiber reinforced plastic gear could provide higher strength than unreinforced plastic gears. The ana- lysis showed that the warpage and shrinkage proper- ties were affected most significantly by the glass fiber percentage in both polymer matrixes. This happened due to the orientation of the fibers along the injection flow direction.showed that the thermal damage was delayed for the gears with modified tooth. The experimental data showed a good agreement with the finite element model to predict the temperature rise.81 CNT-based polymer gears showed torque is reduced by the nano-clay reinforcement.91 Glass-filled polymer gears show better mechanical properties such as Young's modulus, ten- sile strength and flexural strength.84,85 Polymer gears wear resistance in comparison to the unfilled polymer gears due to the improved elastic modulus and com- with fiber reinforcement show poor wear resistance pressive strength.63,92 A study shows that when a trace but an improvement in the thermal resistance is observed.95 Figure 10 shows an average fiber orien- in polymer matrix reduces its capacity of heat gener- ation.88 Fiber reinforcement of region is shown in Figure 11. Fatigue data was obtained for a tensile bar made of the same material which showed a good correlation with gear fatigue data. The detail of the finite element mesh of polymer gear is shown in Figure 12. The values of these stres- ses showed satisfactory results.62 showed that the contact stress at the beginning of the mesh was higher in comparison to that at the end of the mesh, as shown in Figure 13. The simulated results of these gears showed improved load sharing and lower bend- ing and contact stresses compared to the standard gears. Also, the proposed gears showed an involute profile around the face width at all locations. Results showed that the bending stresses decreased with increase in a number of teeth, module, and pressure angle. The simulated results showed that the path of contact extended at the beginning and end of the meshing cycle due to the large tooth deflections of polymer gear teeth. Simulation results showed that the cumulative sliding wear had a significant effect on contact load due to the variation of tooth profile. The calculated results showed that the temperature, rotational speed, and humidity had a significant effect on the load sharing due to the varying viscoelastic properties. The measured values showed a per- fect correlation with the simulated values. Unidirectional models compared to the fiber orienta- tion models showed a difference of less than 8% amount fiber and of Proc IMechE Part J: J Engineering Tribology 232(2) regarding transmission error and less than 3% regard- ing contact pressure. Results showed that the springs model used for steel spur gears were suitable for plas- tic spur gears. He showed that Blok's solution122 could be used to obtain a quasi-steady approximation for mean flash temperature but the Blok's solution was inaccur- ate when the start and end of the gear teeth meshing were considered. The modeling results showed that the carbon fiber reinforced plastic gear could provide higher strength than unreinforced plastic gears.58 found that more thermal damage takes place in case of plastic–plastic gear pair in comparison to the plastic–metal gear pair. The pre- mature contact at the beginning of the meshing cycle was considered to be the cause for pitch line tooth fractures, and the extended contact was found to be the cause of extreme wear of gear tooth. An improvement in the ejection time and warpage of an injection molded polymer spur gear was suggested by Lee and Lin108 using uniform design and Kriging surrogate modeling. This modeling technique was used to con- struct the surrogate models of maximum warpage and ejection time. Modeling and simulation aspects of polymer gears Several research articles are based on the modeling and simulation techniques that provide a beforehand Proc IMechE Part J: J Engineering Tribology 232(2) understanding of the design and performance of the polymer gears.8% using uni- form design. The method pro- vided design information related to load sharing without any reference to gear tooth dimensions, material properties or operating conditions. This model was further refined by a finite element analysis for the adjustment of tooth designs. Conclusion and future scope The article has provided a review on various design features and performance characteristics of polymer and polymer composite gears. However, the effi- ciencies are similar for both gear pairs at high speed. Functionally graded materials based polymer gears can have the capability to pro- duce excellent performance and durability. This is an important aspect to be explored in the field of plastic gearing. The performance of hybrid gear was compared with a stainless steel gear without a polymer coating. In the tooth modification techniques such as dril- ling cooling holes in the gear tooth, the strength of the gear tooth was sacrificed for the improvement in the performance and durability of these gears. Performance parameters of polymer and polymer composite gears In the literature on polymer gears, a large number of studies are focused on the investigation of the per- formance parameters of these gears. The various factors that affect these performance parameters are: type of gear pair, type of reinforcement, and loading condi- tions as listed in Table 2. These factors and their effects on the performance parameters are discussed below: Effect of gear pair In the literature, the performance of polymer gears is studied using two types of gear pairs: plastic–plastic and plastic–metal. An experiment was performed by Evans and Keogh59 to predict the thermal response of a polymer gear running against a steel pinion.61 The study of gears made of dissimilar polymeric materials indicates that acetal (as a driver) against nylon provides better performance in com- parison to the other combinations. Magnesium catalytic cast polyamide 6 performed very well in comparison to the other polymers and polymer composites.79 Gears made of PC/ABS perform satisfactorily under low load but when the load increases, the surface melting of the tooth takes place due to the sudden increase in temperature. Melick and Dijk97 performed a high temperature test- ing using polyamide gears to calculate the correct root stresses by taking tooth bending into account. Modeling and simulation aspects of polymer gears Several research articles are based on the modeling and simulation techniques that provide a beforehand Proc IMechE Part J: J Engineering Tribology 232(2) understanding of the design and performance of the polymer gears. Finite element simulation study performed by Li et al. Conclusion and future scope The article has provided a review on various design features and performance characteristics of polymer and polymer composite gears. Techniques based on the modification in the profile of the gear tooth and their effects on the performance of these gears are also discussed. Performance analysis of polymer–polymer gear pair has not been adequately investigated so far.61 The study of gears made of dissimilar polymeric materials indicates that acetal (as a driver) against nylon provides better performance in com- parison to the other combinations. Modeling and simulation aspects of polymer gears Several research articles are based on the modeling and simulation techniques that provide a beforehand Proc IMechE Part J: J Engineering Tribology 232(2) understanding of the design and performance of the polymer gears. The modeling results showed that the carbon fiber reinforced plastic gear could provide higher strength than unreinforced plastic gears. Conclusion and future scope The article has provided a review on various design features and performance characteristics of polymer and polymer composite gears. Lin and

Title	Year;Author	Abstract	SUMMARY
An investigation on the thermal and wear behavior of polymer based spur gears	2018 Prashant Kumar Singh *, Siddhartha, Akant Kumar Singh	A R T I C L E I N F O This study investigates the potential of three different thermoplastic materials viz. Acrylonitrile Butadiene Styrene Keywords: (ABS), High Density Polyethylene (HDPE) and Polyoxymethylene (POM) to be used in plastic gearing applica- Polymer gears Failure tions. The gears are manufactured by injection molding process. Thermal and wear behavior of these gears are Wear rate examined at different torque levels of 0.8, 1.2, 1.6 and 2.0 Nm along with different rotational speeds of 600, 800, Surface temperature 1000 and 1200 rpm. Also, steady state analysis of the gears is carried out at a torque of 1.4 Nm and a rotational speed of 900 rpm to measure the reduction in the gear tooth, durability and failure modes occurring in these gears. ABS gear fails due to excessive wear of the teeth whereas HDPE gear failure is caused by the cracking at the root of gear teeth. ABS and HDPE gears complete 0.5 and 1.1 million cycles, respectively before failure whereas POM gear completes 2 million cycles without any sign of failure. 1.	The results obtained in this study are concluded as follow: 1. It results in a reduced wear rate of gear tooth at higher rotational speed. It is found that ABS gear shows the best agreement (maximum 8% deviation) with Mao model followed by HDPE and POM gears with the maximum deviation of 10% and 11% respectively. It is found that rise in surface temperature is maximum for POM and minimum for HDPE at all torque levels.4 Nm and a rotational speed of 900 rpm and it is found that ABS gear fails due to excessive wear of gear teeth while HDPE gear fails due to root cracking of gear teeth.) to investigate their performance. machine cut gears) can be used to fabricate polymer gears and their performance can be compared with the gears made by current technique (i. Other form of gears such as helical or bevel gears can be fabricated to investigate the performance.
Accelerated lifetime testing of reinforced polymer gears Jože TAVČAR*, Gašper GRKMAN* and Jože DUHOVNIK** ** Faculty of Mechanical Engineering, University of Ljubljana *Iskra Mehanizmi d.o.o. Lipnica 8, SI-4245 Ljubljana, Slovenia E-mail: joze.tavcar@iskra-		The main advantages of polymer gears compared to metal gears are low manufacturing costs for mass production, vibration damping, and there is no need for a lubricant. In the literature and guidelines, the allowable gear endurance limits for bending and contact stresses are mainly given for polyamides (PA) and polyacetals (POM). A large number of suitable polymer gear materials is available, but the standards offer little support for the lifetime calculations of polymer gears from other materials. Therefore, the testing of gear geometry and materials combinations cannot be avoided in the design of an optimal gear drive. However, gear testing is very time-consuming and expensive, especially when testing several different material combinations in different testing conditions. By applying the upgraded accelerated testing procedure, gear test time and costs can decrease significantly. Determination of the gear temperature during meshing is needed for the precise calculation of plastic gears. The presented temperature calculation model is corrected and improved with input parameters, which were determined from the test results. Accelerated tests were conducted on different combinations of reinforced and unreinforced commercially available materials: PA6, PA66, POM and PPS. Glass and carbon fiber were used for reinforcement. The research goal was characterization of different material pairs with the coefficient of friction, time strength, wear, and the failure mechanism in relation to load cycles and load level. The paper's contribution are some general guidelines for selecting polymer material for gears, such as fiber reinforcement improves the allowable stress level at up to a few million load cycles; unreinforced polymers are better for a higher number of load cycles. Also, PTFE – the internal lubricant significantly reduces a coefficient of friction if added to PA polymers, and is less efficient in combination with POM. Keywords : Reinforced polymer, Glass fiber, Coefficient of friction, Accelerated testing, Gear, Temperature 1.	The paper presents the results of a wide range of commercially available polymer materials, and the results of the tests are summarized in several general rules for gear material pair and reinforcement selection. 3) An important contribution of the paper is a wide range of tests from high to low load levels, and from that coming results. More accurate determination of gears temperature in application enables optimization of gear design. This paper presents a coefficient of friction for several reinforced and unreinforced material pairs. On the other hand, the use of the PTFE in combination with acetal (POM) does not significantly improve the tribological performance of the gears.

Title	Year;Author	Abstract	SUMMARY
Rolling contact fatigue of case carburized steels	2017 ⇑	Article history: Case carburized steels are widely used in high performance ball and rolling element bearings. They are Received 9 June 2016 characterized by the hardened exterior and gradient in the material properties as a function of depth. Received in revised form 31 October 2016 In this investigation, an elastic-plastic finite element model based on micro-indentation tests was devel- Accepted 2 November 2016 oped to investigate the rolling contact fatigue of case carburized steels. A series of micro-indentation tests Available online 4 November 2016 were conducted to obtain the hardness gradient in the case carburized 8620 steel. The results demon- strated that the hardness varies linearly from the surface to the core of the material. The finite element Keywords: modeling approach employs Mises based plasticity model with kinematic hardening to incorporate the Rolling contact fatigue effect of material plasticity. The hardness gradient in the material was modeled by changing the yield Case carburized strength as a function of depth. Linear relationship between hardness and yield strength was assumed. Damage mechanics The FE model was coupled with continuum damage mechanics approach to capture material degradation Voronoi tessellation due to fatigue damage. It considers both; stress and accumulated plastic strain based damage evolution Plasticity laws for fatigue failure initiation and propagation. The residual stress distribution due to carburization process was modeled by modifying the damage evolution law. Material dependent parameters used in the damage evolution laws were determined using the SN results for torsional fatigue of the bearing steel. The effects of topological randomness in the material microstructure are accounted in the model through the use of Voronoi tessellations. The model was used to compare the rolling contact fatigue (RCF) lives of through hardened and case carburized bearing steel with different case depths at contact pressures ranging from 2 to 3.5 GPa. The effect of residual stress distribution on RCF lives was also investigated. The results show that there is an optimum case depth for which maximum RCF lives can be attained. The spall shapes and the depth below the surface where damage initiates were found to be dependent on the case depth. The model was also used to study the effect of initial material imperfections. The fatigue lives and their dispersion quantified by Weibull slopes obtained from the model correlate well with the experiments. (cid:1) 2016 Elsevier Ltd. All rights reserved. machine components has been of significant interest to improve reliability and reduce the maintenance costs. In tribo machineries such as gears, cam-followers, wind tur- bines, rail-wheel contacts; rolling element bearings (REB) are fre- quently used to allow rotary motion while supporting significant amount of load. They also help reduce friction between the moving parts. If REBs are properly loaded and operated under conditions of elastohydrodynamic lubrication, then material fatigue is the lead- ing cause of failure that limits the working life of the machine com- ponent [1]. This is caused by the rolling motion between the rollers and the raceway, which produces alternating contact stress over a small volume. This type of fatigue is known as rolling contact fati- gue (RCF). In rolling element bearings, failure due to RCF can manifests itself in variety of different modes. Surface originated pitting and subsurface initiated spalling [2,3] are the two most dominant modes of RCF damage. Pitting is characterized by the crack 1.	Summary and conclusion This paper presents a numerical model based on micro- indentation tests to study the effect of case carburizing on rolling contact fatigue lives rolling element bearings. It is evident from the results that when material flaws are taken into account, model results show considerable scatter in the fatigue lives. of voids, as the pressure increases the L10 life decreases Table 4 Weibull plots and L10 lives obtained from the model results for through hardened material with initial voids. From the results of the parametric study an equation for the modifying factor to calculate the L10 lives of case carburized steels is derived. Addi- tionally, the model resulted in spall patterns which resemble those commonly observed in experiments. It is evident from the results that when material flaws are taken into account, model results show considerable scatter in the fatigue lives. In order to achieve the objectives, micro-indentation tests were performed to calcu- late Vicker's hardness at various depths along the cross-section.
Different teeth profile shapes of polymer gears and comparison of their performance Damijan ZORKO*, Simon KULOVEC**, Jože TAVČAR* and Jože DUHOVNIK* *Faculty of Mechanical Engineering, University of Ljubljana Aškerčeva 6, Ljubljana 1000, Slovenia E-mail: damijan.zorko@lecad.fs.uni-lj.si **Podkrižnik, d.o.o. Loke 33, Ljubno ob Savinji 3333, Slovenia	This article presents a lifespan testing analysis of polymer gears manufactured by cutting. Compared to injection molding, machine cutting provides higher accuracy of gear geometry. Two different tooth flank geometries were tested; i.e. involute and S-gears. In theory, S-gears have several advantages over involute gears due to the convex/concave contact between the matching flanks. The theoretical tooth flank geometry of S-gears provides more rolling and less sliding between the matching flanks, compared to involute gears. The convex/concave contact leads to lower contact stress, which in combination with less sliding means lower losses due to sliding friction and consequently less heat generated. The goal of our research was to prove that tooth flank geometry affects the lifetime of polymer gears, and to find the mechanisms and quantitative differences in the performance of both analyzed geometries. The gears were tested on specially designed testing equipment, which allows exact adjustment of the central axis distance. Two different material pairs (POM/POM and POM/PA66) of the drive and driven gears were tested. Each test was done at a constant moment load and a constant rotational speed. Several tests were conducted using the same conditions due to repeatability analysis. All the tests were performed till the failure of the gear pair and without lubrication. In lifespan testing, the polymer S-gears showed better performance and longer lifespan than involute polymer gears. Keywords : Polymer gears, Lifespan testing, Temperature, S-gears, Involute 1.	After around 2 million cycles, noise level during the operation of the tested gears increased significantly, which can lead to a conclusion that gear wear is considerable. Conclusion This work has experimentally verified better performance of S-gears, as well as researched and identified the reasons for differences between both geometries, which supports our hypothesis, stated in the beginning. Wear results in the loss of tooth profile shape, the study of which was our goal. Figure 5 shows the results of lifespan tests for this material pair. The results can lead to a presumption of a higher load capacity of S-gears, as the gears with this flank profile geometry yielded better results at all tested loads. When S-gears are manufactured precisely, temperature increases more slowly, compared to involute gears, which – in the case of heat-related defects – results in longer lifetime. This results in lower contact stresses in S-gears (Duhovnik et al., 2016), which in combination with less sliding and smaller sliding velocities means lower heat generation as a result of losses due to friction between tooth flanks. Discussion It was observed during testing that different load levels result in different types of failure modes. The use of identical materials causes strong adhesion between the parts in contact, resulting in increased wear of the tooth flank. Cracks are visible on the teeth of the driven gear, and deformed teeth on the drive gear as a result of overheated material. Figure 10 shows the result of measured surface temperature of an involute and an S-gear pair POM/PA66 at a load of 1. It can be claimed that the shape of S-gears tooth profile improves contact conditions, which results in lower contact stress and the related heat generation. Temperature increase in involute gears is faster, which means higher heat generation as a result of losses due to friction in contact. This time, tests were conducted under high loads in order to obtain results in a reasonable time. Figure 4 shows the lifespan curves, drawn with a 90% probability that the test item would survive. Testing showed differences between both geometries, however, a rather small number of operational cycles was achieved at tested loads of 0. Figure 5 shows the results of lifespan tests for this material pair.5 Nm, shown in Fig.c shows wear of an involute gear after 9.a shows an S-gear pair that yielded after 0.b shows an S-gear pair that failed under a load of 1.a shows an involute gear pair that failed at a moment of 1.b shows the defects on an involute gear pair after transferring 1. Figure 10 shows the result of measured surface temperature of an involute and an S-gear pair POM/PA66 at a load of 1. Based on temperature measurement, it has been found that the course of temperature increase in S-gears is different from that in involute gears. Such testing is time consuming, however, it yields a knowledge basis, necessary for the use of polymer gears in real applications. Testing showed differences between both geometries, however, a rather small number of operational cycles was achieved at tested loads of 0. A worn gear will still transfer moment and thus fulfil its main function, however, noise and vibration levels are too high for use in a real-life application, and moment transfer via worn tooth flanks is no longer constant. In these types of test loads, S-gears lasted more operational cycles, however, the type of failures was the same, i. Such a gear can still transfer moment, however, the gear ratio is no longer constant, vibrations and noise levels are high, which makes such a gear unsuitable for operation. It can be observed that the temperature increase gradient is similar, however, in the initial operation phase, S-gears heat up less than the involute ones. Three tests were performed for POM/POM gear pairs at each load level. Only one test for each load value was performed, which makes it impossible to discuss the probability of survival at a specific load level. Conclusion This work has experimentally verified better performance of S-gears, as well as researched and identified the reasons for differences between both geometries, which supports our hypothesis, stated in the beginning.

Appendix B Design of the trial mould cavity

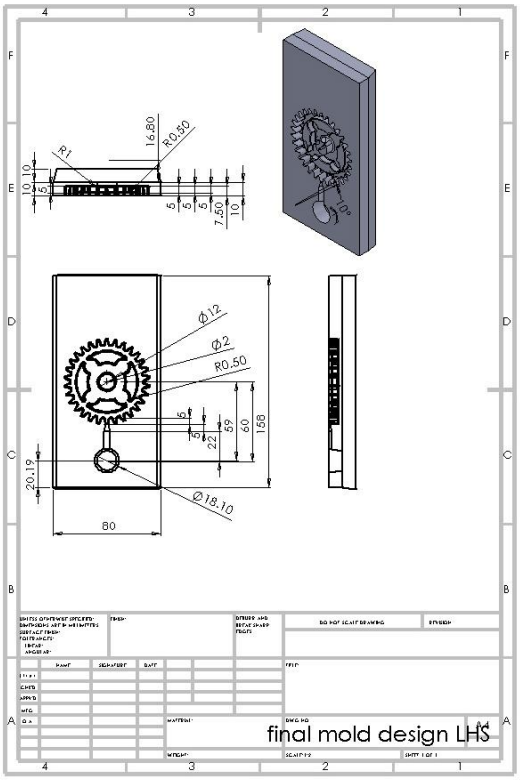

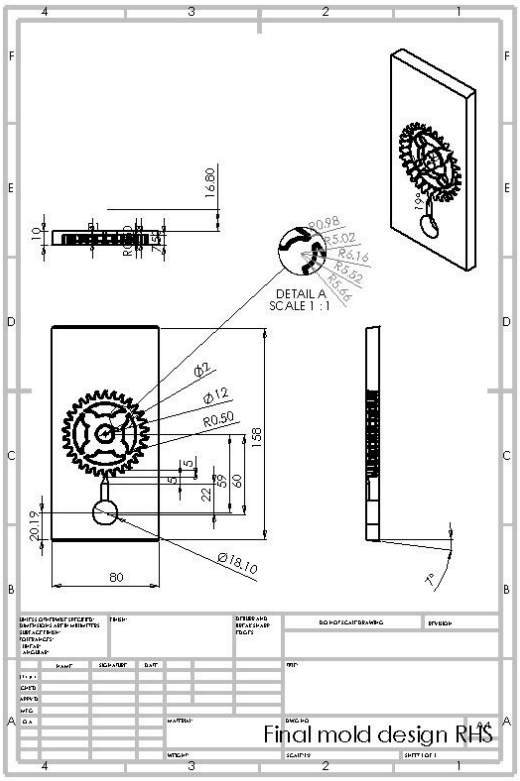

Appendix C Design of the final edition mould